MODELLING, TRANSIENT SIMULATIONS AND PARAMETRIC STUDIES OF PARABOLIC TROUGH COLLECTORS WITH THERMAL ENERGY STORAGE

A THESIS SUBMITTED TO
THE GRADUATE SCHOOL OF NATURAL AND APPLIED SCIENCES
OF
MIDDLE EAST TECHNICAL UNIVERSITY

BY

TUFAN AKBA

IN PARTIAL FULFILLMENT OF THE REQUIREMENTS
FOR
THE DEGREE OF MASTER OF SCIENCE
IN
MECHANICAL ENGINEERING

OCTOBER 2014

Approval of the thesis:

MODELLING, TRANSIENT SIMULATIONS AND PARAMETRIC STUDIES OF PARABOLIC TROUGH COLLECTORS WITH THERMAL ENERGY STORAGE

submitted by **TUFAN AKBA** in partial fulfillment of the requirements for the degree of **Master of Science in Mechanical Engineering Department, Middle East Technical University** by,

Prof. Dr. M. Gülbin Dural Ünver _____
Dean, Graduate School of **Natural and Applied Sciences**

Prof. Dr. Tuna Balkan _____
Head of Department, **Mechanical Engineering**

Assoc. Prof. Dr. Almıla Güvenç Yazıcıoğlu _____
Supervisor, **Mechanical Engineering Dept., METU**

Assoc. Prof. Dr. Derek K. Baker _____
Co-Supervisor, **Mechanical Engineering Dept., METU**

Examining Committee Members:

Assoc. Prof. Dr. İlker Tarı _____
Mechanical Engineering Dept., METU

Assoc. Prof. Dr. Almıla Güvenç Yazıcıoğlu _____
Mechanical Engineering Dept., METU

Assoc. Prof. Dr. Derek K. Baker _____
Mechanical Engineering Dept., METU

Asst. Prof. Dr. Feyza Kazanç _____
Mechanical Engineering Dept., METU

Dr. Mustafa Zeki Yılmazoğlu _____
Mechanical Engineering Dept., Gazi Uni.

Date: 17.10.2014

I hereby declare that all information in this document has been obtained and presented in accordance with academic rules and ethical conduct. I also declare that, as required by these rules and conduct, I have fully cited and referenced all material and results that are not original to this work.

Name, Last name : Tufan AKBA

Signature :

ABSTRACT

MODELLING, TRANSIENT SIMULATION AND PARAMETRIC STUDY OF PARABOLIC TROUGH COLLECTOR WITH THERMAL ENERGY STORAGE

Akba, Tufan

M.S., Department of Mechanical Engineering

Supervisor : Assoc. Prof. Dr. Almıla Güvenç Yazıcıoğlu

Co-Supervisor : Assoc. Prof. Dr. Derek K. Baker

October 2014, 134 pages

In this thesis, a mathematical model of a parabolic trough collector field with a two-tank molten salt thermal energy storage is developed. The model is built in TRNSYS and by using MatLab, novel valve and thermal energy storage control algorithms are implemented. The model is sensitive to transient states inside the components and variations in weather and demand.

Optimum parabolic trough collector length is determined for different insolation values to show the relation between direct normal insolation and collector string length. The mathematical model is used in an economic model, which contains initial investment costs of the parabolic trough collector field and thermal energy storage costs only.

Depending on the economic model, different sizes of plants are created at fixed initial investment costs by changing collector field area and storage size in the mathematical model. A parametric study is done by using economic model data and by simulating the mathematical model at various initial investment costs, two different locations in Turkey, and four different load profiles. As result of the parametric study, maximum solar fraction cases are selected and a generalized trend is observed. Effect of thermal energy storage on solar fraction is discussed and the change in thermal energy storage with optimum plant size is investigated. After an optimum investment, linear increment behavior of solar fraction is disappears and increases asymptotically by increasing the plant and/or storage size. Above this limit, hybridizing with other energy sources are advised. Later in the thesis, significance of load profile is emphasized, which should be one of the major design parameters for solar powered energy systems.

Keywords: Solar Energy, Concentrating Solar Power, Parabolic Trough Collector, Thermal Energy Storage, Two-Tank Thermal Energy Storage

ÖZ

ISIL ENERJİ DEPOLAMALI PARABOLİK OLUKLU KOLEKTÖRLERİN MODELLENMESİ, ZAMANA BAĞLI BENZETİMİ VE PARAMETRİK ÇALIŞMASI

Akba, Tufan
Yüksek Lisans, Makina Mühendisliği Bölümü
Tez Yöneticisi : Doç. Dr. Almıla Güvenç Yazıcıoğlu
Ortak Tez Yöneticisi : Doç. Dr. Derek K. Baker
Eylül 2014, 134 sayfa

Bu tezde, iki tank ergimiş tuzlu ısıl enerji depolamalı parabolik oluklu kollektör tarlasının matematiksel modeli geliştirilmiştir. Model TRNSYS'te oluşturulmuş ve MatLab kullanılarak özgün bir valf ve ısıl enerji depolama kontrol algoritması modele dahil edilmiştir. Model, elemanların içerisindeki zamana bağlı durumlara, hava durumu ve talepteki değişikliklere duyarlıdır.

Doğrusal dik ışınım ve kollektör uzunluğu arasındaki ilişkiyi göstermek için farklı güneş ışınımlarında en uygun parabolik oluklu kollektör uzunluğu hesaplanmıştır. Matematiksel model yalnızca parabolik oluklu kollektör tarlası ve ısıl enerji depolamanın ilk yatırım maliyetlerini içeren bir ekonomik modelin içerisinde kullanılmıştır.

Ekonomik modele bağlı olarak, matematiksel modelde, sabit ilk yatırım maliyetinde kollektör tarlası alanı ve depo büyüklüğünü değiştirerek farklı büyüklükte santraller

oluşturulmuştur. Birçok ilk yatırımı maliyetinde, Türkiye'deki iki farklı şehirde ve dört farklı yük profilinde ekonomik model verilerini ve matematiksel model benzetimlerini kullanarak parametrik bir çalışma yapılmıştır. Parametrik çalışmanın sonucunda, en fazla güneşlenme oranının olduğu durumlar seçilmiş ve genel bir davranış gözlemlenmiştir. Isıl enerji depolamanın kollektör tarlasından üretilen enerjiye olan etkisi tartışılmış ve ısıl enerji depolamanın en uygun santral boyutlarındaki değişimi gözlenmiştir. Uygun bir yatırım limitinden sonra, artan kolektör tarlası ve/veya depolama büyüklüğüne bağlı olarak; güneşlenme oranının doğrusal artışı kaybolur ve asimtotik artar. Bu limitin üstünde, diğer enerji kaynaklarıyla hibritleme tavsiye edilmiştir. Tezin sonraki bölümünde güneş enerjisinde temel tasarım parametrelerinden bir tanesi olan yük profilinin önemi vurgulanmıştır.

Anahtar Kelimeler: Güneş Enerjisi, Yoğunlaştırılmış Güneş Enerjisi, Parabolik Oluklu Kolektör, Isıl Enerji Depolama, İki Tanklı Isıl Enerji Depolama

To my family,

ACKNOWLEDGEMENTS

First of all, I would like to thank my supervisors Assoc. Prof. Derek K. Baker for his guidance, support, perspective, and criticism throughout this thesis study and Assoc. Prof. Dr. Almıla Güvenç Yazıcıoğlu for her kindly advices and being my primary advisor when everything got messed up.

I sincerely like to thank Can Uçkun and other members in CERES (Clean Energy Research, Education, and Service) group for their valuable support, comments and suggestions about my study. I would also like to express my appreciation to my co-workers and very close friends Ulaş Akova and Bilgehan Tekin for their friendship and support during my assistantship and in two other jobs in the last three years.

I am also grateful to Ali Karakuş for his advice and always sharing his coffee and office with me. I would like to thank to Gökhan Bayar for showing me completely different points of view for the model used in this thesis.

In addition, for providing TRNSYS 17 license, GUNAM (Center for Solar Energy Research and Application) is gratefully acknowledged.

Finally, I would like to thank my family for their endless support and encouragement during my life. I know it was always late when I studied.

TABLE OF CONTENTS

LIST OF TABLES

LIST OF FIGURES

LIST OF SYMBOLS AND ABBREVIATIONS

A	Nodal Aperture Area $[m^2]$
a	Constants for Heat Transfer from Heat Collecting Element to Environment
b	Constants for Incidence Angle Modifier
c	Constants for Pump Power Consumption Polynomial
C_c	Cold Side Heat Capacity Rate of Heat Exchanger $[kW/°C]$
C_h	Hot Side Heat Capacity Rate of Heat Exchanger $[kW/°C]$
C_{max}	Maximum Heat Capacity Rate of Heat Exchanger $[kW/°C]$
C_{min}	Minimum Heat Capacity Rate of Heat Exchanger $[kW/°C]$
c_p	Constant Pressure Specific Heat of the Fluid $[kJ/kg\ K]$
$\dot{E}_{in}$	Rate of Energy Input $[kJ/s]$
$\dot{E}_{out}$	Rate of Energy Loss $[kJ/s]$
F	The Focal Length of the Collector $[m]$
$f_{bellows}$	Function that Accounts for Shading of the Mirror by the Bellows
f_{dust}	Function that Accounts for Losses due to the Dust on the Glass Envelope
$f_{endloss}$	Function that Accounts for the Geometric Inaccuracies of the Parabolic Mirror
f_{misc}	Function that Accounts for Miscellaneous Losses from the System
f_{par}	Fraction of Parasitics Converted to Fluid Thermal Energy
$\dot{H}_{fluid,in}$	Rate of Enthalpy Flow of Inlet Fluid $[kW]$
$\dot{H}_{fluid,out}$	Rate of Enthalpy Flow of Outlet Fluid $[kW]$
L_{coll}	Length of One Collector along the Length of the Mirror $[m]$

m	Mass $[kg]$
$\dot{m}_c$	Cold Side Mass Flow Rate for Heat Exchanger $[kg/s]$
$\dot{m}_{in}$	Inlet Mass Flow Rate $[kg/s]$
$\dot{m}_h$	Hot Side Mass Flow Rate for Heat Exchanger$[kg/s]$
$\dot{m}_{out}$	Outlet Mass Flow Rate $[kg/s]$
$\dot{m}_{pump}$	Mass Flow Rate of Pump $[kg/s]$
m_{tank}	Mass of Tank $[kg/s]$
P_{pump}	Power Consumption of Pump $[kW]$
$\dot{Q}$	Heat Transfer Rate $[kW]$
$\dot{Q}_{absorbed}$	Rate of Heat Transfer Absorbed to HCE $[kW]$
$\dot{Q}_{losses}$	Rate of Heat Transfer Lost from HCE $[kW]$
T	Temperature $[°C]$
T_{amb}	Ambient Temperature $[°C]$
$T_{c,in}$	Cold Side Inlet Temperature of Heat Exchanger $[°C]$
$T_{c,out}$	Cold Side Outlet Temperature of Heat Exchanger $[°C]$
T_{in}	Inlet Temperature $[°C]$
$T_{h,in}$	Hot Side Inlet Temperature of Heat Exchanger $[°C]$
$T_{h,out}$	Hot Side Outlet Temperature of Heat Exchanger $[°C]$
T_{out}	Outlet Temperature $[°C]$
u	Internal Energy $[°C]$
U'	Heat Loss Coefficient from Heat Collecting Element to Environment $[kJ/hr\ m]$
UA	Overall Heat Transfer Coefficient of Heat Exchanger $[kW/K]$
$(UA)_t$	Overall Conductance for Heat Loss from Tank $[kW/K]$
U_L	Heat Transfer Coefficient between Heat Collecting Element to Environment $[kW/m^2\ K]$
W_{aper}	Aperture Width of Collector Mirror $[m]$
V	Volume $[m^3]$

GREEK SYMBOLS

$\alpha_{coating}$	Absorptance of the Coating on the Absorber Tube
β	Slope [°]
γ	Azimuth Angle [°]
γ_{sgn}	Control Signal for Pump
γ_S	Solar Azimuth Angle [°]
δ	Declination [°]
ε	Effectiveness
θ	Angle of Incidence [°]
θ_z	Zenith Angle [°]
φ	Latitude [°]
ω	Hour Angle [°]
Δt	Time Step [hr]

ABBREVIATIONS

CLFR	Compact Linear Fresnel Reflectors
CPV	Concentrated Photovoltaics
CRS	Central Receiver Systems
CSP	Concentrating Solar Power
CST	Concentrating Solar Thermal
DLR	German Aerospace Center
DNI	Direct Normal Insolation
DSG	Direct Steam Generation

HEX	Heat Exchanger
HTF	Heat Transfer Fluid
IAM	Incidence Angle Modifier
IEA	International Energy Agency
LCOE	Levelized Cost of Electricity
LFR	Linear Fresnel Reflectors
OECD	Organization for Economic Co-operation and Development
ORC	Organic Rankine Cycle
O&M	Operation and Maintenance
PSA	Plataforma Solar de Almeria
PTC	Parabolic Trough Collectors
PV	Photovoltaics
SEGS	Solar Electric Generating Systems
SM	Solar Multiple
SSSPS/DCS	Small Solar Power System Project / Distributed Collector System
SunLab	Sandia National Laboratories

CHAPTER 1

1. INTRODUCTION

1.1. Motivation

Fossil fuels were used even before the invention of Watt's steam engine in 1781, which initiated the industrial revolution. Subsequently, the need for fossil fuels has increased rapidly. In the textile industry, steam engines increased production capacity and created new markets. Steam engines allowed access to new and distant markets by their use in locomotives and ships. But a new problem occurred, which has continued since the industry revolution: in a fast growing world, how can the increasing demands for fossil fuels are supplied?

The very first solution was a new fossil fuel, which is oil. It has a higher heating capacity with respect to coal. After refining, it allows efficient burning with low ash and due to purification continuous work and consistent output can be supplied. Oil allowed internal combustion engines to spread commercially and resulted in the rise of automobile and aviation industries. Today oil has replaced coal for many applications and it is the major fossil fuel. But still, oil cannot be a sustainable solution of meeting the increasing need for fuel. The time when oil will be depleted is still unclear but it is known that it will, and when oil becomes depleted a new

alternative fuel source is necessary that can be used in industry and daily life for running engines and generating electricity.

The oil crisis, which occurred in 1973, is another oil related problem. By the end of the crisis in 1974, the crude oil market price quadrupled as shown in Figure 1.1 (nominal prices rose from 3.22 to 12.52 USD per barrel) (U.S. Energy Infomation Administration, 2014). Stock markets crashed as a result. More importantly, it showed that the results of a global oil embargo were catastrophic and suggested the next crisis would be worse in a world with increasing fuel demand if it was dominantly powered by oil. At the end of the embargo, finding an alternative energy source became vital to decrease the world's dependence on oil. For this purpose, an intergovernmental organization was established named the Organization for Economic Co-operation and Development (OECD) to reduce the effect of disruptions in oil supplies.

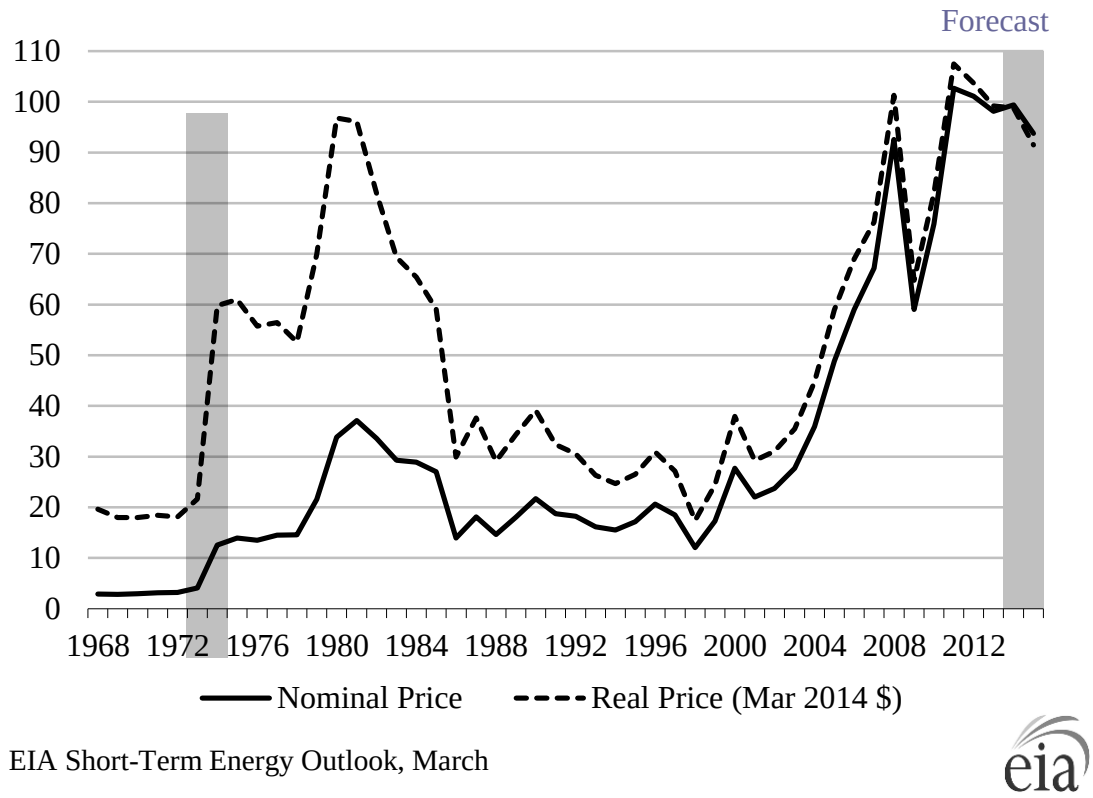

Figure 1.1 Annual Imported Crude Oil Price [dollar per barrel], (U.S. Energy Infomation Administration, 2014)

The new alternative fuel source could not be a fossil fuel (processed coal, shale gas, etc.) because of two reasons. First, CO_2 emissions became an important issue due to climate change, which required that the next generation of fuels not have a large carbon footprint. Second, the new energy source must not cause the next energy crisis. And it also should have the advantages of oil such as easily supplied when in demand and easy storage. Considering these reasons, renewable energy sources became attractive, as they are clean and they increase energy security by allowing the harvesting of domestic energy sources rather than importing energy from another country. Today there is new point of view for energy independency; self-generated electricity makes the user no longer dependent on the grid.

The motivation of this thesis is demonstrating that solar energy can be a good future energy source. Unlike fossil fuels, which have negative environmental impacts and makes the user dependent on the fuel supplier, solar is a clean energy source and it gives independence to users. Even though solar energy input varies, day and night times are precisely known and with good storage designs and control algorithms a consistent and sustainable output can be provided.

1.2. Principles of Concentrating Solar Power (CSP) Technologies

Solar energy conversion technologies harness the light or heat emitted by the sun using various technologies such as solar architecture, solar illumination, solar heating and cooling, solar photovoltaic (PV), solar thermal electricity, artificial photosynthesis etc. (International Energy Agency, 2011), (Black, 2014). In concentrating solar power (CSP), solar radiation is focused to a specific smaller surface using mirrors or lenses. Depending on the application, concentrated surfaces can directly generate electricity (concentrating photovoltaic), or the surface can a heat medium to a high temperature, which can be used to drive a heat engine for electricity generation, mechanical power or process heat (concentrated solar thermal).

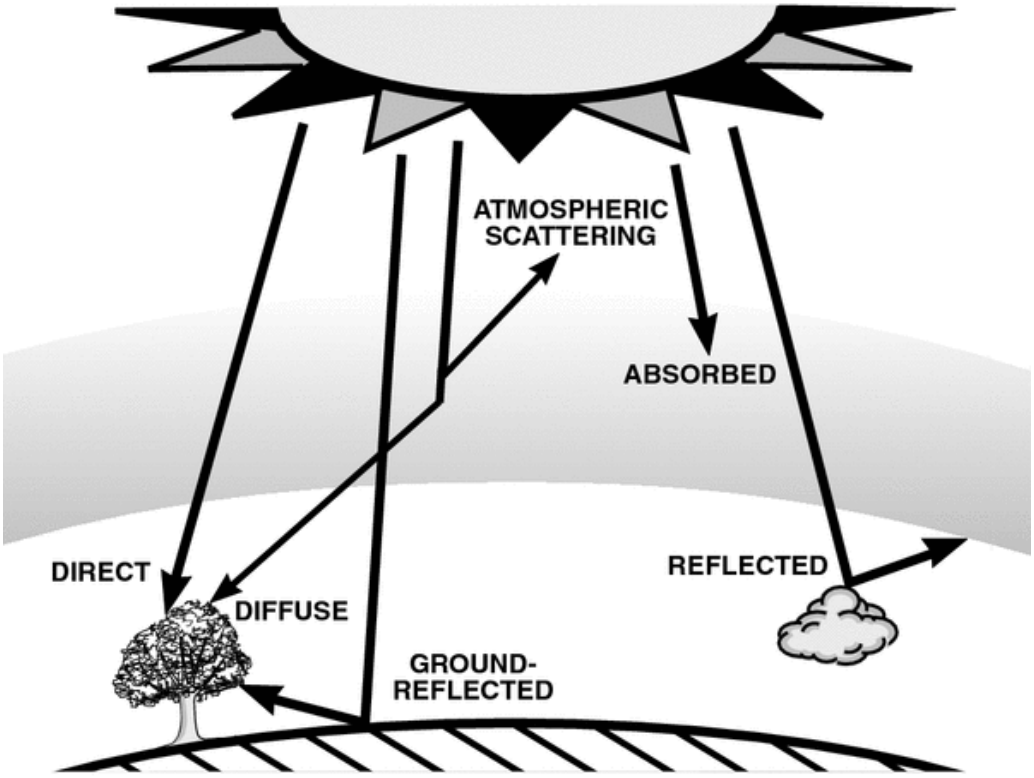

Figure 1.2 The Total Global Radiation and Its Components (Newport Corporations, 2014)

In order to understand the working principles of CSP systems, several terms need to be clearly defined as illustrated in Figure 1.2. **Total Solar Radiation (Global Radiation)** is the total solar radiation incident on a specific surface, and is the combination of beam (direct), diffuse, and reflected radiation as shown in Figure 1.2. **Beam Radiation** is the solar radiation striking the earth without having been scattered by the atmosphere or reflected by terrestrial objects. Beam radiation is directional, and depending on the geometry with which the beams hit, it can be reflected in the desired direction or concentrated to a smaller area for obtaining a high radiative flux. Beam radiation is the only type of solar radiation used for CSP applications. On the other hand, **Diffuse Radiation** is the solar radiation scattered due to molecules and particles in the atmosphere. Diffuse radiation can be used for non-concentrating solar applications, but since it cannot be specularly reflected or

concentrated, it cannot be used for CSP. **Reflected Radiation** is the solar radiation reflected from terrestrial objects (buildings, ground, oceans, etc.). Although reflected radiation can be classified as a part of diffuse radiation, reflected radiation is much less spatially uniform than diffuse radiation since a surface next to a white wall will have much more reflected radiation than a nearby surface next to a black wall. **Irradiance** is the rate of radiant energy flux on a surface at a specific instance in time. **Irradiation** is the integration of irradiance over a time, usually on an hourly or daily basis. **Insolation** is the term specific to solar energy irradiation. Irradiance, irradiation, and insolation can be used for extraterrestrial, total, beam and diffuse radiation (Duffie & Beckman, 2006).

Concentration ratio is a non-dimensional ratio of the insolation achieved after concentration to the normal insolation (Steinfeld & Palumbo, 2001).

There are four major CSP technologies which can be sorted by their focus and receiver types as shown in Table 1.1, and detailed information is given in the following paragraphs and in the literature review.

Table 1.1 The Four CSP Technology Families (International Energy Agency, 2010)

	Line Focus	**Point Focus**
Fixed Receiver	Linear Fresnel Reflectors (LFR)	Central Receiver Systems (CRS)
Mobile Receiver	Parabolic Trough Collectors (PTC)	Parabolic Dishes

The focus types can be linear or point. Linear focus systems require the collectors to track on a single axis and focuses solar radiation on a line. The main advantage of a line focus is single axis tracking which makes tracking simpler and cheaper with respect to point focus. Point focus systems require the collectors to track in two-axes

(azimuth and elevation), which results in tracking with lower angle of incidences (ideally always zero) and allows higher temperatures to be reached.

Receiver types can be fixed or mobile. Fixed receivers are located at a stationary position and are separate from the focusing device. Fixed receivers make it easier to transport the heat transfer fluid (HTF) since HTF is not distributed to a piping network for heating to the power block or, in case of process heat applications, the end-use. Mobile receivers move continuously with the focusing device. They collect more energy, which allows reaching higher temperatures.

Requirements define the selection of technology. For large scale electricity production, usually Parabolic Trough Collectors (PTC) and Central Receiver Systems (CRS) are preferred. On the other hand, if the cheapest solution is required and efficiency is not a concern, Linear Fresnel Reflectors (LFRs) are preferred, which have the additional advantage of allowing easy dual land use such as having plants grow beneath the collectors or placing the collectors on rooftops. Parabolic dishes can reach the highest temperature, which maximizes Carnot efficiency, and they can operate without using any cooling water. When a CSP plant is built in arid regions or where water sources are not available, parabolic dishes are sometimes the preferred technology, but their initial investment cost and commercialization prospects still need to be improved. In Table 1.2, a summary of the main characteristics for each CSP technology is given.

Table 1.2 Performance Characteristics of CSP Technologies, (Kalagirou, 2009), (Greenhut, 2010)

	Capacity range [MW]	**Concentration Ratio**	**Peak solar eff. (%)**	**Solar to electric eff. (%)**	**Land use [m^2/MWh-a]**
PTC	10-200	10-100	8-12	8-12	6-8
LFR	10-200	25-100	<10	9-11	4-6
CRS	10-150	300-1000	12-18	12-18	8-12
Parabolic dishes	0.01-0.4	600-3000	15-30	15-30	8-12

1.2.1. Parabolic Dishes

Parabolic dishes use a parabolic-shaped concentrator (50-100 m^2 area) that concentrates solar radiation to power an energy conversion unit, which is a Stirling engine or a micro-turbine, at the focal point of the parabola. They have the highest concentration ratios (1000-3000), which allows accessing very high temperatures (above 1000 ^oC), and as a result have the highest Carnot efficiency with respect to other CSP technologies. The axis of symmetry of the parabolic dish points to the sun which requires the parabolic dish to track in two-axes as shown in Figure 1.3.

Figure 1.3 Front and Back Views of EURODishes, (Plataforma Solar de Almería, 2014)

Unlike the other CSP technologies, each parabolic dish acts as an individual power generation unit and generates around tens of kW power. To obtain a large scale power plant, a field of parabolic dishes needs to be installed. Since parabolic dishes do not require active cooling, they can be installed in isolated and distant places like deserts which results in two advantages: first, deserts have very high direct normal insolation (DNI), and second generation of off-grid electricity is easy. Also parabolic dishes can be used with concentrated photovoltaics (CPV) using high temperature durable multi-layer photovoltaics (International Energy Agency, 2010).

The immaturity of Stirling engine technology, very high relative initial investment cost and inability to easily integrate energy storage are the main disadvantages of this system. To solve these problems, several initiatives and companies have been founded and focused on specific points about this issue such as Stirling Energy

Systems (1996), Schlaich Bergermann und Partner (1998), Infinia (2006), Australian National University and a number of additional small and early stage initiatives (Vogel & Kalb, 2010).

1.2.2. Central Receiver Systems

Central receiver systems (CRS) (or power tower or heliostat systems) use flat or slightly curved reflectors (reflective area of approximately 16-20 m^2) to concentrate solar radiation to an absorber which is top of a tower to heat up a Heat Transfer Fluid (HTF) as shown in Figure 1.4. Thermal power is then supplied to the load via the HTF (e.g., when water is used as the HTF) or through a heat exchanger (e.g., when molten salts are used as the HTF). Depending on the design, there can be more than one absorber to control the phase and superheat temperatures. Concentration ratio up to 1000 is common. Experimental central receiver systems typically work in the 600 – 1200 $°C$ range but commercial plants work in the 400 – 600 $°C$ range (Vogel & Kalb, 2010), (Greenhut, 2010), with the operating temperature depending on the HTF properties, size of the heliostat field and receivers, and for commercial plants on the Levelized Cost of Electricity (LCOE).

Figure 1.4 Central Receiver Solar Power Plant, (Abengoa, 2012)

CRSs consist of a heliostat field, receiver, storage reservoir and a power cycle (optional) if electricity is generated. There are several different configurations of the heliostat fields and receivers. One such configuration works on the "beam-down" principle (Rabl, 1976), which uses a hyperbolic curvature mirror at the top of the tower to reflect the concentrated solar radiation down the tower and which allows the absorber to be located at the bottom of the tower. Using a hyperbolic mirror allows further concentration of the radiation and creates a funnel-shaped concentrator. Moreover, locating the absorber at the bottom reduces HTF pressure losses by decreasing pipe lengths and requires a smaller pump since the HTF does not have to be pumped to the top of the tower.

Unlike parabolic dishes, the power section of CRSs use a turbine (typically a Rankine cycle but sometimes a Brayton cycle), which is a very mature technology. Using turbines allows relatively low cost solar-powered electricity generation and significant operation and maintenance experience. For large scale CSP cases (100

MW_e and higher), CRSs have the lowest cost, easiest storage, and easiest hybridization to provide firm power. Compact and optimized heliostat fields decrease land use and in the near future many CSP experts predict CRS systems will be the dominant CSP technology.

CRS and PTC systems can use a significant amount of HTF. Most HTFs commonly used in commercial systems are highly toxic and flammable; in case of spillage, leakage or fire, a significant amount of environmental damage can occur. Currently significant efforts are underway to develop advanced HTFs that are cheaper, non-flammable and non-toxic.

1.2.3. Linear Fresnel Reflectors

Fresnel concentrators have two different variations as shown in Figure 1.5: the Fresnel lens concentrator (left) and linear Fresnel reflectors (LFR) (right). The main characteristic of Fresnel concentrators is collimating or focusing a large aperture using a short focal length. Fresnel lenses are mostly used for final focusing, especially in concentrating PV (CPV) applications. The design of Fresnel Reflectors is different from a parabolic trough in that they use a number of planar (or slightly curved) mirrors located at the same height. These reflectors track the sun on one axis longitudinally, and focus the solar radiation to the absorber tube located above as shown in Figure 1.5.

Figure 1.5 Comparison between Fresnel Lens (1) and Normal Lens (2), (Wikipeadia, 2014) and LFR, (Alstom, 2014)

LFR is still an immature CSP technology. The current plants were developed over the last 15-20 years and pioneered by Australia and Belgium (Solarmundo Project, 2001). Several different absorber tube configurations, HTF selections, and frame structure exist and their combination must be optimized for the optimal design of LFR plants.

Compact Linear Fresnel Reflectors (CLFR) is a new concept in which individual mirrors are not associated with a specific receiver. Multiple towers (with each tower containing the linear absorber) are used and the area coverage is significantly reduced by partially inter-meshing two adjacent single tower arrays (Mills, 2004) as shown in Figure 1.6.

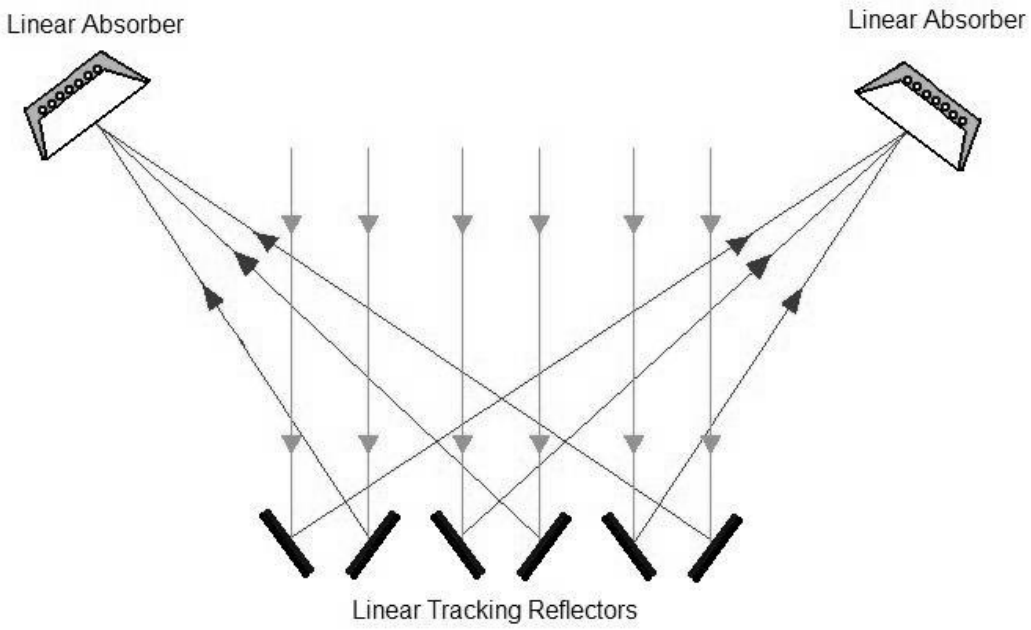

Figure 1.6 CLFR Working Principle, (Wikipedia, 2014)

LFRs have relatively wide range of concentration ratios (25-100) with respect to PTC. For low concentration ratios, they are appropriate for Organic Rankine Cycle (ORC) plants for small scale electricity generation and for direct steam generation (DSG) at low temperatures for industrial use. For higher concentration ratios, LFRs can be used for electricity generation using a conventional Rankine (steam) cycle. LFRs are relatively cheap and easy to assemble, need less maintenance, and therefore they can easily be built in distant places which have high DNI or low land cost.

Since the heat collecting elements for LFRs are stationary and therefore have no moving parts, it provides better sealing and makes using DSG and air as a HTF easier. Water and air are more chemically stable than the oils commonly used as HTFs. Using air or water as a HTF allows 500 $°C$ outlet temperature for high concentration ratio fields, while common oil HTFs are limited to 400 $°C$. Unlike other CSP technologies, LFR can more easily accommodate dual land use such as using the land beneath the collectors for agricultural purposes or locating the

collectors on roofs, which allows sharing land costs with agriculture or very low land costs by using roofs.

1.2.4. Parabolic Trough Collectors

In Parabolic Trough Collectors (PTCs) light is concentrated by long (25 – 150 m) parabolic cross section mirrors to a glass enveloped vacuum absorber tube placed at the focal point of the parabola as shown in Figure 1.7. The absorber tube has a selective absorbent coating that maximizes absorption of solar radiation (high absorbance for short wavelengths) and minimizes near-infrared losses (low emittance for near-infrared region). The glass envelope is used to create a vacuum region between the absorber tube and the glass tube that minimizes convective and conductive losses from the absorber tube to the air. Also the outer glass tube transmits solar radiation but is opaque to the near-infrared radiation predominately emitted by the absorber tube, which further helps to keep heat in the glass annulus. For low temperature systems (below $250\ °C$) an evacuated glass envelop may not be a cost effective solution due to the challenges in maintaining the vacuum over long time periods. The HTF passing through the absorber tube is heated using concentrated solar energy and is then pumped to a heat exchanger where this thermal energy can be transferred to a power block for electricity generation or stored for later use. While most commercial PTCs use a thermal oil as the HTF and are coupled to the load by a heat exchanger, Direct Steam Generation (DSG) systems are under development in which water is used as the HTF in the PTC and this water in the form of steam is sent directly to the load, which eliminates the need for the heat exchanger.

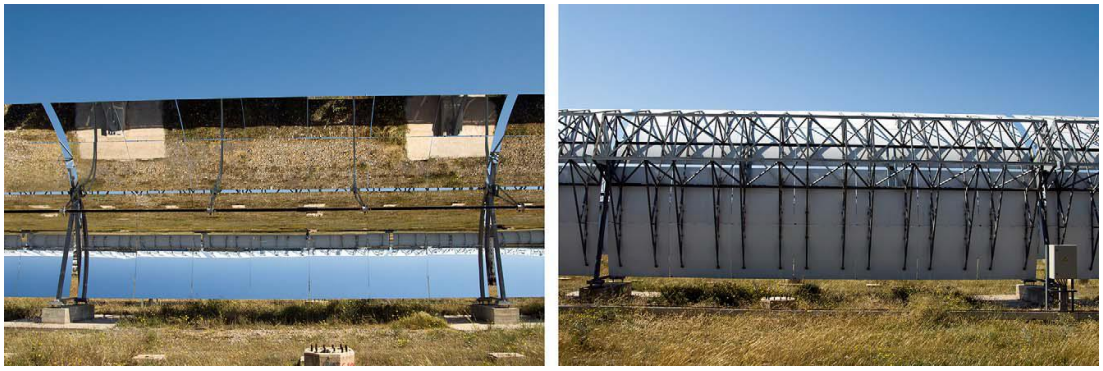

Figure 1.7 Front (left) and Rear (right) Views of EuroTrough Collector (Fernandez-Garcia, Zarza, Valenzuela, & Perez, 2010)

PTCs use single axis tracking and have working temperatures up to 400 – 500 $°C$ through the use of a long series of heat collecting elements; therefore, longer collector modules are manufactured, easing the assembly process. Collectors can be oriented with their axes in the north-south or east-west directions. Ideal tracking about an east-west axis results in a zero angle of incidence at solar noon but as is subject to large end-losses at early and late times in the day, and overall for an annual basis tracking about a north-south axis typically maximizes the collector output.

Solar Electric Generating Systems (SEGS) consist of 9 generations of PTC power plants located in California, USA. Every generation of the SEGS represents an improvement based on the experiences from previous plants in terms of outlet temperature and dispatchability as shown in Table 1.3. SEGS were the highest capacity CSP power plants built (354 MW_e turbine power) until 2013. The first two plants were built in Daggett, CA, a power park of five SEGS power plants (SEGS 3 through7) were built in Kramer Junction, CA, and the last two plants were built in Harper Lake, CA. All the plants were designed, built and sold by Luz International. Due to the extensive operation and maintenance experience with SEGS, the PTC technology is the most mature CSP technology. The design of the plants evolved after each generation. To increase the power output, efficiency and dispatchability of each successive plant, the maximum outlet temperature and collector field area were

increased, the collector type was changed, and the dispatchability method of the solar field was revised.

Table 1.3 Characteristics of SEGS Plants (National Renewable Energy Laboratory)

			Solar Field		
SEGS Plant	**First Year of Operation**	**Net Output (MW_e)**	**Outlet Temperature ($°C$)**	**Area (m^2)**	**Dispatchability Provided by**
I	1985	13.8	307	82,960	3 hours TES
II	1986	30	316	190,338	GF* superheater
III/IV	1987	30	349	230,300	GF boiler
V	1988	30	349	250,500	GF boiler
VI	1989	30	390	188,000	GF boiler
VII	1989	30	390	194,280	GF boiler
VIII	1990	80	390	464,340	GF HTF heater
IX	1991	80	390	483,960	GF HTF heater

*GF: Gas-fired

There are several small scale ORC plants driven using PTCs that utilize different designs, power scales (around 50 kW to 100 MW), operating temperature (50 – 450 $°C$) and HTFs, which affect the behavior of the plant due to two-phase flow and

different thermal characteristics (National Renewable Energy Laboratory, 2010). The economic viability of integrating thermal energy storage (TES) with PTC plants makes PTC systems with TES attractive. There are several PTC power plants with TES. In general adding TES to PTCs increases both dispatchability and initial investment costs, but overall causes a decrease in the levelized cost of electricity (LCOE). On the other hand, common storage media are often dangerous for the environment since they are often toxic and flammable.

1.2.5. Thermal Energy Storage

Solar energy requires high initial investment cost, but has no fuel cost. This trade-off can allow the LCOE to decrease to a preferable level. But the nature of the uncertainty in weather generated power cannot guarantee that the demand can always be met and the inconsistency between demand and supply creates interruptions or over energy input to the grid. To prevent this problem, hybridization with an auxiliary heater is the simplest solution but using fuel to fire the auxiliary heater can increase the LCOE. In order to decrease LCOE, a capacitance can be implemented to the plant which can easily be charged and discharged during the day with changing weather and demand. Since there is not any fuel used and excess energy is not wasted, the LCOE can decrease significantly.

Thermal energy storage (for CSP) is the capacitance which stores excess energy of the HTF using its storage medium through either temperature changes (sensible heat storage) or phase changes (latent heat storage) for later dispatch. There are several types of TES; the most common methods for CSP applications are concrete thermal storage, thermocline, and two-tank thermal energy storage.

Concrete thermal storage has several pipes passing through a concrete block as shown in Figure 1.8 which heats up and stores energy in concrete. It is a simple and relatively cheap solution but inefficient with respect to other technologies. Heat transfer depends on the pipes (configuration and size) but is relatively slow. It is still

in the early stages of development and needs testing for long term thermal fatigue. Low heat transfer rates make concrete thermal storage appropriate only for base load plants.

Thermocline is a term used mostly in oceanography, and is defined by Britannica as an oceanic water layer in which the water temperature decreases rapidly with increasing depth (Brittanica, 2013). As for the CSP point of view, thermocline thermal storage uses a single tank containing a fluid with a thermal gradient running vertically through the tank as shown in Figure 1.8. In this tank, the hotter fluid is at the top due to its low density and the colder fluid at the bottom due to its high density. The separation of different temperatures creates a thermal potential. Using low cost thermal fillers increases the potential more by separating the mediums more, prevents convective mixing and reduces the required amount of the storage medium (Pacheco, Showalter, & Kolb, 2002).

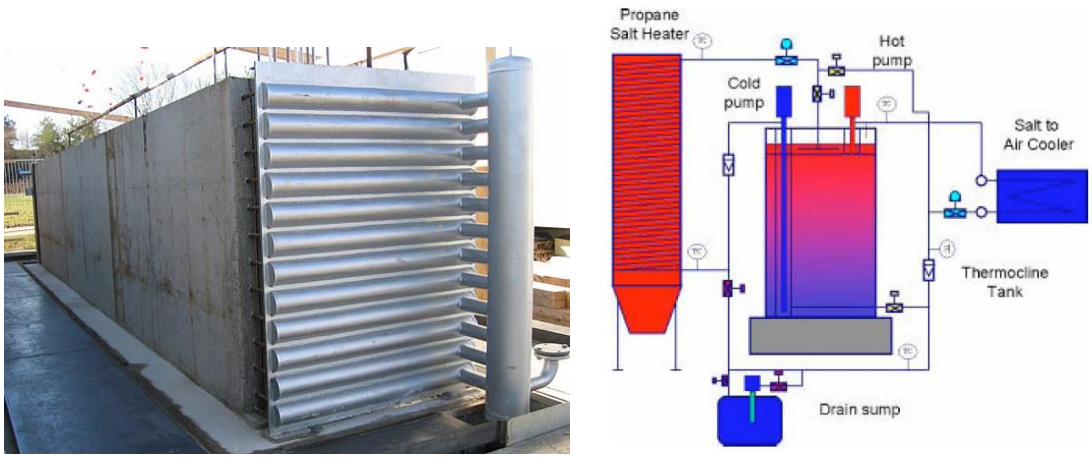

Figure 1.8 Concrete (DLR) and Thermocline (Brosseau, Hlava, & Kelly, 2004) TES

Two-tank thermal energy storage consists of separate hot and cold tanks. For charging the TES, the storage pump pumps the TES HTF from the cold tank through the heat exchanger where it is heated and into the hot tank, and in the process empties the cold tank and fills the hot tank. For discharging, the process works in

reverse. Two-tank TES has been demonstrated in several applications already. One important application of PTC power plant with two-tank TES, by the consortium of the Solar Millennium A.G., ACS Cobra, MAN Ferrostaal, Marquesado Solar SL, is the Andasol 1-3 power plants. Each power plant has a 50 MW turbine and contains a two-tank TES. Each of the tanks has an approximately 36 m diameter and 14 m height, and can hold 28,500 tons of storage medium. When full, the TES can provide 7.5 hours of full-load turbine capacity (Solar Millennium, 2014). The Andasol plants proved that PTC plants with TES can provide base load power for 24 hours. The layout of the plant is shown in Figure 1.9.

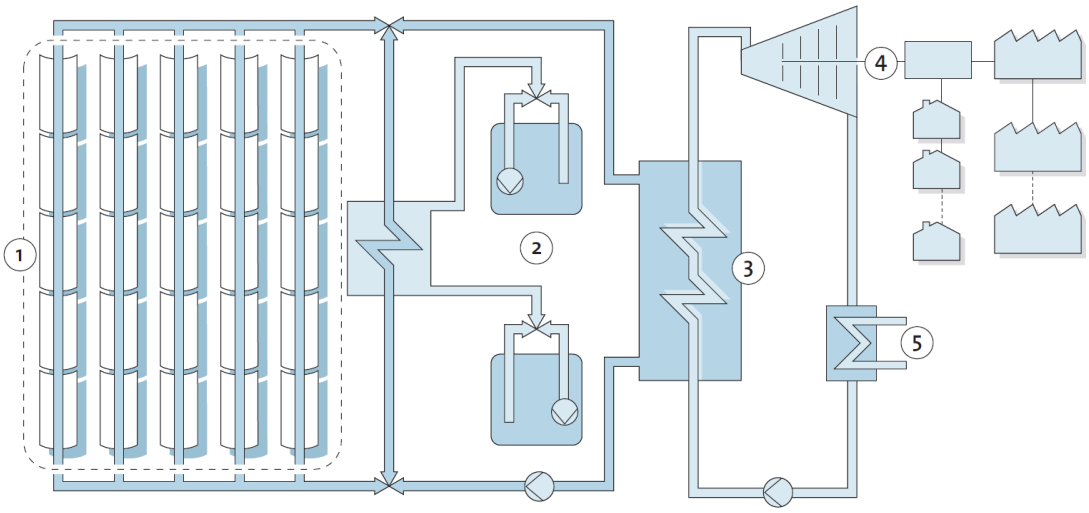

1. Solar Field, 2. Storage, 3. Heat exchanger, 4. Steam turbine and generator, 5. Condenser

Figure 1.9 Andasol Power Plants Layout and Indirect Two-Tank TES (RWE Innogy)

TES can be implemented to a PTC plant in a direct or indirect way. In the direct storage scheme, the HTF passes through the TES and then goes to the power block to transfer its thermal energy. Direct TES is relatively easy to control compared to the indirect scheme. For the indirect storage scheme, the HTF passes through the TES in a separate piping system and the TES is used when the collector field cannot meet the load. A separate piping system allows discharging without using the PTC field at

night or in low DNI cases (defined as conditions for which the PTC field would cool rather than heat the HTF passing through it).

The storage medium is the most important characteristic of two-tank TES. A preferable storage medium should have high thermal capacity, low solidification temperature, and be cheap, non-corrosive, non-toxic and inflammable. Today, efficient PTC plants should work above 400 $°C$, therefore future storage media should be chemically stable above 400 $°C$. Also having the storage medium serve as the PTC HTF improves plant efficiency significantly, reduces initial investment and simplifies the storage system by reducing the number of pumps and heat exchangers required for TES.

1.3. Brief History of PTC

Solar power generation is an ancient technology. By harvesting the sun, there were several applications from domestic water heating to high heat flux weapons in history. This thesis is concentrated on solar thermal energy generation by using PTC technology. The next sections are mainly focused on PTC rather than CSP generally. However, many scientists and engineers in solar sciences are working on other technologies in addition to PTC.

Although the very first application of CPS is a legend[1], the first documented PTC was designed and built by a Swedish engineer named John Ericson. It had a 3.25 m^2 aperture area and drove a 373 W steam engine. In 1883, Ericson improved the system by replacing the polished metal reflectors with flat strips of silvered-glass reflectors with 16.415 m^2 aperture area. As a result of the improvement, Ericson's PTC could produce 0.24 MPa saturated steam to drive a 120 rpm, 0.153 m diameter and 0.2 m single stroke piston (Lovegrove & Stein, 2012).

[1] In ancient times, Archimedes invented a way, using concave mirrors in heliostat principle, to flee Roman warships by burning their sails before invasion initiated in Syracuse, Sicily.

The first PTC plant was built in Maadi, Egypt, by Frank Shuman in 1912 for irrigation of a cotton field next to the Nile River. His plant ran a pump with a capacity of 6000 gallons (22.7 m^3) of water per minute. In August 22, 1913, his plant was tested and it had maximum 40.1% collector efficiency (solar to steam) with 55.5 bhp (41.4 kW) maximum output. Also on the same day, the plant ran five hours continuously with maximum and minimum powers of 55.5 and 46.2 bhp (41.4 and 34.0 kW) respectively (Kryza, 2003).

A mathematician professor Giovanni Francia built the first solar power tower in Sant'llario, near Genoa, Italy in 1968 and it had a capacity of 1 MW with 100 bar and 500 $°C$ superheated steam (Perlin, 2013). He was also a pioneering researcher on Linear Fresnel Reflector concentrators in Italy.

After the 1973 oil crisis, the U.S. began investing heavily in renewable energy sources and as a result of this act and from the CSP point of view, the SEGS plants were built. The SEGS plants are the first large scale CSP application. Nine commercial plants were built in the Mojave Desert (average direct normal insolation, DNI, up to 2, 727 kWh/m^2 year) in California for supplying electricity for peak demand hours to the grid. Several improvements were implemented while plants SEGS-1 to SEGS-9 were sequentially being built. SEGS-1 was built with direct two-tank storage of HTF as shown in Figure 1.10 (110 MWh storage capacities, which is equivalent to 3-hours full-load turbine capacity) and a natural-gas fired super heater. After high DNI hours, the storage discharges and the hot HTF produces steam which passes through the super heater before the turbine. The aim of storage is to allow electricity generation to vary with peak demand to sell the electricity produced with the highest profit. In 1999, the storage was damaged by fire and it was not restored. In SEGS-2 a different approach was selected and a natural-gas fired boiler was integrated into plant as an auxiliary heater. The plant does not have a storage unit and the auxiliary heater heats up the HTF when it is necessary (high demand or low DNI cases). In SEGS-2, steam is superheated only by the HTF and no heater is used. The contribution of the natural-gas fired boiler is limited to 25% of the total effective

annual thermal plant energy input to meet renewable energy legislation (Price, et al., 2002).

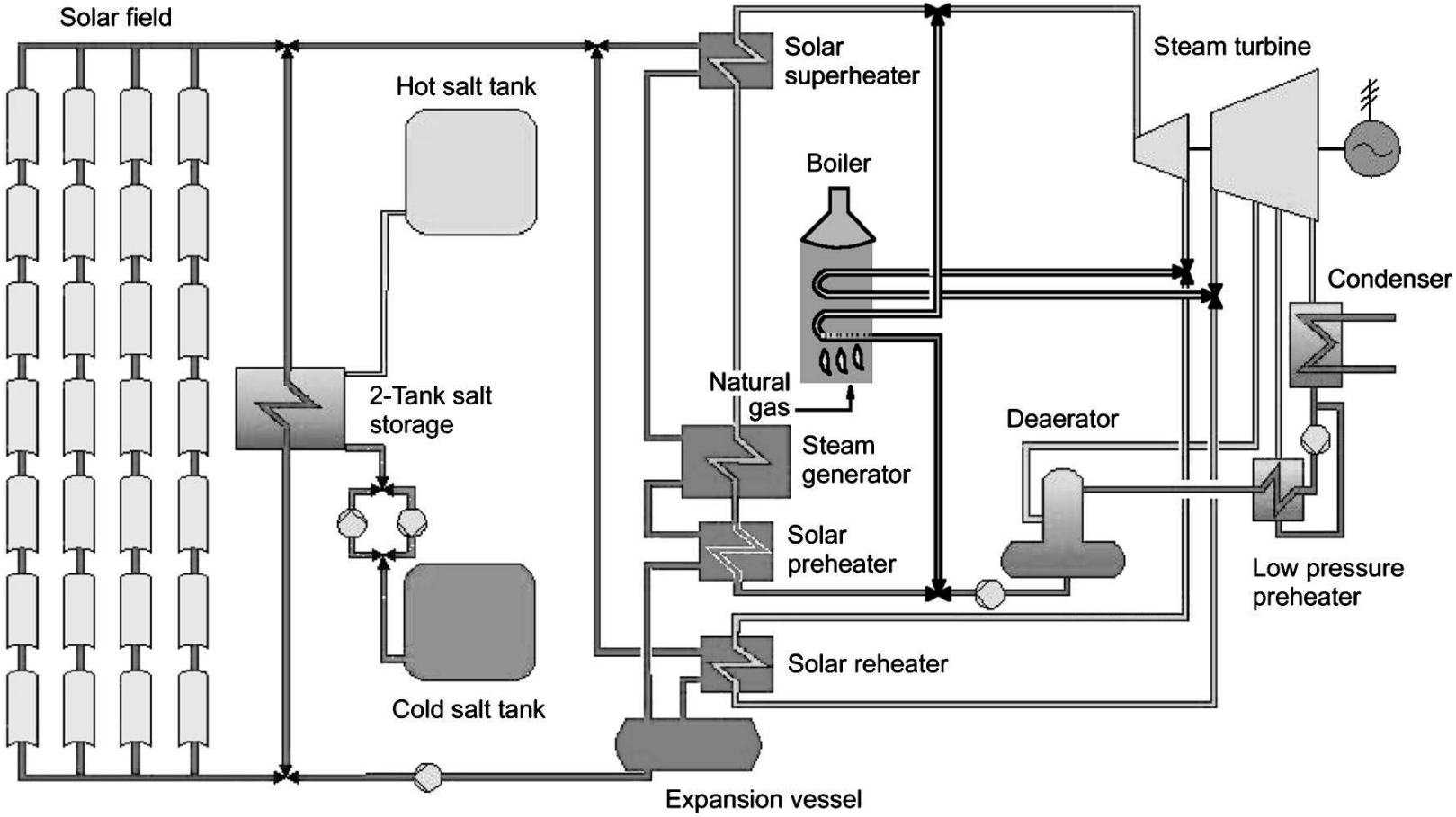

Figure 1.10 Process Flow Schematic of SEGS-1 Power Plant (Herrmann, Geyer, & Kearney, 2003)

Another major improvement achieved in the SEGS plants (specifically done in SEGS-3, 4, 5, 6, and 7, which are the plants located in Kramer Junction) was a six-year project to reduce operation and maintenance (O&M) costs, started in 1993 by Sandia National Laboratories (SunLab) and the Kramer Junction Operating Company. As a result of this project, improvements were achieved in solar energy harvesting units, solar field loop and plant operation strategy. In environmental aspects, improvements were made through the reduction in costs spent on environmental regulations. Overall, a 37% reduction in O&M costs were achieved (Cohen, Kearney, & Kolb, 1999).

While feasibility analyses of the SEGS plants were being conducted, there were some improvements done in Europe. Plataforma Solar de Almeria (PSA) and German Aerospace Center (DLR) co-lead an International Energy Agency (IEA) sponsored program to build experimental CSP plants in Spain. This project was called Small Solar Power System Project/ Distributed Collector System (SSPS/DCS). Nine countries and several solar companies built their components (collector, receiver, TES components and turbine) and tested them in this facility. The project was initiated in 1977 and the research continues today (Fernandez-Garcia, Zarza, Valenzuela, & Perez, 2010).

One of the major PTC applications in Spain is the Andasol 1-2 power plants. They are the first PTC plants in Spain. The importance of Andasol plants is their storage capacity, which demonstrated that in the future CSP can provide base load power for 24 hours. Each plant has 1010 MWh_t two-tank indirect molten salt TES, which allows the plant to run at full-load for 7.5 hours. Charge and discharge temperatures of the TES are 385 and 295 $°C$ respectively. Also each plant has two auxiliary heaters to heat the HTF and prevent solidification of the molten salts (SOLAR MILLENNIUM AG, 2014).

1.4. Literature Review of PTC Design, Development and Optimization

There are several efforts spent on simulation of performance models, benchmarking these simulations with several PTC plants, and optimization of different parameters and locations.

A PTC field consists of rows of PTC modules connected in series, and then these rows are connected in parallel until the desired thermal performance is achieved. A 50 MW_e PTC plant without TES was tested with different solar multiples (SM) (1.03 to 1.55) by increasing the number of rows in parallel. SM is defined as the ratio of the thermal power produced by the solar field ($\dot{Q}_{th\,SF}$) at design point and the thermal power required by the power block at nominal conditions ($\dot{Q}_{th\,PB}$) as shown in Equation 1.1. The effect of different SMs on performance is shown in Figure 1.11. For SM = 1, the output of the PTC at design conditions perfectly matches the thermal powered required by the power block at nominal conditions. But as SM is increased beyond 1, the PTCs produce excess thermal energy at design conditions, and this excess thermal energy must be dumped by defocusing some of the PTC modules (essentially turning these PTCs off) or by using the excess thermal energy to charge TES that can be discharged at a later time to make the plant feasible. Steady-state finite-time difference analyses have been done at the design point and part-load conditions to understand the behavior of the plant. Annual electricity output and LCOE from 1996 to 2000 were presented (Montes, Abanades, Martinez-Val, & Valdes, 2009).

$$SM_{design\ point} = \left.\frac{\dot{Q}_{th\,SF}}{\dot{Q}_{th\,PB}}\right|_{design\ point} \qquad 1.1$$

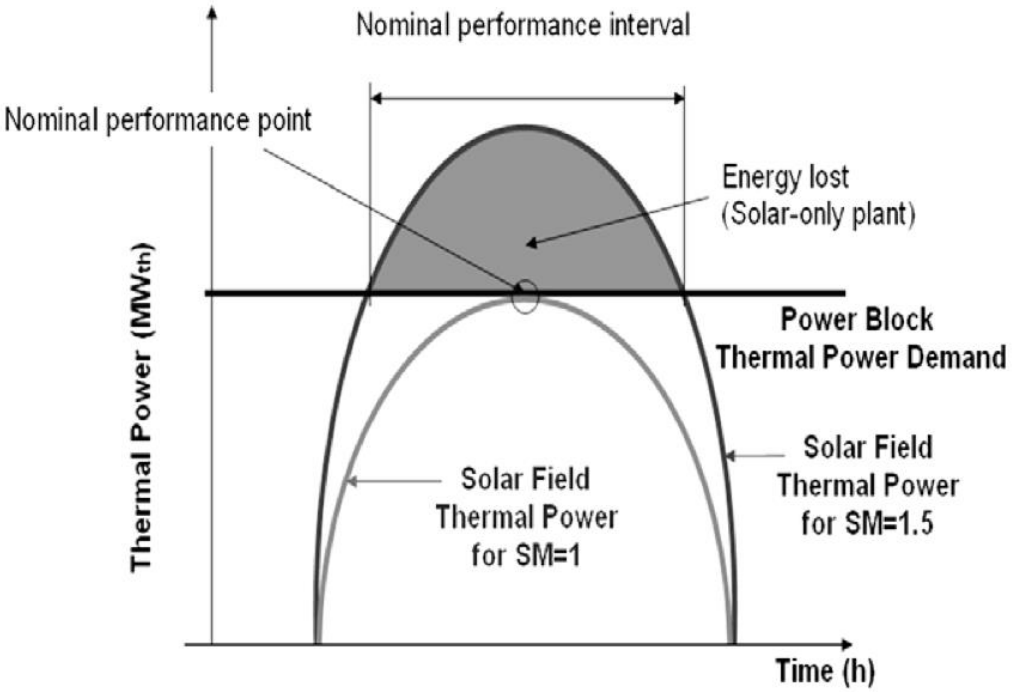

Figure 1.11 Daily Thermal Power Production for Different SM (Montes, Abanades, Martinez-Val, & Valdes, 2009)

On an LCOE basis, the performance model is validated with SEGS 1 plant operational data and then used for parametric studies to compare different capacities (1, 3, 6, 9, 12, and 15 hours TES capacity) of two-tank molten salt TES. Cost estimation is performed and a 50MW_e nominal power generating plant with 12 hours storage capacity gives the lowest LCOE with 128.2 USD/MWh (Herrmann, Geyer, & Kearney, 2003)

Oil (Therminol VP-1), molten salt and Direct Steam Generation (DSG) are tested as the HTF in a 20 MW_e power block for a variety of collector lengths, absorber tube diameters, working temperature and pressure. While DSG is found to be the most efficient solution, its efficiency values are close with respect to the other HTFs (Montes, Abanades, & Martinez-Val, 2010).

A parametric study is performed for Cyprus with different sizes of PTC power plants (25-50-100 MW nominal capacity). This study focuses on operation hours (from 5 to 24 hours per day), resulting in CO_2 footprint saving, economic benefits of tax incentives by using renewables and land use. It shows that PTC plants could be profitable and feasible for the Mediterranean region by using the location and annual average DNI value (2000 kWh/m^2) of Cyprus (Poullikkas, 2009).

A 50 MW_e PTC plant performance model is benchmarked with the Andasol-2 plant's operating data. The model is consistent with actual plant results for the given period (June 26th – August 6th 2010, for 42 days). This model has a very detailed control algorithm that is adaptive depending on part load and hours, has different operation modes, and is sensitive to transient inputs of weather by using a small time span of 10 minutes (Garcia, Alvarez, & Blanco, 2011).

Since the first data collected for solar power plants was from the SEGS plants, modeling of SEGS plants is an important step for PTC plant simulation, feasibility analysis and plant optimization. Several theses have been completed about modeling of solar thermal power plants, but unlike traditional coal or natural gas plants, the importance of solar energy power plant modeling of part-load behavior is emphasized. Unlike solar power plant modeling, fossil fuel plants are built in a modular manner and part-load behavior only depends on demand. Depending on the demand, part-load behavior is mostly achieved by closing one or several boilers of the plant. However, for solar power plants part-load conditions depend not only on demand and but also the weather input and they must be evaluated simultaneously in order to have a proper plant model.

Lippke simulated SEGS-6 plant (30 MW_e) operating at full-load and two part-loads conditions. Lippke compared these results with the SOLERGY model (Stoddard, Faas, Chiang, & Dirks, 1987), optimized the plant by changing the solar field output temperature and reducing solar field pressure loss on selected clear summer, fall and winter days. In conclusion, changing the plant's maximum HTF temperature on

colder days (fall and winter) allows 1.5% more electricity to be generated annually (Lippke, 1995).

Later, a model of the SEGS-6 plant was used by Stuetzle for generating a linearized model to build an automatic controller algorithm. Due to differences between solar power plants and traditional fossil fuel power plants, controlling solar power plants is harder, since solar input needs to be considered in addition to demand. The model with the controller is tested for four different days in 1998 and results are compared with actual plant operating data (Stuetzle, 2002).

Forristall built a linearized model for the heat transfer in the absorber assembly of the PTC, which is termed the Heat Collecting Element (HCE), (Forristall, 2003). Later, this model was used in PTC field models that are more sensitive to more transients. McMahan used this model for design and optimization of an ORC solar-thermal power plant model with storage. McMahan shows that low-cost, small size PTC plants can be an attractive solution to generate electricity and TES allows tailoring the generated electricity based on demand (Mcmahan, 2006). Patnode investigated performance degradation of PTC plants over several years due to loss of vacuum in the HCE annulus, optimized plant performance by changing the mass flow of the HTF, and tested different condensers to show changes in the cooling water required (Patnode, 2006). Usta simulated SEGS-6 using Antalya weather data for one year (Usta, 2010). Uçkun modeled a DSG PTC plant and did a parametric study of collector inlet temperature, working pressure and different DNI values (Uçkun, 2013).

1.5. Thesis Overview

The main weakness of solar power is its inability to generate energy at night or on cloudy days. Fossil fuels backups are the most common solution for intermittency of the plant. Storing energy allows improved dispatchability and reduces fossil fuel

needs of the plant. But still there are missing points in the literature about optimum control algorithms of the power plants with thermal energy storage.

1.5.1. Thesis Objectives

The main purpose of this study is developing a model of a PTC plant with TES for Turkey and optimizing the plant design for different investment costs, load profiles and locations. The main objectives of the thesis are listed as follows:

- Optimizing PTC string length by average DNI of the location,
- Optimizing PTC and TES sizes in a solar plant to maximize solar fraction,
- Investigating the change in solar fraction for different optimized PTC and TES sizes,
- Investigating optimized cost ratio of PTC to TES in different sizes of plants.
- Adapting plant to different locations and investigating how the solar fraction, PTC field and TES vary with location,
- Investigating the change in solar fraction for different load profiles.

1.5.2. Thesis Scope

The present work focuses on PTC field with two-tank TES system. This work can also be adapted to other CSP technologies and different kinds of TES systems when their specific characteristics are included in the model.

Since the main purpose of this study is simulating PTC with TES in different configurations, various complexities are simplified in plant size and component size while still conserving the main characteristics of the PTC, TES and pumps.

1.5.3. Thesis Organization

In Chapter 1, first, a brief history and general information about CSP and TES technologies have been provided. PTC and TES technologies have been identified and discussed after this introduction.

The remainder of the thesis is organized as follows. In Chapter 2, components in the plant model are explained and references are provided for readers interested in learning about the details of these models.

In Chapter 3, the model described in Chapter 2 is simulated under different conditions, the plant is optimized for maximizing solar fraction, and simulation results are presented.

In Chapter 4, the work in the thesis is summarized, the benefits and weaknesses of the model are discussed, and possible ways for improving the methodology are given. Suggestions for prospected researchers are also advised in this Chapter.

CHAPTER 2

2. MODEL DESCRIPTION

The model of the system is composed of the following sub-models: Parabolic Trough Collector (PTC), Heat Transfer Fluid (HTF) pump, HTF tank, load model, Thermal Energy Storage (TES) sub-model which contains hot and cold TES tanks and TES pumps for charging and discharging processes. The control algorithm (valves, pumps and TES control) is built in MatLab and connected to TRNSYS (TRaNsient SYStem Simulation). TRNSYS is the major simulation program used for the simulations, and the system model is constructed by linking existing TRNSYS library items for various components with novel control algorithms developed in MatLab. At each time step during the simulations, TRNSYS calls MatLab and iteratively solves the set of equations based on the valve control due to the operating state of the plant, inputs and outputs. Each of these sub-models is described in detail in the following sections.

2.1. Collector Model

The Collector Model consists of a solar geometry calculation model, which calculates the Direct Normal Insolation (DNI) and angle of incidence from Typical

Meteorological Data (TMY2) input, and PTC model, which heats HTF using data transferred from solar resources model.

2.1.1. Solar Geometry Calculation

In order to estimate the performance of a solar collector, the solar energy input needs to be estimated accurately. Insolation on the collector and the angle between the sun and the collector surface must be calculated. In this part, calculation of solar angles and resulting solar energy input on the collector's Heat Collecting Element (HCE) is explained. To calculate the position of the sun relative to the collector, the location, time of day, day of year, and orientation of the collector are required, which are described using the definitions and sign conventions explained below, with the definitions being taken almost directly from (Duffie & Beckman, 2006) for solar calculations:

Latitude (φ), the angular location north or south of the equator, north positive; $-90° \leq \varphi \leq 90°$

Declination (δ), the angular position of the sun at solar noon with respect to the plane of equator, north positive; $-23.45° \leq \delta \leq 23.45°$

The declination angle is represented in Figure 2.1:

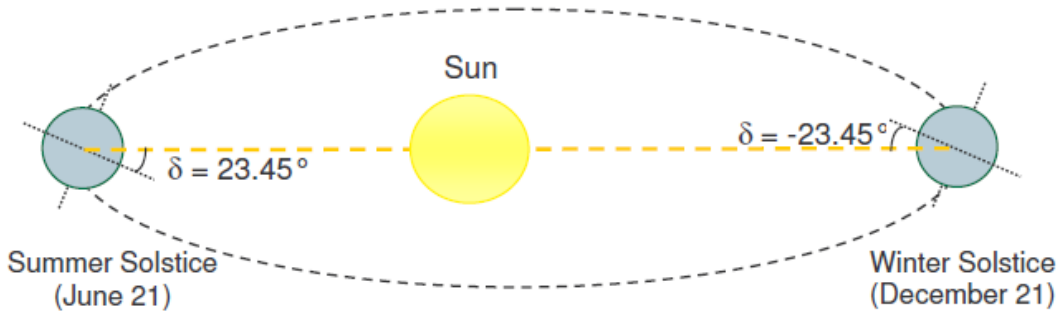

Figure 2.1 Declination Angle due to Earth's Tilt (Patnode, 2006)

Declination angle can be found using Equation 2.1 (Iqbal, 1983):

$$\delta = 23.45 \sin\left(360 \frac{284 + n}{365}\right) \quad 2.1$$

where n is the day of the year, with $n = 1$ for January 1 and $n = 365$ for December 31.

Slope (β), the angle between the plane of the surface in question and the horizontal, $\beta > 90°$ for downward-facing component; $0° \leq \beta \leq 180°$.

Surface Azimuth angle (γ), the deviation of the projection on a horizontal plane of the normal to the surface from the local meridian, with zero being due south, east of due south negative, and west of due south positive; $-180° \leq \gamma \leq 180°$.

Hour angle (ω), the angular displacement of the sun east or west of the local meridian due to rotation of the Earth on its axis at $15°$ per hour, morning is negative, solar noon is zero, and afternoon is positive; $-180° \leq \omega \leq 180°$

Angle of incidence (θ), the angle between the beam radiation on a surface and the normal to that surface; $0° \leq \theta \leq 180°$

Figure 2.2 illustrates the angle of incidence between beam radiation and collector normal on a PTC.

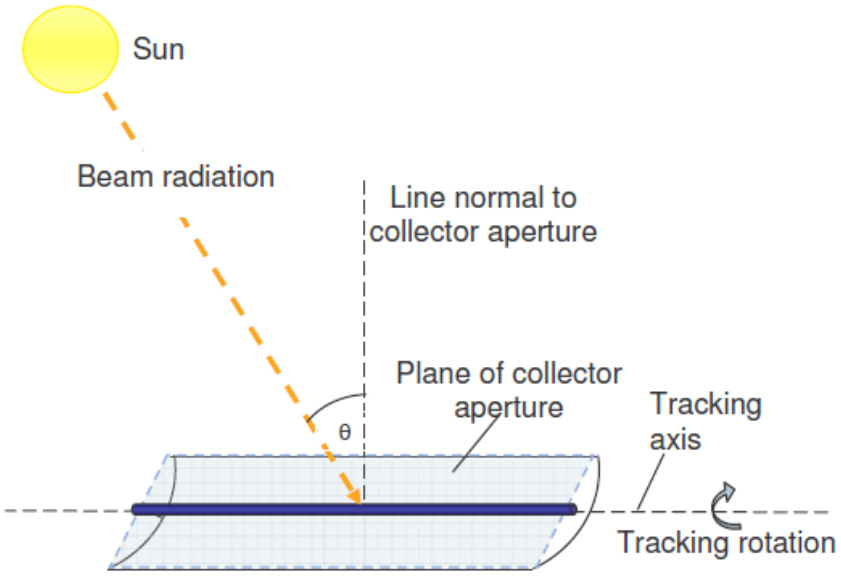

Figure 2.2 Angle of Incidence on a PTC (Patnode, 2006)

Zenith angle (θ_z), the angle between the vertical and the line to the sun, that is, the angle of incidence of beam radiation on a horizontal surface; $0° \leq \theta_z \leq 180°$

Solar altitude angle ($\boldsymbol{\alpha_z}$), the angle between horizontal surface and the line to sun, that is, the angle of incidence of beam radiation on a horizontal surface; $0° \leq \alpha_z \leq 180°$

The difference between zenith angle and angle of incidence is shown in Figure 2.3**.**

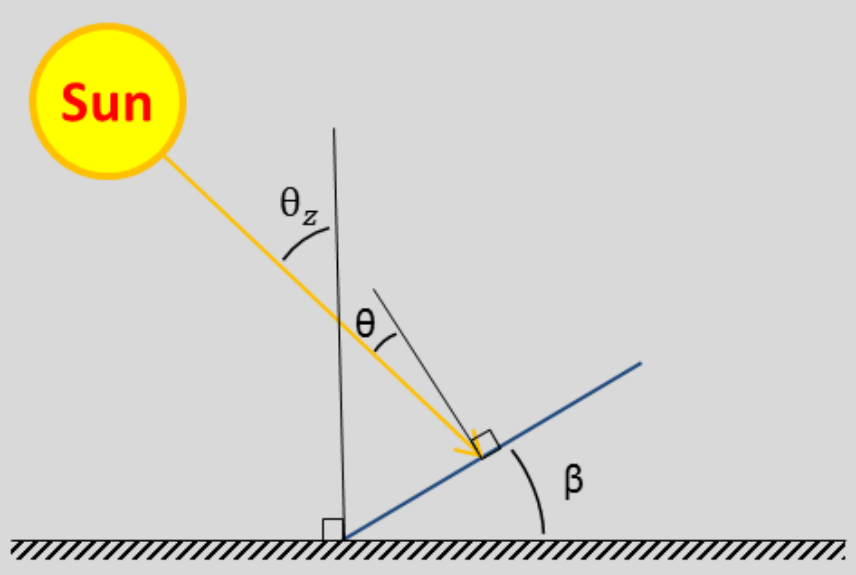

Figure 2.3 Angle of Incidence, Zenith Angle and Slope (Uçkun, 2013)

Solar azimuth angle (γ_s), the angular displacement from south of the projection of beam radiation on the horizontal plane, similar to surface azimuth angle with zero being due south, east of due south negative, and west of due south positive; $-180° \leq \gamma_s \leq 180°$,

In the Figure 2.4, some of the various solar and surface angles illustrated by Uçkun (Uçkun, 2013) are presented.

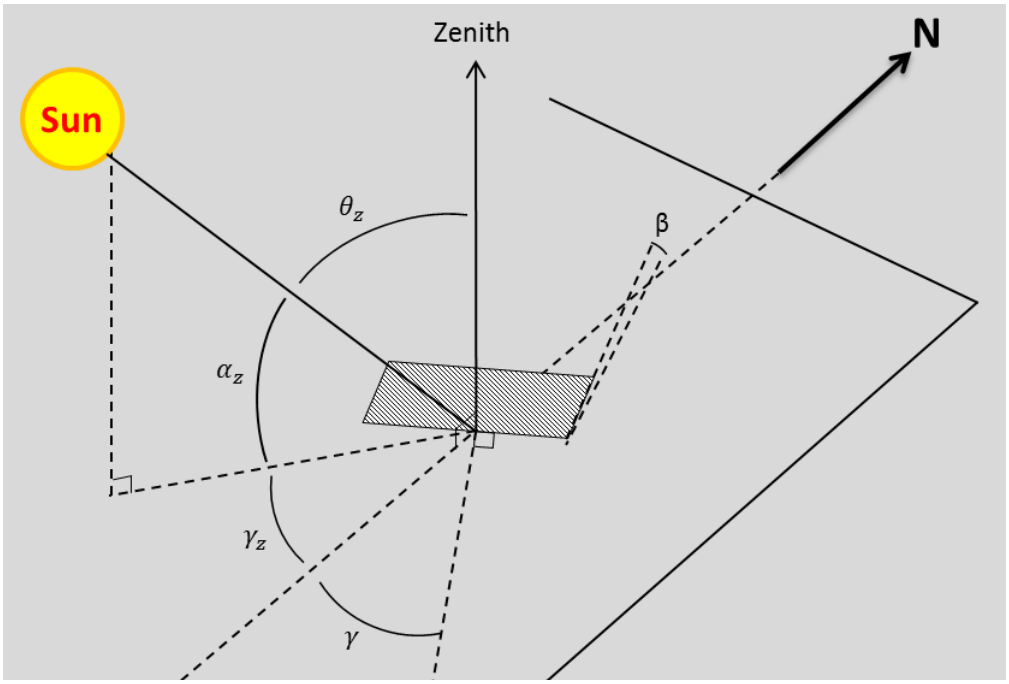

Figure 2.4 Representation of Slope (β), Zenith Angle (θ_z), Solar Altitude Angle (α_z), Surface Azimuth Angle (γ) and Solar Azimuth Angle (γ_s) (Uçkun, 2013)

There are two generalized formulas for angle of incidence:

$$\cos\theta = \sin\delta\sin\phi\cos\beta - \sin\delta\cos\phi\sin\beta\cos\gamma + \cos\delta\cos\phi\cos\beta\cos\omega + \cos\delta\sin\phi\sin\beta\cos\gamma\cos\omega + \cos\delta\sin\beta\sin\gamma\sin\omega \quad 2.2$$

Or

$$\cos\theta = \cos\theta_z\cos\beta + \sin\theta_z\sin\beta\cos(\gamma_s - \gamma) \quad 2.3$$

Equations 2.2 and 2.3 are the generalized formulas, and there are special cases for which angle of incidence calculation can be simplified as below.

- For horizontal surface (zero slope ($\beta = 0°$)), using Equation (2.3) angle of incidence is equal to the zenith angle.

- For 2-axis collectors, in ideal tracking conditions, collectors always point toward the sun during the day time, and therefore $\theta = 0°$.
- For 1-axis tracking there are two main configurations depending on the azimuth angle of the collector. For east-west axis tracking system (azimuth angle of collector is $0°$ or $180°$) the angle of incidence is given in Equation 2.4:

$$\cos\theta = (1 - \cos^2\delta \sin^2\omega)^{1/2} \qquad 2.4$$

- For north-south axis tracking system (azimuth angle of the collector is $-90°$ or $90°$), the angle of incidence is given in Equation 2.5:

$$\cos\theta = (\cos^2\theta_z + \cos^2\delta \sin^2\omega)^{1/2} \qquad 2.5$$

In this thesis, analyses have been done for a north-south axis tracking system, and in the next section the thermal model of a nodal PTC model oriented in north-south direction is explained.

2.1.2. PTC model

In this model a collector string is divided into a series of fixed length nodes and each node is modeled in a fixed time step defined by the user. TRNSYS uses the Runge-Kutta method for solving for the time rate of change of temperature and the model requires a predefined Runge-Kutta step.

The PTC model assumes that an incompressible HTF passes through a constant volume HCE. Thermodynamic properties (density, enthalpy and internal energy) are dependent only on temperature due to the incompressible fluid assumption. The properties of the HTF and the fluid for the Thermal Energy Storage (TES) are modeled as a quadratic function of temperature.

For a single node, the time rate form of an energy balance can be written for a constant volume where changes in potential and kinetic energies are assumed negligible,

$$\frac{d(mu)}{dt} = \dot{E}_{in} - \dot{E}_{out} \tag{2.6}$$

where m is the mass, u is the internal energy inside the constant volume and $\dot{E}_{in}$ and $\dot{E}_{out}$ are the rate of input and output energy, respectively.

For the case of a PTC, the energy input rates are the enthalpy flow rates of the inlet fluid ($\dot{H}_{fluid,in}$) and absorbed insolation ($\dot{Q}_{absorbed}$) and energy output rates are the thermal losses from the HCE ($\dot{Q}_{losses}$) and enthalpy flow rate of the outlet fluid ($\dot{H}_{fluid,out}$). After defining heat transfer rates of inputs and losses, Equation 2.6 becomes,

$$\frac{d(mu)}{dt} = \dot{Q}_{absorbed} + \dot{H}_{fluid,in} - \dot{Q}_{losses} - \dot{H}_{fluid,out} \tag{2.7}$$

Applying the product rule to the time rate of change of the total internal energy of the constant volume, the left-hand side of the Equation 2.7 can be rewritten as,

$$\frac{d(mu)}{dt} = m\frac{du}{dt} + u\frac{dm}{dt} \tag{2.8}$$

For solving for the time rate of change of temperature, the time rate of change of the mass should also be defined as a time rate of change of temperature by applying the chain rule as in Equation 2.9,

$$\frac{dm}{dt} = \frac{dm}{dT}\frac{dT}{dt} \tag{2.9}$$

Since the system is constant volume, the changes in its total volume are assumed negligible,

$$\frac{dm}{dT} = \frac{d(\rho V)}{dT} = V\frac{d\rho}{dT} \quad 2.10$$

As noted above, this model assumes that the properties of incompressible fluids in the model can be described as quadratic functions of temperature, and using this assumption the density of the HTF can be described as Equation 2.11,

$$\rho(T) = r_0 + r_1 T + r_2 T^2 \quad 2.11$$

Substituting Equation 2.11 to Equation 2.10 gives,

$$\frac{dm}{dt} = \frac{d(\rho V)}{dT} = V\frac{d\rho}{dT} = V\ (r_1 + 2r_2 T) \quad 2.12$$

The following approach is used to model the du/dt term in Equation (2.8),

$$\frac{du}{dt} = u_1 + 2u_2 T \quad 2.13$$

Substituting equations 2.12 and 2.13 into 2.8 gives;

$$\frac{d(mu)}{dt} = (uVr_1 + 2uVr_2 T)\frac{dT}{dt} + (mu_1 + 2mu_2 T)\frac{dT}{dt} \quad 2.14$$

Rearranging:

$$\frac{d(mu)}{dt} = (uVr_1 + 2uVr_2 T + mu_1 + 2mu_2 T)\frac{dT}{dt} \quad 2.15$$

After arranging the left-hand side of Equation 2.6 to yield Equation 2.15, each parameter on the right-hand side of Equation 2.6 can be described as follows.

The absorbed heat transfer rate is derived from (Patnode, 2006) as shown in Equation 2.16,

$$\dot{Q}_{absorbed} = A\ DNI \cos\theta\ \ IAM\ f_{endloss}\ f_{dust}\ f_{bellows}\ \tau_{glass}\ \alpha_{coating}\ f_{misc} \qquad 2.16$$

Here A is the collector aperture area of one node, IAM is an incidence angle modifier and the remaining parameters are collector specific constants described below.

IAM is defined by Dudley in Equation 2.17, based on experimental data (Dudley, et al., 1994) where b_0, b_1, and b_2 are constants and the angle of incidence is defined in degrees.

$$IAM = b_0 + b_1 \frac{\theta}{\cos\theta} + b_2 \frac{\theta^2}{\cos\theta} \qquad 2.17$$

The collector model accounts for end losses (f_{endloss}) using an equation given by Lippke (Lippke, 1995). End losses quantify the fraction of the absorber tube that is illuminated by the reflected solar radiation and $0 \leq f_{endloss} \leq 1$.

$$f_{endloss} = 1 - \frac{F \tan\theta}{L_{coll}} \qquad 2.18$$

In Equation 2.18, F is the focal length of the collector and L_{coll} is the length of one row of collectors.

The remaining parameters in Equation 2.16 all scale between 0 and 1 and are described below:

f_{dust} : a factor which accounts for dust on the glass annulus (1=no dust)

$f_{bellows}$: a factor which accounts for the shading of the mirror by the collector bellows (1=no shading)

τ_{glass} : the transmittance of the receiver glass to solar radiation (1=perfect transmission)

$\alpha_{coating}$: the absorptance of the coating on the absorber tube

(1= all insolation absorbed)

f_{misc} : a factor which accounts for miscellaneous losses from the collection system (1=no miscellaneous losses).

The enthalpy flow rate of the inlet fluid to the constant volume is defined as,

$$\dot{H}_{fluid,in} = \dot{m}_{in} h_{in} \quad 2.19$$

Similarly, the enthalpy flow rate of the exit fluid from the constant volume is defined as,

$$\dot{H}_{fluid,out} = \dot{m}_{out} h \quad 2.20$$

The time rate of change of the mass flow rate is described as Equation 2.21 but for a small temperature change this transient term can be neglected,

$$\dot{m}_{out} = \dot{m}_{in} - \frac{dm}{dt} \quad 2.21$$

The inlet and outlet mass flow rates are assumed equal,

$$\dot{m} = \dot{m}_{out} = \dot{m}_{in} \quad 2.22$$

The thermal loss from the HCE to the environment is a complicated heat transfer problem. It is a mixture of conduction, convection and radiation (with varying emission due to temperature and reflection due to the existence of insolation). Forristall (Forristall, 2003) developed a linearized approach that accounts for the dominant heat transfer mechanisms as described in Equation 2.23;

$$U' = a_0 + a_1 T + a_2 T^2 + a_3 T^3 + DNI(a_4 + a_5 T^2) \quad (2.23)$$

where U' is the heat loss coefficient from the HCE to the environment per unit length of collector. Equation 2.23 is developed for a single ambient temperature at 25 °C. In order to modify the equation for varying ambient temperatures (T) in °C, the following equation can be used.

$$U_L = \frac{U'}{W_{aper}(T - 25)} \quad (2.24)$$

By dividing the test value by the aperture width (W_{aper}) and temperature difference, the new parameter U_L is defined, which is the heat transfer coefficient between the device and the surrounding air per unit collector aperture area. After defining U_L, the heat loss from the HTF to the ambient can be modeled as a simple convection phenomenon as follows:

$$\dot{Q}_{losses} = U_L A(T - T_{ambient}) \quad (2.25)$$

After defining and expanding all the parameters in the Equation 2.6, the energy balance can be rewritten as,

$$\begin{aligned}&(uVr_1 + 2uVr_2 T + mu_1 + 2mu_2 T)\frac{dT}{dt} \\ &= A\ DNI \cos\theta\ \ IAM\ f_{endloss}\ f_{dust}\ f_{bellows}\ \tau_{glass}\ \alpha_{coating}\ f_{misc}\ +\ \dot{m}h_{in} \\ &-\ U_L A(T - T_{ambient}) -\ \dot{m}h\end{aligned} \quad (2.26)$$

Rearranging Equation 2.26 for solving for the time rate of temperature change:

$$\frac{dT}{dt} = \frac{A\ DNI \cos\theta\ \ IAM\ f_{endloss}\ f_{dust}\ f_{bellows}\ \tau_{glass}\ \alpha_{coating}\ f_{misc}}{[uV(r_1 + 2r_2T) + m(u_1 + 2u_2T)]} + \frac{\dot{m}(h_{in} - h)}{[uV(r_1 + 2r_2T) + m(u_1 + 2u_2T)]} - \frac{U_L A(T - T_{ambient})}{[uV(r_1 + 2r_2T) + m(u_1 + 2u_2T)]} \quad 2.27$$

TRNSYS solves this equation numerically using a second order Runge-Kutta method for each time step for all nodes.

2.2. Pump Model

There are three pumps (one HTF pump (see Figure 2.9) and two identical pumps for charging and discharging (see Figure 2.6) inside TES model) used in the model, two of which are identical to simplify the model. One is the main pump used for HTF circulation and the other two are identical pumps used for TES medium circulation. For discharging and charging of TES, in actual systems, one pump is used. In contrast, herein the discharge and charging operations are modelled separately since the piping is not included. Therefore two identical pumps, which do not work at the same time, are used to model the system.

The pump model requires a control signal in which zero means the pump is off and one means the pump is at maximum power. The fluids passing through the pumps are assumed to be incompressible and a constant specific heat approach is used for heat transfer calculations. A predefined parameter is used for the fraction of energy lost to environment added to the fluid as heat input as in actual cases. Inlet and exit fluid mass flow rates are assumed equal for simplicity. The unknowns in the model are consumed power and outlet temperature of the fluid.

The outlet temperature of the pump is calculated as follows:

$$T_{out} = T_{in} + \frac{P_{pump}\, f_{par}}{\dot{m}_{pump}\, c_p} \qquad 2.28$$

T_{out} and T_{in} are outlet and inlet temperatures respectively, $\dot{m}_{pump}$ and P_{pump} are the mass flow rate and power consumption of pump, and f_{par} is the fraction of lost energy converted to fluid thermal energy.

Inlet and outlet mass flow rates are simply related with the control signal γ_{sgn} as defined in Equation 2.29;

$$\dot{m}_{pump} = \gamma_{sgn}\dot{m}_{max} \qquad 2.29$$

where $\gamma_{sgn} = 0$ if the pump is off and the consumed power can be defined as a polynomial as;

$$P_{pump}(\gamma) = P_{max}\left[c_0 + c_1\gamma_{sgn} + c_2\gamma_{sgn} + \cdots + c_i\gamma_i\right] if\ \dot{m}_{pump} > 0 \qquad 2.30$$

When the pump is off $\left(if\ \gamma_{sgn} = 0\ then\ P_{pump} = 0, T_o = T_{in}\ and\ \dot{m}_{pump} = 0\right)$, the inlet temperature is assumed equal to the outlet temperature even though there is no flow. This is an action done for keeping continuity of information transfer in the simulation time steps. Also power consumption is assumed as zero, which is the same as actual cases when transient effects are neglected.

Depending on the pump characteristics, the power polynomial Equation 2.30 can be a constant or a higher order polynomial. In this thesis, the pump is modeled as a quadratic function which has zero power when it is off $\left[P_{pump}(0) = 0\right]$ and the consumed power is the maximum power when the signal is one $\left[dP_{pump}/d\gamma_{sgn}\,\big|_{\gamma_{sgn}=1} = 0\ and\ P_{pump}(1) = P_{max}\right]$. So, the power consumption of the pump is characterized as;

$$P_{pump} = P_{max}(2\gamma_{sgn} - \gamma_{sgn}^2) \quad 2.31$$

2.3. Variable Volume Tank

The tank model used is lumped with a variable volume of constant cross sectional area without any heater inside. When the tank is at its minimum level (may not be defined as completely empty), the exit flow is zero and inlet and exit flows are not equal. When the tank is at its maximum level (may not be defined as completely full), the exit flow is equal to the inlet flow. In each time step, the tank model calculates mass and energy balances in order to find the tank temperature, volume ratio (which scales between zero and one, and corresponds to minimum and maximum levels, respectively) and exit flow rate. Outlet temperature is assumed equal to tank temperature since the tank is assumed as lumped. This model uses a constant specific heat approach for calculating the temperature change. Mass and energy balances are defined as follows;

$$\frac{dm_{tank}}{dt} = \dot{m}_{in} - \dot{m}_{out} \quad 2.32$$

And assuming an incompressible liquid $(c_p = c_v)$

$$c_p \frac{d(m_{tank}T)}{dt} = \dot{m}_{in}c_pT_{in} - \dot{m}_{out}c_pT - (UA)_t(T - T_{amb}) \quad 2.33$$

where c_p is the constant pressure specific heat of the fluid, m_{tank} is the mass inside the tank, and $\dot{m}_{in}\ and\ \dot{m}_{out}$ are the mass flow rates in and out. T is the temperature of tank and of the outlet, and T_i and T_{amb} are the inlet fluid and environment temperatures respectively. $(UA)_t$ is the overall heat transfer coefficient for heat loss from tank to environment. For the sake of simplicity, dividing by c_p gives;

$$\frac{d(m_{tank}T)}{dt} = \dot{m}_{in}T_{in} - \dot{m}_{out}T - \frac{(UA)_t(T - T_{amb})}{c_p} \quad 2.34$$

Applying the product rule to the derivative,

$$m_{tank}\frac{dT}{dt} + T\frac{dm_{tank}}{dt} = \dot{m}_{in}T_{in} - \dot{m}_{out}T - \frac{(UA)_t(T - T_{amb})}{c_p} \quad 2.35$$

Substituting Equation 2.32, to Equation 2.35 gives,

$$m_{tank}\frac{dT}{dt} + T(\dot{m}_{in} - \dot{m}_{out}) = \dot{m}_{in}T_{in} - \dot{m}_{out}T - \frac{(UA)_t(T - T_{amb})}{c_p} \quad 2.36$$

Cancelling common terms on both sides and rearranging gives;

$$m_{tank}\frac{dT}{dt} = \dot{m}_{in}(T_{in} - T) - \frac{(UA)_t(T - T_{amb})}{c_p} \quad 2.37$$

For each time step $(t + \Delta t)$ and by assuming a constant inlet temperature, mass flow rate and time rate of temperature change for the tank, the temperature and mass inside the tank can be defined as;

$$m_{tank_{(t+\Delta t)}}\frac{dT}{dt} = \dot{m}_{in}\left(T_{in} - T_{(t+\Delta t)}\right) - \frac{(UA)_t(T_{(t+\Delta t)} - T_{amb})}{c_p} \quad 2.38$$

Applying backward finite difference formula to the differential temperature term, Equation 2.38 becomes;

$$m_{tank_{(t+\Delta t)}}\frac{T_{(t+\Delta t)} - T_t}{\Delta t} = \dot{m}_{in}\left(T_{in} - T_{(t+\Delta t)}\right) - \frac{(UA)_t(T_{(t+\Delta t)} - T_{amb})}{c_p} \quad 2.39$$

Rearranging,

$$\left(\frac{m_{tank_{(t+\Delta t)}}}{\Delta t}+\dot{m}_{in}+\frac{(UA)_t}{c_p}\right)T_{(t+\Delta t)}=\dot{m}_{in}T_{in}+\frac{m_{tank_{(t+\Delta t)}}}{\Delta t}\,T_{(t)}+\frac{(UA)_t}{c_p}\,T_{amb} \quad 2.40$$

The mass of the material inside the tank for final time step can be defined as follows;

$$m_{tank_{(t+\Delta t)}}=m_{tank_{(t)}}+(\dot{m}_{in}-\dot{m}_{out})\Delta t \quad 2.41$$

Dividing Equation 2.41 by the time step (Δt) gives,

$$\frac{m_{tank_{(t+\Delta t)}}}{\Delta t}=\frac{m_{tank_{(t)}}}{\Delta t}+(\dot{m}_{in}-\dot{m}_{out}) \quad 2.42$$

and the final temperature is,

$$T_{(t+\Delta t)}=\frac{\dot{m}_{in}}{C}T_{in}+\frac{\left[\frac{m_{tank_{(t)}}}{\Delta t}+(\dot{m}_{in}-\dot{m}_{out})\right]}{C}T_{(t)}+\frac{\frac{(UA)_t}{c_p}}{C}\,T_{amb} \quad 2.43$$

where C is a constant multiplier of final temperature in Equation 2.40 which is

$$C=\frac{m_{tank_{(t)}}}{\Delta t}+2\dot{m}_{in}-\dot{m}_{out}+\frac{(UA)_t}{c_p} \quad 2.44$$

2.4. Heat Exchanger Model

The Heat Exchanger (HEX) model used is for a counter flow HEX with constant effectiveness. Fouling of the HEX is not included in the model. Likewise to using identical pumps in the model, two identical HEXs are used for charging and discharging operations. The HEX model is covered in Incropera et al. (Incropera, DeWitt, Bergman, & Lavine, 2007). Definitions for the HEX calculation are explained below. Heat capacity rates are defined as follows:

$$C_c = \dot{m}_c c_{p,c} \tag{2.45}$$

$$C_h = \dot{m}_h c_{p,h} \tag{2.46}$$

where subscript c and h are refer to cold and hot sides respectively. For calculating the effectiveness of the HEX (ε),

$$C_{max} = \max(C_c\ ,\ C_h) \tag{2.47}$$

$$C_{min} = \min(C_c\ ,\ C_h) \tag{2.48}$$

where C_{max} and C_{min} refer to maximum and minimum heat capacity rates, and the effectiveness is,

$$\varepsilon = \frac{1 - \exp\left(-\frac{UA}{C_{min}}\left(1 + \frac{C_{min}}{C_{max}}\right)\right)}{1 - \left(\frac{C_{min}}{C_{max}}\right)\exp\left(-\frac{UA}{C_{min}}\left(1 - \frac{C_{min}}{C_{max}}\right)\right)} \tag{2.49}$$

The outlet temperatures of each exit are calculated based on the heat transfer rate

$$\dot{Q} = \varepsilon C_{min}(T_{h,in} - T_{c,in}) \tag{2.50}$$

and the outlet temperatures are:

$$T_{h,out} = T_{h,in} - \frac{\dot{Q}}{C_h} \tag{2.51}$$

$$T_{c,out} = T_{c,in} + \frac{\dot{Q}}{C_c} \tag{2.52}$$

2.5. Weather Model

The simulation program (TRNSYS) used in the thesis provides various location specific meteorological data from locations all over the world in several formats. In the model, Typical Meteorological Data (TMY2) format is used for simulation. In this thesis, TMY2 data of Konya and Muğla are used, which are provided by TRNSYS. Weekly simulations have been done from the 195th day (July 14th) to the end of the 201st day (July 21st). The model uses ambient temperature and DNI provided from the TMY2 data. Sample data of Muğla and Konya are shown in Figure 2.5. Average DNI for Muğla and Konya are 1226.1 (340.58) and 1035.2 (287.56) $kJ/(hr\ m^2)$ (W/m^2) (15.6% less than Muğla) respectively and average ambient temperatures are 25.7 and 22.9 $°C$ respectively.

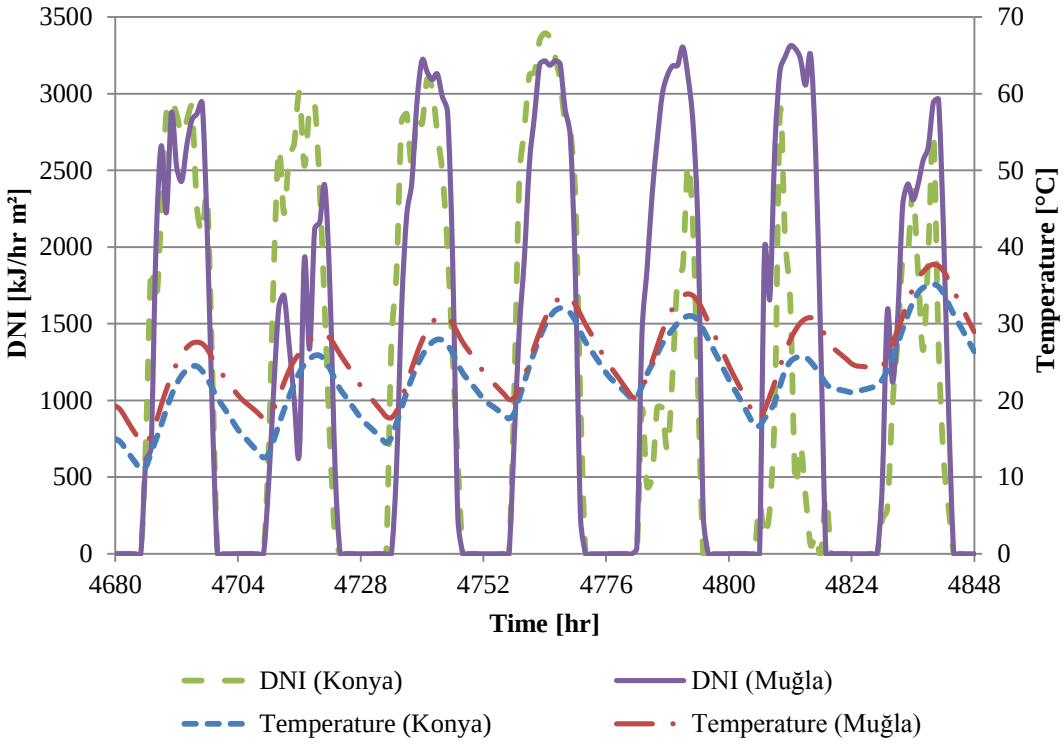

Figure 2.5 Weekly DNI and Temperature versus Time Data for Muğla and Konya (July 14th - 21st)

TMY data are an hourly data set of solar radiation and other meteorological elements over a year. TMY data sets are constructed by analyzing approximately 30 years of measured meteorological data for a specific location, and then for each month choosing the year that is “most typical” based on statistical measures. Therefore a TMY data set may consist of January data from 1998, February data from 2005, etc. When compared to average data which tend to model all days in a series as being very similar, TMY data more accurately model daily fluctuations in meteorological conditions, such as having sunny days followed by cloudy days, etc. The main intention of creating a TMY data set is for their use in computer simulations for solar energy applications; especially solar plants and building systems. As mentioned in the TMY2 manual (Marion & Urban, 1995), TMY data are not a good indicator for one or five year’s prediction. Rather, they represent average conditions over a long period, such as 30 years. Since it uses typical rather than extreme meteorological conditions, worst-case analyses should not be simulated using TMY data sets. TMY2 and TMY3 are newer data sets with more detailed information included and longer time-spans used for generating the data sets with respect to TMY data sets. From a solar energy point of view and relative to TMY data sets, TMY2 data account for recent climate changes and more accurate values of solar radiation for several reasons stated below (Marion & Urban, User's Manual for TMY2s, 1995).

- Better model for estimating values,
- More measured data, some of which are DNI,
- Improved instrument calibrations methods,
- Rigorous procedures for assessing quality of data.

2.6. TES Model

The model of the two-tank molten salt TES system is a combination of models for several units explained in the previous sections and a controller model which is built in MatLab. The model includes two tanks (hot and cold tanks), two pumps and two HEXs. To simplify the model, charging and discharging processes are modeled using

different but identical components, but in reality these processes use a single common component rather than two identical components. Specifically, in the model two pumps and two HEXs have the same predefined parameters as shown in Figure 2.6. The TES model in TRNSYS is shown schematically in Figure A.1 in the design conditions for the TES are presented in Appendix B.

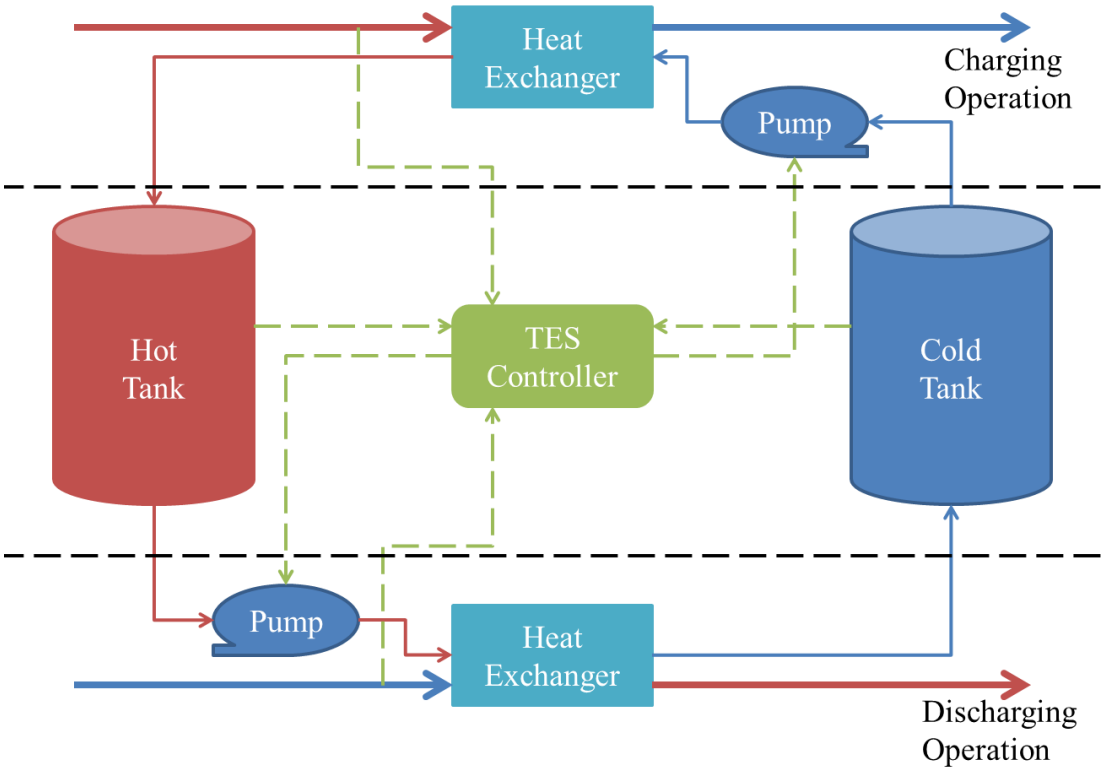

Figure 2.6 Schematic Representation of TES Model (Blue and red lines refer to cold and hot lines respectively, solid lines indicate mass flows, with a thick line for HTF flow and a thin line for storage medium flow, green dashed lines are information signals and all of them are connected to/from controller.)

Horizontal black dashed lines emphasize regions of charging and discharging operation in Figure 2.6. Depending on the direction of information signals, the information can either be controller inputs or outputs. For the TES model, controller outputs only go to the pumps as a pump control signal. The control code is written in MatLab and presented in Appendix C.2.

The modeled storage medium is a eutectic mixture of molten salts. For charging the TES, the storage medium flows from the cold tank to the hot tank by passing through the pump and the charging HEX where the storage medium is heated. Similarly, except in reverse, for discharging the TES, the storage medium flows from the hot tank to the cold tank by passing through the pump and the discharging HEX where the storage medium gives up its heat. The flow chart of TES controller is shown in Figure 2.7.

In each time step, the mass flow rates, the HTF's inlet temperature, the level of the tanks and temperature data are sent to the TES controller. Then, the controller calculates the required mass flow rate of storage medium that should be pumped. Finally, after comparing this rate with pump parameters, the controller evaluates the pump controller signal.

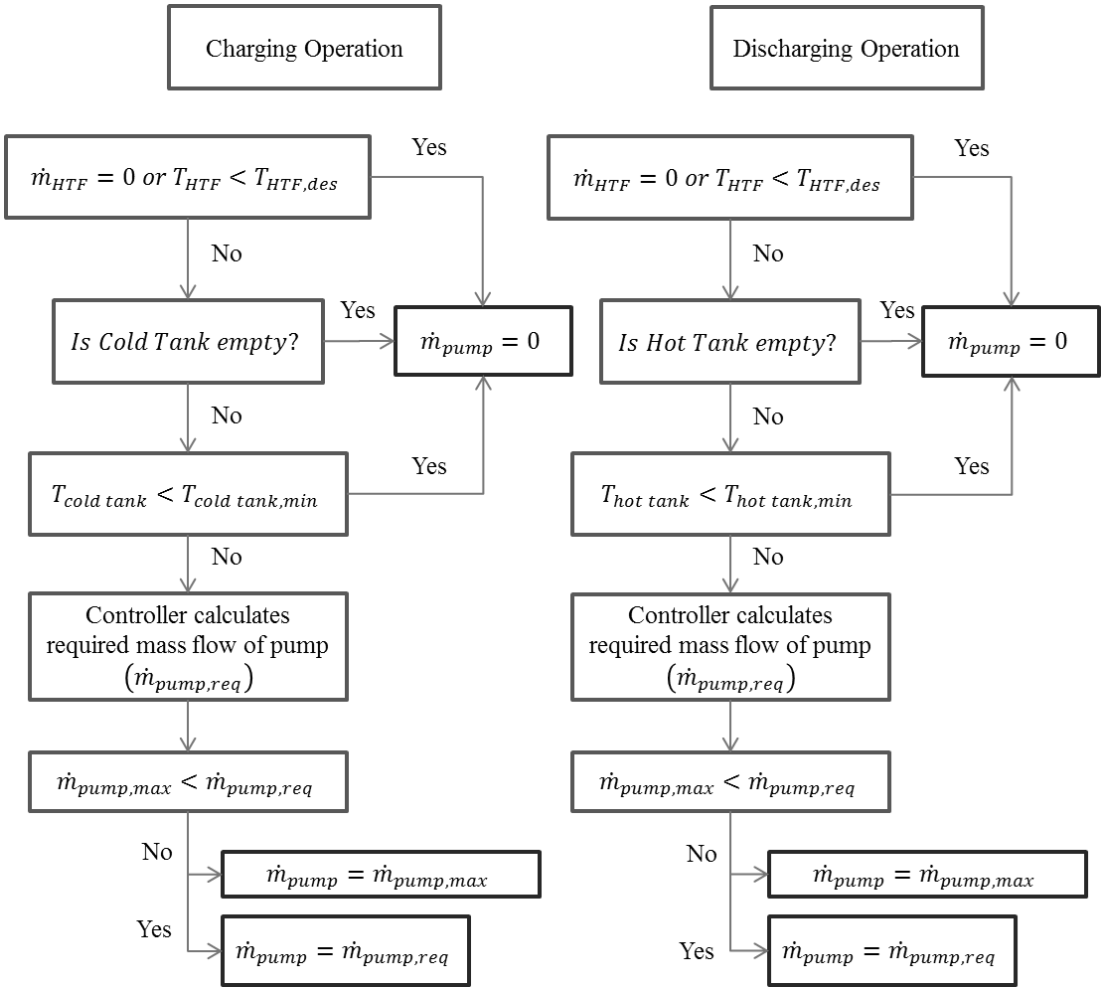

Figure 2.7 Flow Chart of TES Controller

For the charging operation, the controller does not allow pumping if either of the following criteria are not met:

- if there is not any HTF flow or the temperature of the HTF entering the hot tank is lower than the required temperature,
- if the cold tank (input reservoir of pump) is empty
- if the cold tank is colder than the required tank temperature

In this thesis, storage tank models do not have auxiliary heaters; therefore in case of empty cooled cold storage tank, charging is not possible. But this occurs in 3-4 weeks depending on the ambient temperature. Since weekly simulations have been

done, this case is not encountered none of the simulations. It is advised that model should be improved by replacing storage tanks with auxiliary heaters in future work section (Section 4.3.).

After all conditions are good for pumping, the controller calculates the amount of required storage medium $(\dot{m}_{pump,req})$ and compares with maximum allowable pump mass flow rate $(\dot{m}_{pump,max})$ then sends pump signal to pump.

For discharging operation, the only difference is pump reservoir. In this case, the controller checks the hot tank as input reservoir instead of the cold tank.

In charging and discharging operations, the amount of fluid pumped is calculated by following equations.

The rate of heat transfer for the HEX can be calculated by using the logarithmic mean temperature difference as (Incropera, DeWitt, Bergman, & Lavine, 2007),

$$\dot{q} = UA\Delta T_{lm} \qquad 2.53$$

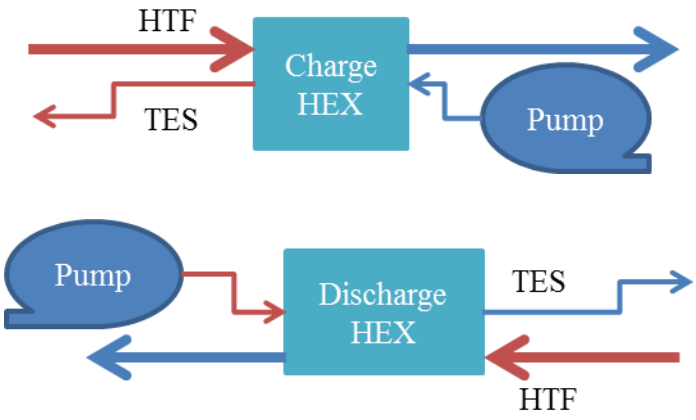

Figure 2.8 Charging (Top) and Discharging (Bottom) Operations Inside TES (Thick lines are HTF and thin lines are storage medium, blue and red lines refer to cold and hot lines respectively)

Recalling the charging (top) and discharging (bottom) systems in TES in Figure 2.8, and log mean temperature can be expressed for a counter flow HEX as,

$$\Delta T_{lm} = \frac{\Delta T_1 - \Delta T_2}{\ln \frac{\Delta T_1}{\Delta T_2}} = \frac{\left(T_{HTF,in} - T_{TES,out}\right) - \left(T_{HTF,out} - T_{TES,in}\right)}{\ln \frac{T_{HTF,in} - T_{TES,out}}{T_{HTF,out} - T_{TES,in}}} \quad 2.54$$

Heat transfer from/to the HTF is,

$$\dot{q}_{HTF} = \dot{m}_{HTF}\, c_{p,HTF} \left(T_{HTF,in} - T_{HTF,out}\right) \quad 2.55$$

Since heat transfer Equation 2.53 and Equation 2.55 are equal and the only unknown is $T_{HTF,out}$, by solving Equation 2.53 and Equation 2.55 simultaneously $T_{HTF,out}$ can be calculated. For a faster calculation and to obtain only physically meaningful results, $T_{HTF,out}$ value is bounded between $T_{HTF,in}$ and $T_{TES,in}$ since counter-flow HEX is used.

After $T_{HTF,out}$ is calculated, $\dot{m}_{TES}$ can be calculated as follows,

$$\dot{m}_{TES} = \frac{\dot{m}_{HTF}\, c_{p,HTF} \left(T_{HTF,in} - T_{HTF,out}\right)}{c_{p,TES} \left(T_{TES,out} - T_{TES,in}\right)} \quad 2.56$$

2.7. Plant Model

The plant model consists of an HTF tank, an HTF pump (main pump), a PTC collector field, a TES system and a load model, six diverter valves and six mixing valves as shown in the Figure 2.9. It is shown in Figure A.2 and input file of the model in TRNSYS is written in Appendix D.

In Figure 2.9the red lines are hot HTF and blue lines are cold HTF, which are at lower than required load temperature. Dashed lines are bypass lines which direct

inlet fluid to HTF tank. Diverter valves and HTF pump is controlled by a plant controller in MatLab and code for plant controller is given in Appendix C.1.

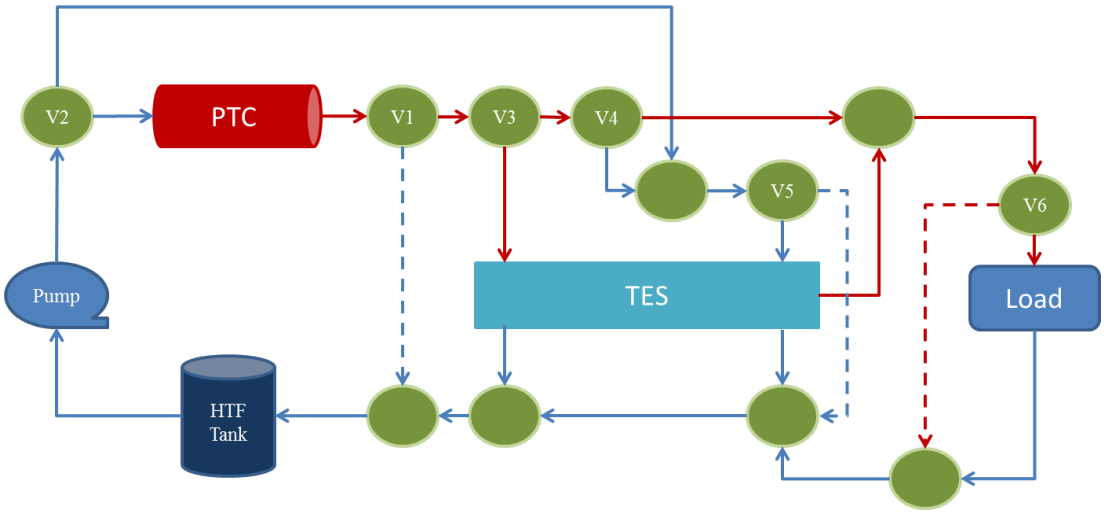

Figure 2.9 Plant Layout (Blue Lines are Cold HTF, Red Lines are Hot HTF and Dashed Lines are Bypass Lines; Green Circles are Valves, where diverters are the circles with text inside. From V1 to V6, the valves are: Main Bypass Valve, PTC – TES Valve, Charging Valve, Discharging Valve, Discharging Bypass Valve and Load Bypass Valve, respectively)

Unlike the common plant models, this model does not have predefined system operation modes. Rather, the system modes are defined at the valve and pump levels and various modes can be generated at the system level. The controller collects weather data and plant states (TES tanks' fluid volume and temperature, PTC output fluid temperature and mass flow rate and demand) then controls the valves and pump in the model. Each valve has a specific task and depending on the valves' states, the pump signal is calculated at the end of the algorithm. The control scheme of the valves and pump are explained below.

2.7.1. Main Bypass Valve (V1):

A flow diagram of the main bypass valve is shown in Figure 2.10. This valve works in two modes; either it directs the HTF to the TES system or bypasses by directing the HTF back to the PTC field via the HTF Tank.

This valve is controlled based on the outlet temperature and mass flow rate of the PTC field, and the state of the TES. If the TES is empty, in order for the fluid to pass from the valve to the TES, the PTC outlet temperature and mass flow rate must sustain the load. Otherwise, the valve directs the fluid to the HTF tank (bypasses the TES). If the TES is not empty, the outlet temperature and mass flow rate of the PTC field are determined and fed to the TES controller. According to the result of the HEX calculation in the TES model, if the temperature is sufficient to sustain the load, the fluid is directed to the TES system.

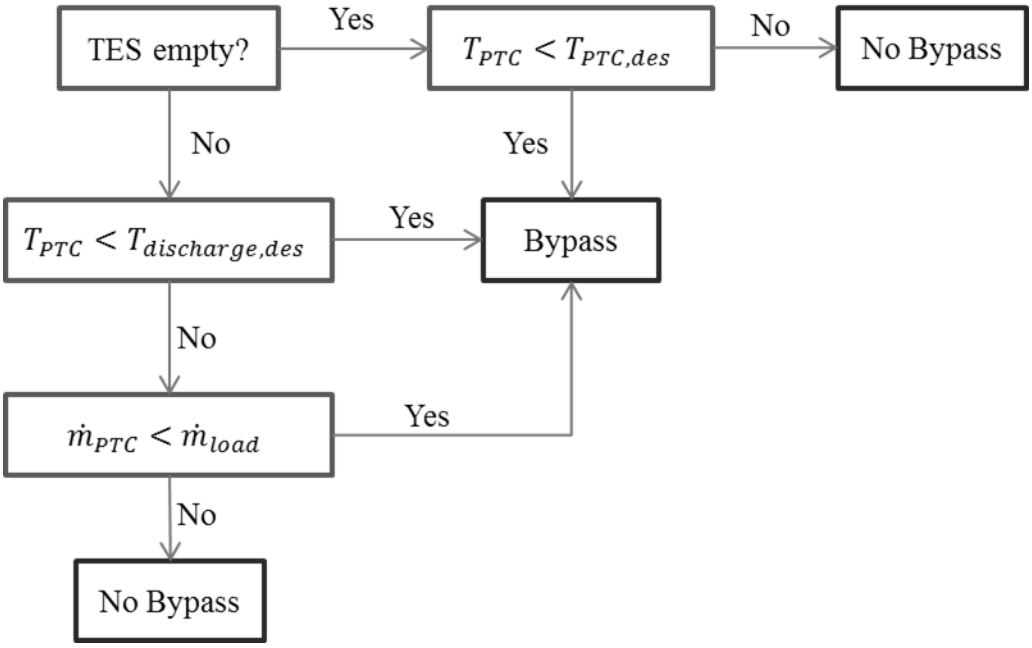

Figure 2.10 Flow Diagram of Bypass Valve

2.7.2. PTC – TES Valve (V2)

This valve checks the day or night condition (by checking DNI), TES states, and bypass valve state as explained above. Note that day and night refer to the presence (day) or lack (night) of DNI resources here, and not to the presence or lack of daylight (DNI + diffuse solar resources). Since only DNI solar resources can be used by a PTC, in terms of PTCs a day with no DNI is equivalent to night. The model also classifies the condition under which the PTCs are completely shaded due to row shadowing as night.

Unlike the main bypass valve, the PTC-TES valve can divert fluid partially to the TES and PTC at the same time. At night time this valve directs all fluid to the TES. During the daytime, the controller checks the bypass mode first to determine whether the HTF is being warmed up or if hot HTF can be obtained from the outlet of the PTC. If fluid bypasses valve 1 (Bypass valve on = No), the fluid is diverted to the PTC for warming up. In the case of empty TES or the hot TES tank is too cold, flow passes from the PTC directly to the load and the TES is charged later. When PTC warmup is necessary and TES can be discharged at the same time, the mass flow required for the load passes from the TES and amount of fluid required for warming up passes from the PTC. When the pump is at its maximum flow rate, the mass flow rate required for the load is directed to the PTC and the rest of the fluid is diverted to TES. This case occurred in peak demand analyses when DNI dropped from a high value (cloudy summer noon). The flow diagram of PTC – TES valve is shown in Figure 2.11.

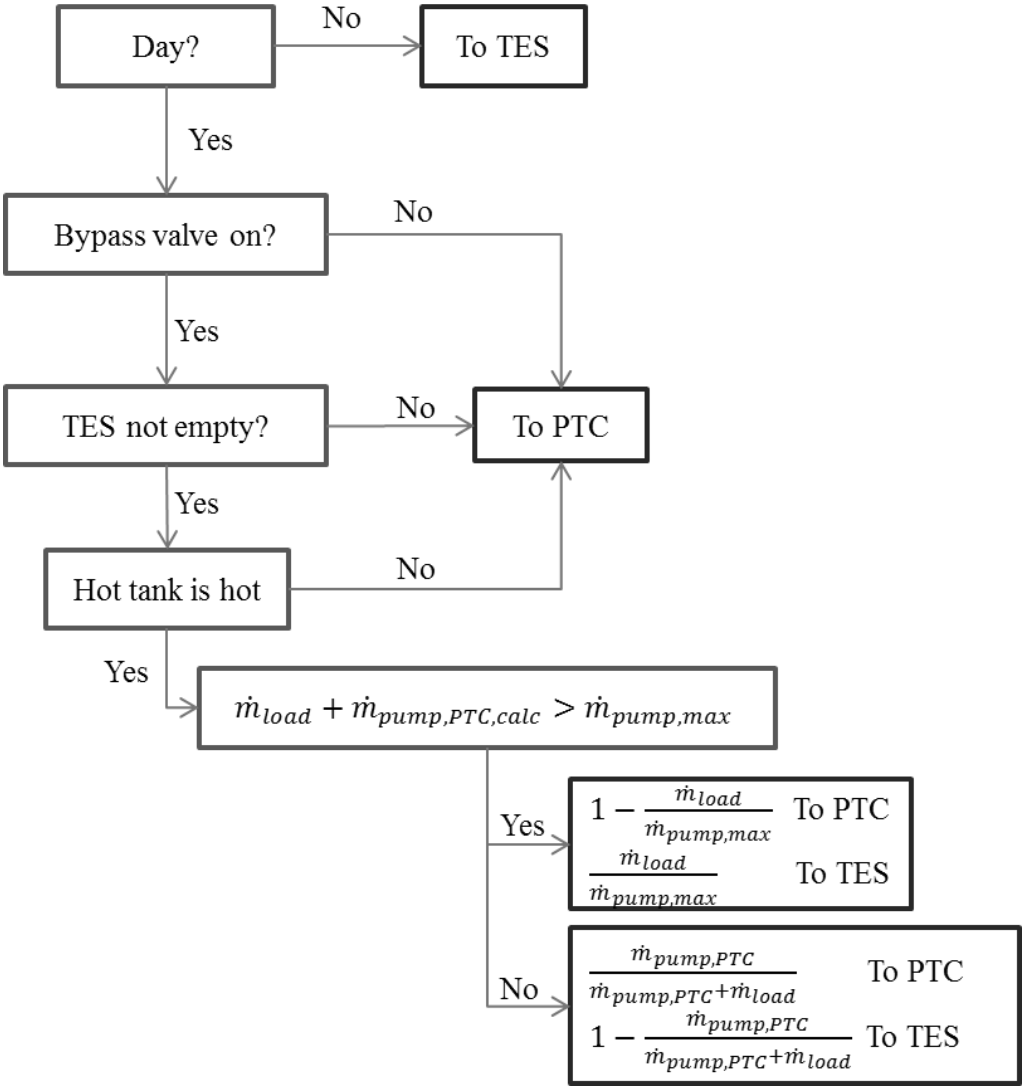

Figure 2.11 Flow Diagram of PTC – TES Valve

2.7.3. Charging Valve (V3)

The charging valve checks the mass flow rate of the load and PTC outlet. When the outlet mass flow rate of the PTC exceeds the load, the charging valve diverts the excess fluid to the TES for charging. Charging does not occur when the TES is full

or the temperature of the PTC outlet is not high enough for charging the TES. The flow diagram of charging valve is presented in Figure 2.12.

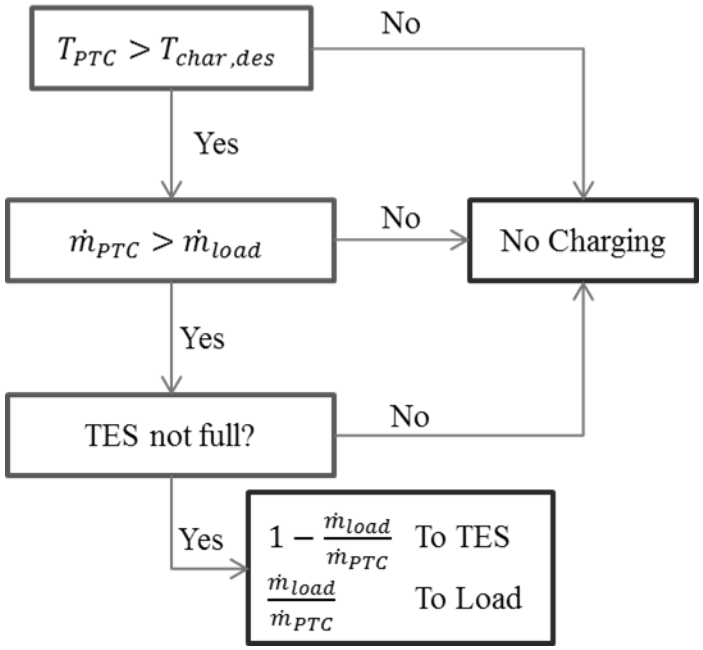

Figure 2.12 Flow Diagram of Charging Valve

2.7.4. Discharging Valve (V4)

The discharging valve checks the states of the TES, the outlet temperature and mass flow rate of the PTC and the required load temperature. This valve works in an on-off mode like the main bypass valve, and it diverts fluid completely to the TES for discharging or to the load for dispatching. The controller for the discharge valve checks the TES level; if it is empty, the valve does not divert to the TES. If the TES is not empty and the temperature of the PTC outlet is sufficiently hot for discharging, the valve controls the inlet mass flow rate and load temperature. At the last step, the controller checks the hot tank temperature; if it is too cold the valve does not allow discharging. When all conditions are satisfied, the discharge valve directs all the

fluid to discharging the TES. In Figure 2.13, the flow diagram of the discharging valve is shown.

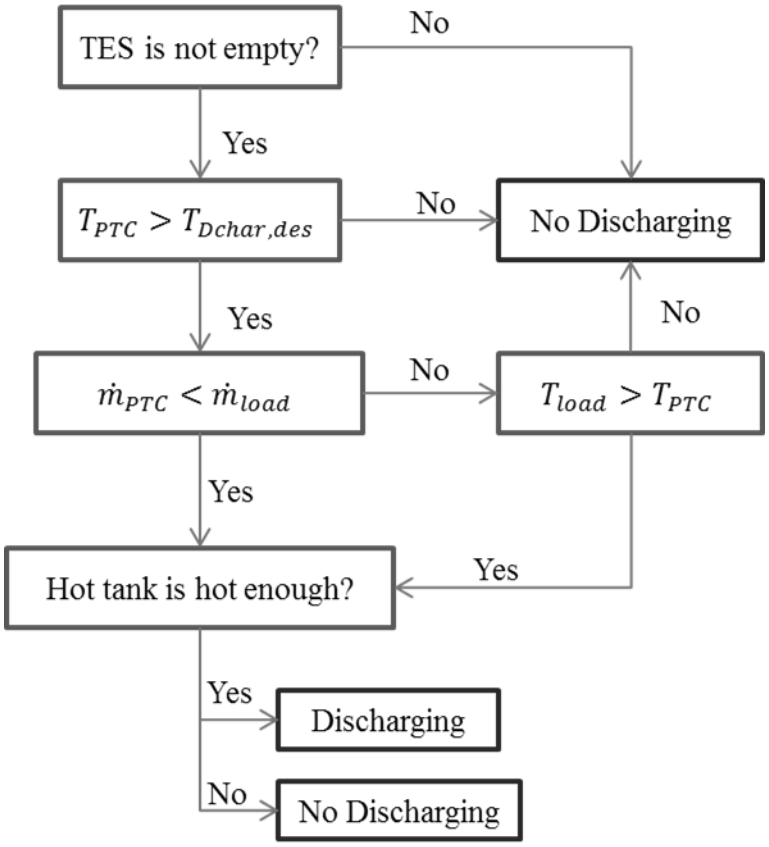

Figure 2.13 Flow Diagram of Discharging Valve

2.7.5. Discharge Bypass Valve (V5) and Load Bypass Valve (V6)

In Figure 2.14, the flow diagram for discharge bypass valve (left) and load bypass valve (right) are shown. The controller for these valves checks the mass flow rate of the TES inlet and the amount of excess bypasses when the inlet flow to this valve is more than the maximum limit for discharging or is more than the load. The maximum discharge capacity and load profile are defined before the simulation is started.

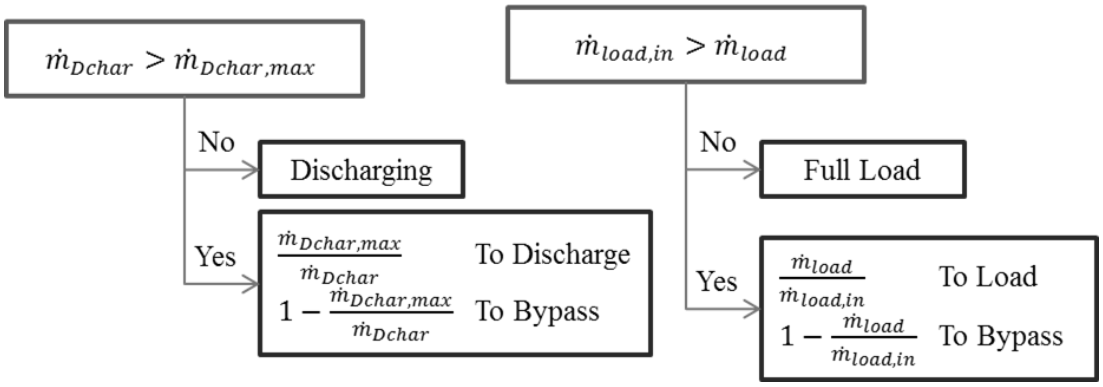

Figure 2.14 Flow Diagram of Discharge (Left) and Load (Right) Bypass Valve

2.7.6. Pump Controller

Flow diagram of the main pump is shown in Figure 2.15. For controlling the pump, the plant controller evaluates the valves, DNI, TES states and outlet PTC temperature and mass flow rate. The pump controller gathers the required mass flow rates for the PTC and the load from the initial time step. The controller sends one of four mass flow rate outputs to the pump:

- Zero mass flow rate (plant closed)
- PTC mass flow rate (mass flow rate calculated by DNI at initial time step)
- Dispatch mass flow rate (mass flow required for sustaining the load, calculated at the initial time step)
- PTC and dispatch mass flow rate.

During the simulation, even when the valve states are not changed, the mass flow can be changed due to changes in DNI or the TES becoming full or empty.

First, the plant controller checks for day or night conditions based on DNI. At night when the TES is empty or the hot tank is cold for charging, the pump does not work (zero mass flow). If the TES is not empty and the hot tank is sufficiently hot, only the mass flow rate to meet the load is pumped for dispatching the load (dispatch mass flow) until the TES becomes depleted.

For the PTC warm-up case (the bypass valve is diverted to the HTF tank), if the TES cannot charge (empty TES or cooled hot tank), all the fluid is diverted to the PTC at the PTC mass flow rate. In case of warm-up and chargeable TES, the pump runs at the sum of the PTC and dispatch mass flow rates, and the valves divert the flow accordingly.

For day time, after PTC warmup (bypass valve is not on), the plant controller checks whether the TES can be discharged or not; if discharge is not possible, the mass flow rate is set to the PTC mass flow. If the TES can be discharged, the plant checks whether the collector field output HTF needs to be discharged by checking the outlet temperature and mass flow. If the temperature or mass flow rate is lower than the load, the system diverts the HTF from the TES by passing though the PTC field at load mass flow rate. Otherwise the PTC field can sustain the load at the PTC mass flow rate by itself and TES is not used.

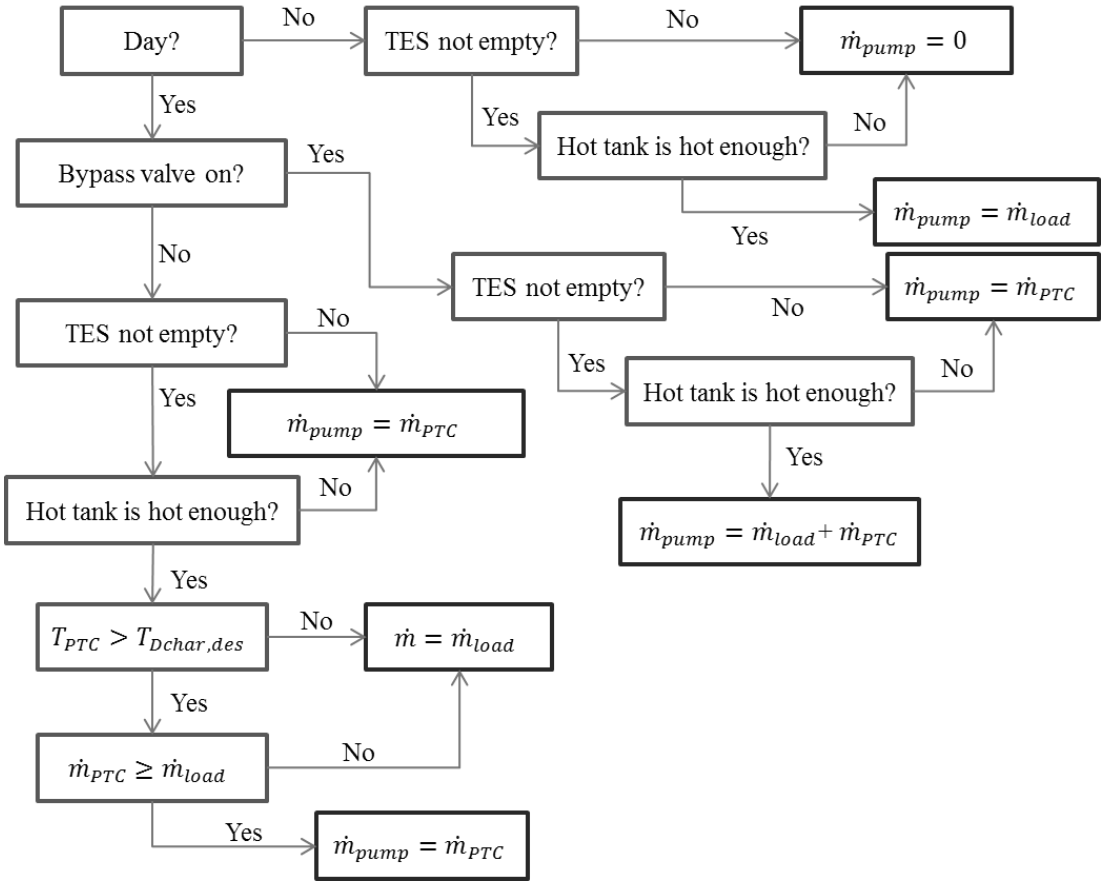

Figure 2.15 Flow Diagram of Main Pump

CHAPTER 3

3. PARAMETRIC ANALYSES

Before starting the parametric studies, the Parabolic Trough Collector's (PTC's) Heat Collecting Element's (HCE's) string length is optimized for Muğla. The main reason for optimizing the string length is adapting the plant to different places and meteorological conditions. The calculation of the optimum HCE length depends on location, DNI, maximum PTC plant outlet temperature and HTF mass flow rate when the same collector type is used. Optimization is done for the LS-3 collector and this collector is used for all simulations. The LS-3 is designed by Luz Int. Ltd and used in SEGS 7, 8, and 9 (Fernandez-Garcia, Zarza, Valenzuela, & Perez, 2010). The main characteristics of the LS-3 collector are shown in Table 3.1.

Table 3.1 Main Characteristics of LS-3 Collector (Fernandez-Garcia, Zarza, Valenzuela, & Perez, 2010)

Max. operating temperature [$°C$]	390
Aperture area [m^2]	507.2
Aperture width [m]	5.76
Length [m]	99
Focal length [m]	1.71
Absorber tube diameter [mm]	70
Reflectance	0.94
Transmittance	0.96
Absorptance	0.96
Emittance (at temp. [$°C$])	0.15 (350)

The collector string length is optimized for Muğla. The inlet and outlet temperatures of the PTCs are taken from the SEGS plants as 290 $°C$ and 391 $°C$ respectively. For the period simulated, Muğla has an average daily DNI of 5.313 kWh/m^2 and approximately 12 hours of solar radiation can be harvested in a day (average DNI 442.7 W/m^2). On the other hand, the SEGS plants (Daggett, CA) have an average DNI of 637.2 W/m^2 , which is 43.9% greater than Muğla.

In the SEGS plants, each string has 16 HCEs in series. To adapt the plant to Muğla, the number of HCEs is increased and 18 HCEs is found as the optimum value (12.5% longer), which can reach 390 $°C$ and sustain the load without TES.

3.1. Base Analysis

In this section, the plant is simulated at a constant initial investment value (50 M USD) and the maximum solar fraction of the plant is found by changing the TES size and collector field area. Solar fraction is defined as the ratio of sustained load time to total load time during simulation. For the initial investment calculation, costs projected for 2010 and 2020 are used from the S&L report (Sargent & Lundy LLC Consulting Group, 2003) and are linearly interpolated to 2014 values. In Table 3.2, the interpolated initial investment costs are shown.

Table 3.2 Interpolated Initial Investment Values for 2014 (Sargent & Lundy LLC Consulting Group, 2003)

Solar field $[USD/m^2]$	245
HTF system $[USD/m^2]$	90
TES system $[USD/kWh_t]$	80

For the sample plant calculation, the TES capacity is calculated as follows, where a higher heat capacity can be obtained by changing the fluid and reservoir temperatures.

$$Q_{TES} = \forall_{TES} \times \rho_{TES} \times c_{p,TES} \left(T_{Hot\ Tank} - T_{Cold\ Tank}\right) \quad 3.1$$

Q_{TES} is the heat capacity of the TES. Recall that a 2-tank TES design is assumed with a cold and a hot tank, and the TES fluid is heated or cooled as it flows in a single pass between the two tanks. The reservoir temperatures for the hot ($T_{Hot\ Tank}$) and cold ($T_{Cold\ Tank}$) TES tanks are 380 °C and 290 °C respectively. Other TES parameters are volume ($\forall_{TES}$), density (ρ_{TES}) and constant specific heat $\left(c_{p,TES}\right)$ of the storage medium.

After calculating the heat capacity of the TES, the initial cost is calculated as,

$$Ini.Cost = (Q_{TES} \times TES\ Sys.) + \left(Coll.Area\ \times (Solar\ Field + HTF\ Sys.)\right) \quad 3.2$$

In the base simulations, the maximum solar fraction is calculated by changing the TES size and collector area. During this parametric study, the initial investment cost is kept constant (50 M USD). The demand profile is constant at $150\ kg/s$ mass flow rate and $370\ °C$. The total thermal power of the plant is calculated as follows.

$$P_{plant} = \dot{m}_{load}\ \times c_{p,load} \times \left(T_{load,in} - T_{load,out}\right) \quad 3.3$$

which is,

$$P_{plant} = 150\ kg/s\ \times 2.3\ kJ/kg\ K \times (370\ °C - 270°C) = 34.5\ MW_t \quad 3.4$$

This constant demand profile of $34.5\ MW_t$ is used both in the present base analysis and for the comparison between Muğla and Konya (Section 3.4). In the demand analysis (Section 3.5), different load profiles with the same daily total energy are investigated. The results of the base simulations are shown in Table 3.3.

Table 3.3 Results of Base Analysis (Fixed Initial Investment Cost at 50M USD for Muğla)

Tank Radius $[m]$	**Tank Vol.** $[m^3]$	**TES Heat Capacity** $[kWh_t]$	**TES Cost [M USD]**	**Coll. Area** $[m^2]$	**Coll. Area Cost [M USD]**	**Solar Fraction**
0	0	0	0.0	149,254	50.0	33.9%
2	25	999	0.1	149,015	49.9	34.5%
4	201	7,992	0.6	147,345	49.4	35.3%
6	679	26,974	2.2	142,812	47.8	37.3%
7	1,078	42,833	3.4	139,025	46.6	38.8%
8	1,608	63,938	5.1	133,985	44.9	40.9%
9	***2,290***	***91,036***	***7.3***	***127,514***	***42.7***	***42.1%***
10	3,142	124,878	10.0	119,432	40.0	41.5%
11	4,181	166,213	13.3	109,561	36.7	38.5%
12	5,429	215,790	17.3	97,722	32.7	32.9%

The maximum solar fraction (42.1%) is observed at 9 m tank radius, which has a 2,290 m^3 tank volume and a 127,514 m^2 collector area. The results in Table 3.3 show that the solar fraction is increasing with increasing TES up to a maximum, after which the collector becomes too small to dispatch the load or charge the TES efficiently. The change in the solar fraction with TES tank volume is shown in Figure 3.1 with a parabolic curve fitted. It can be observed that there is only one peak and using curve fit the highest efficiency point can be calculated.

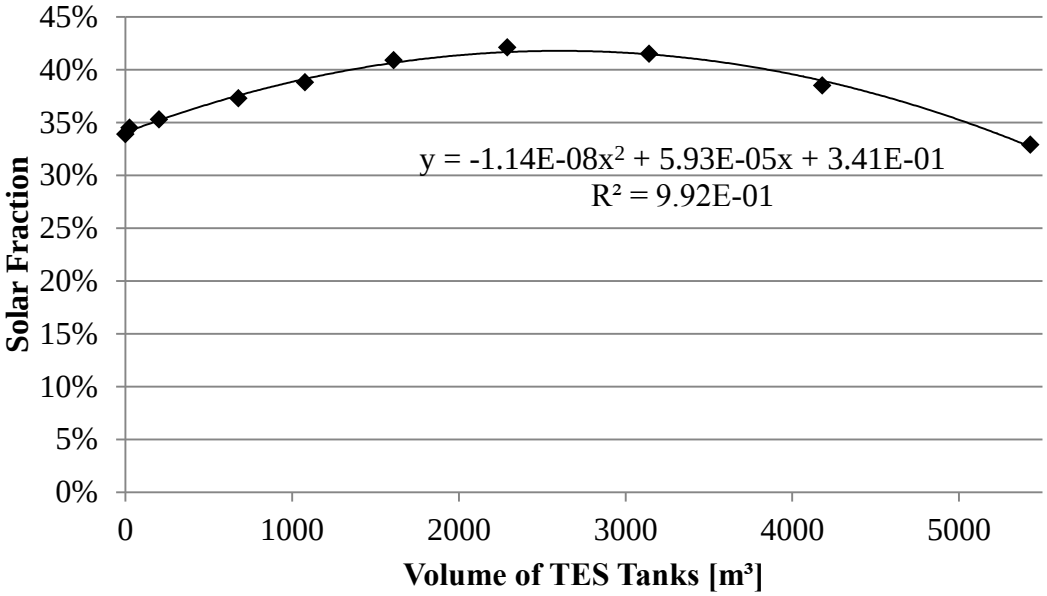

Figure 3.1 Change in Solar Fraction with Volume of TES Tank (Fixed Initial Investment Cost at 50M USD for Muğla. Markers Represent Simulation Results)

3.2. Initial Investment Analysis

In this analysis, the base simulations are repeated for different initial investment values and the capacity rate is investigated. Initial investments are investigated from 30 M USD to 65 M USD to observe the change in solar fraction. In Figure 3.2, the change in solar fraction with the volume of TES tanks is shown.

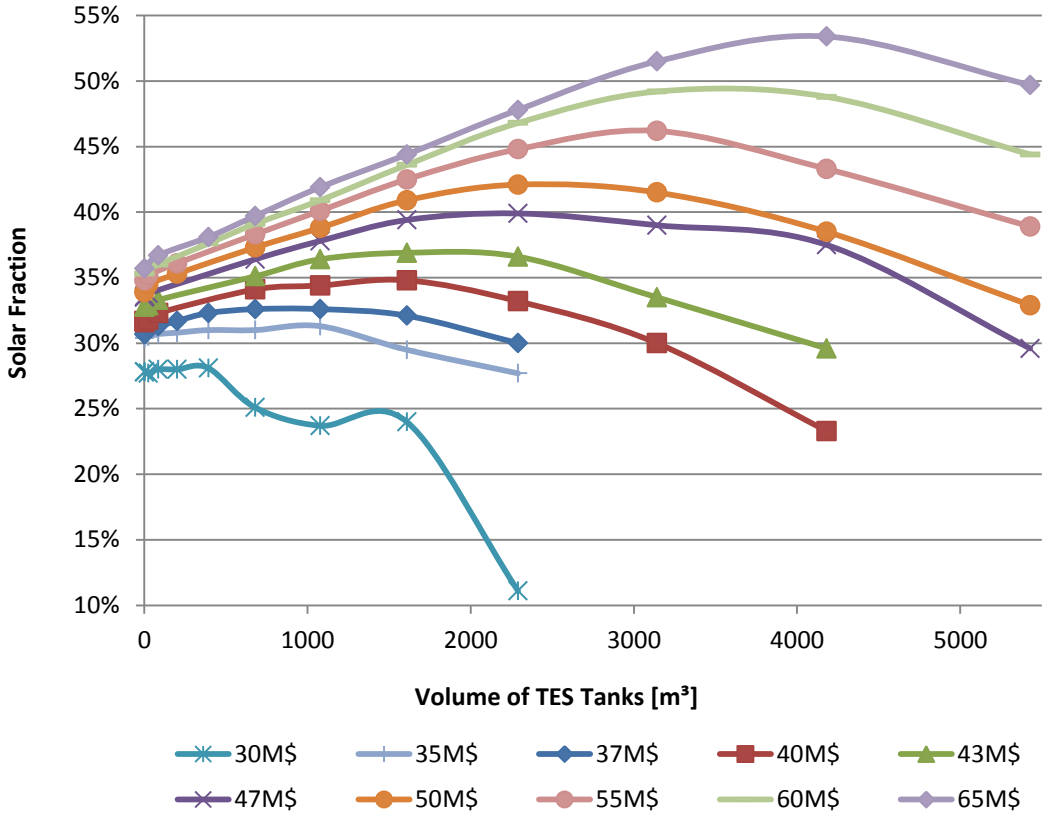

Figure 3.2 Change in Solar Fraction with Volume of TES for Different Initial Investment Costs (30 – 65M USD) for Muğla (Markers Represent Simulation Results)

In the figure, the curves do not intercept with each other even for the no TES (zero tank volume) condition, and they all show a single peak and roughly parabolic behavior except the 30 M USD case.

The reason for simulating the 30 M USD case is observing the sensitivity of the plant's performance at small collector and storage conditions. The results show that the plant's performance is extremely sensitive to daily DNI variations and the simulated results are unstable at very low initial investment values. For small storage cases, the plant completely charges the TES but the TES also depletes very quickly, and the maximum solar fraction is observed when tank volume is 393 m^3.

For large storage cases, the collector area becomes insufficient for the load and only day time interruptions (intermittent cloud) can be dispatched. After reaching the peak solar fraction with increasing TES size, the solar fraction decreases with further increases in TES size because collectors cannot charge the TES and hardly dispatch the load.

With increasing initial investment, the plant can better compensate for daily variations and the oscillations in solar fraction with tank volume for small initial investment seen in Figure 3.2 disappear. For higher investment cases, collector area increases and the maximum solar fraction shifts to larger TES volumes as expected.

The variation in maximum solar fraction with increasing initial investment is shown in Figure 3.3. Over this range of initial investment costs, the solar fraction increases linearly with initial investment cost when optimized parameters are used. Note however, as will be shown in Section 3.3, the maximum solar fraction approaches 1 for larger initial investment costs.

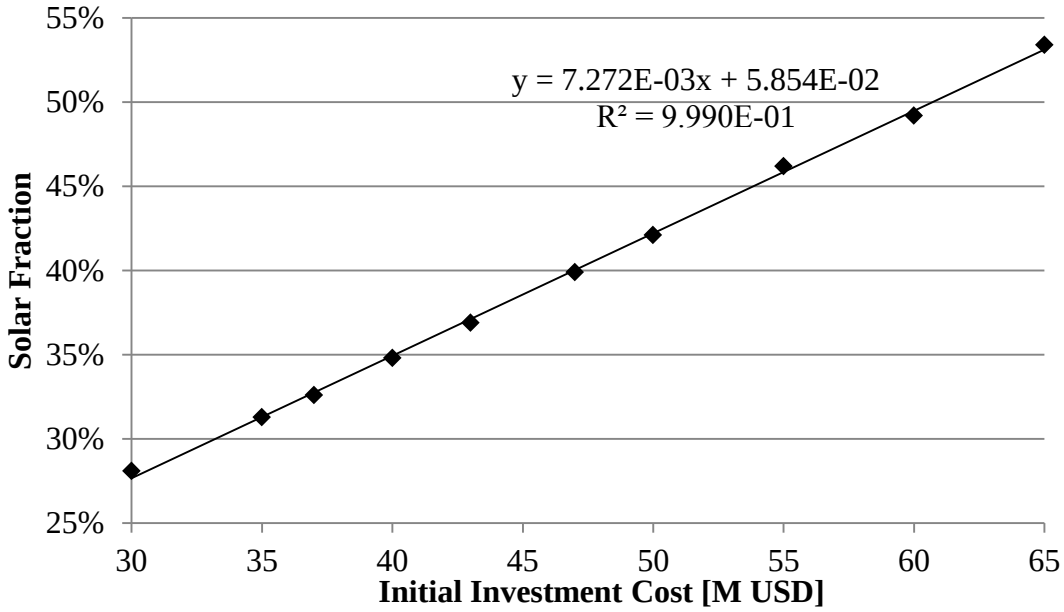

Figure 3.3 Change in Maximum Solar Fraction with Increasing Initial Investment Costs (30 – 65M USD) for Muğla

The ratio of PTC and TES costs with initial investment costs are shown in Figure 3.4. The fluctuations in the TES cost ratio are caused by low resolution discretization, but an overall trend can be observed, which shows that the optimum fraction of investment costs devoted to TES increases with investment costs as expected.

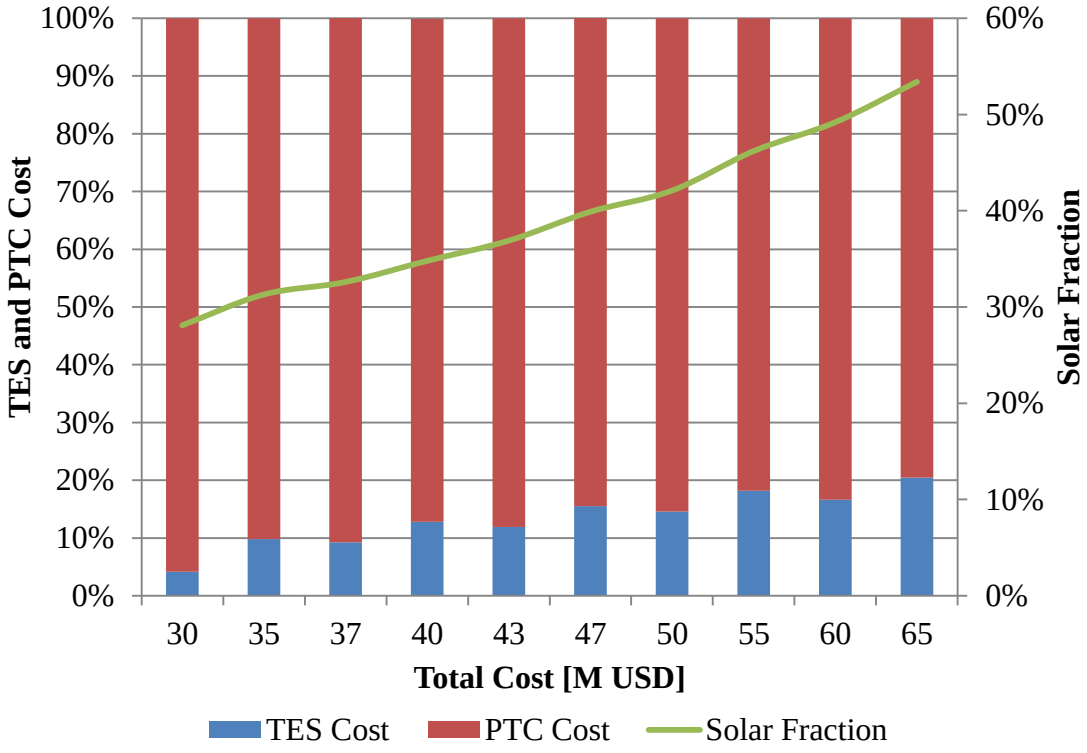

Figure 3.4 Change in PTC and TES Cost and Solar Fraction with Increasing Initial Investment Cost (30 – 65M USD) for Muğla (PTC Cost is Summation of Solar Field and HTF Costs)

3.3. High Initial Investment Analysis

In the initial investment analysis in the previous section (Section 3.2), the limits of initial investment are kept in a reasonable range to show that solar fraction increases linearly with increasing initial investment. As initial investment increases, the load becomes significantly smaller with respect to the generated energy. At high initial

investment costs, the plant sustains the load, and charges the TES until the HTF heats up to a critical level. In real plants, over temperature of the HTF is dangerous due to over expansion of the HCE and the chemical instability of the HTF. For preventing overheating, defocusing is applied to collect less insolation than the allowable limit by tilting the PTCs by a few degrees. Defocusing is not modeled explicitly in the PTC model; rather it is modeled by keeping the plant maximum temperature below a constant limit. For all simulations, the collector output temperature is not allowed to exceed 400 $°C$, which is the maximum allowable HTF temperature limit in the SEGS plants. In the high investment analysis, defocusing becomes significant and even when the initial investment increases with very high steps; the solar fraction asymptotically approaches 1 as shown in the Figure 3.5 and as expected.

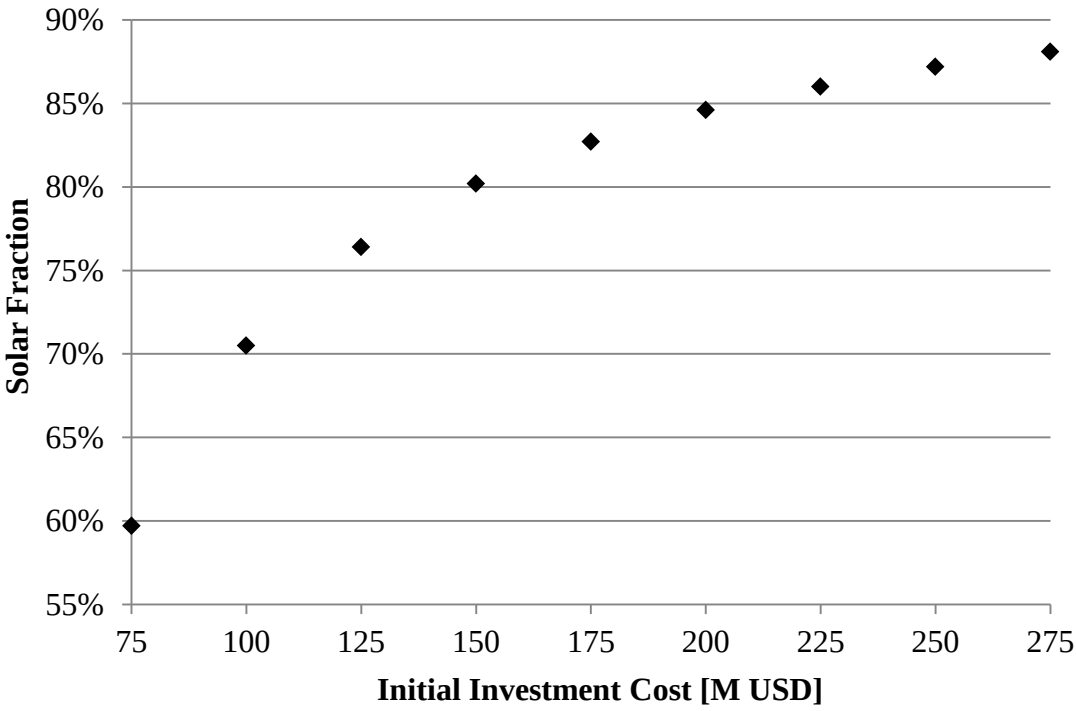

Figure 3.5 Change in Maximum Solar Fraction with Increasing High Initial Investment Costs (75 – 275M USD) for Muğla

It is clear that over investment is not realistic and the linear increment in solar fraction with initial investment has a limit. For showing the asymptotic behavior, the

solar fraction is plotted in Figure 3.6 with the inverse of initial investment cost, and a linear relation is observed.

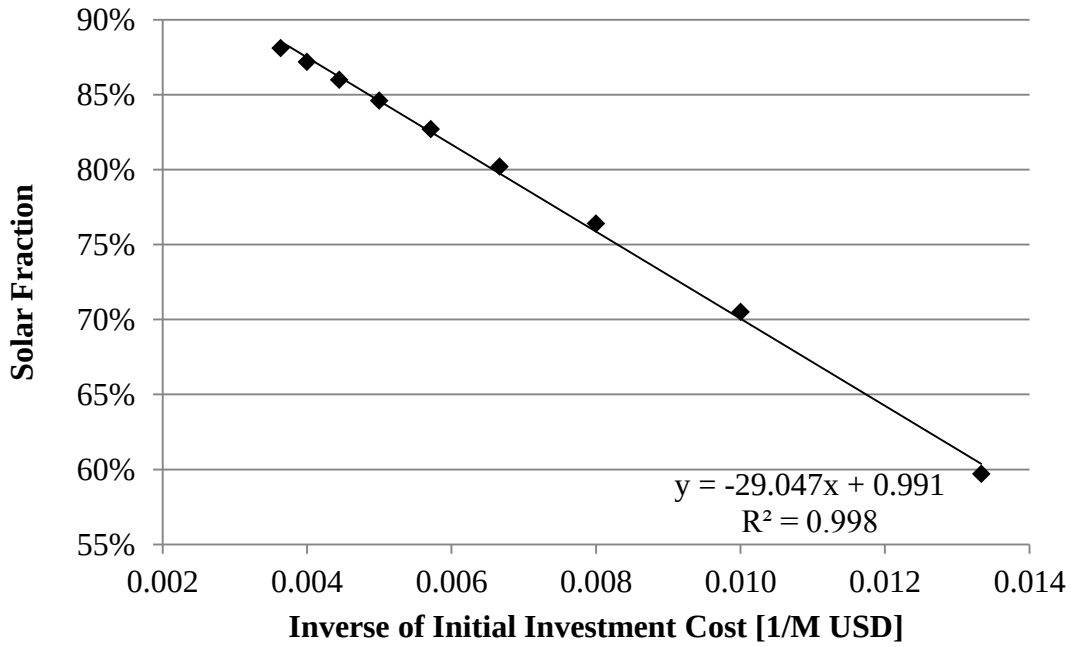

Figure 3.6 Solar Fraction Change with Inverse of Initial Investment Costs

For illustrating the overall change in solar fraction with respect to initial investment, the solar fraction is redrawn from 30 M USD to 275 M USD in Figure 3.7.

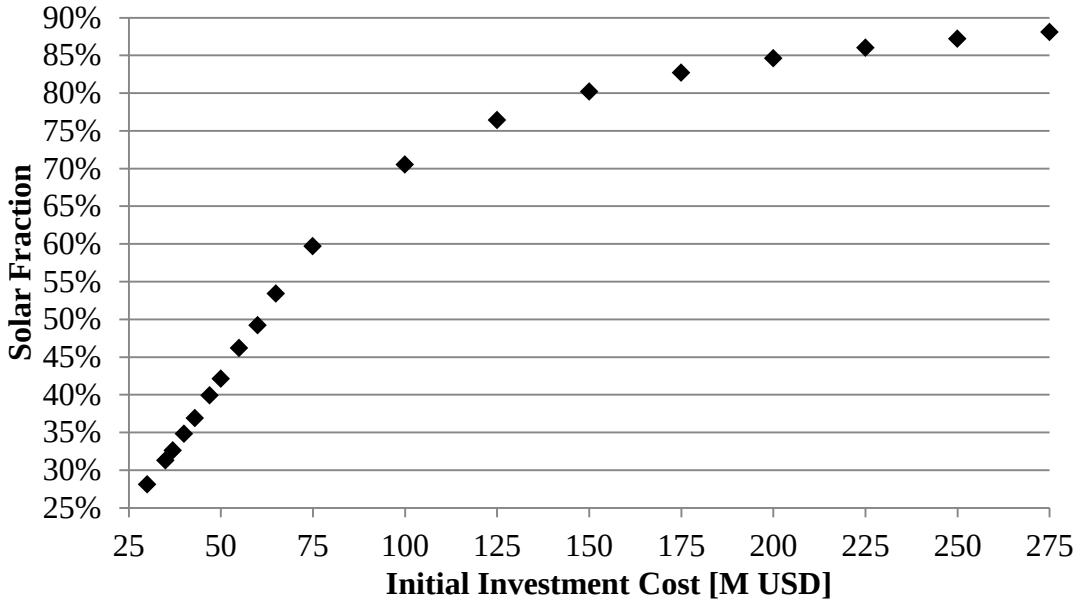

Figure 3.7 Change in Maximum Solar Fraction with All Initial Investment Costs (30 – 275M USD) for Muğla

When high initial investment is considered, asymptotic increment of solar fraction is observed. It can be concluded that solar plants need to be hybridized with alternative energy sources for sustaining dispatchable base load rather increasing investment.

3.4. Comparison of Muğla and Konya

In this part, initial investment analyses are done for another TMY2 data set, Konya, Turkey. Until this section the effect of plant size is investigated by evaluating the solar fraction. The results from the Konya simulations in terms of maximum solar fraction versus initial investment are shown in Figure 3.8, along with Muğla data. This current comparison of Muğla and Konya gives an idea about the change in solar fractions with different weather data (Konya is cloudier, has lower average DNI and lower ambient temperature than Muğla.).

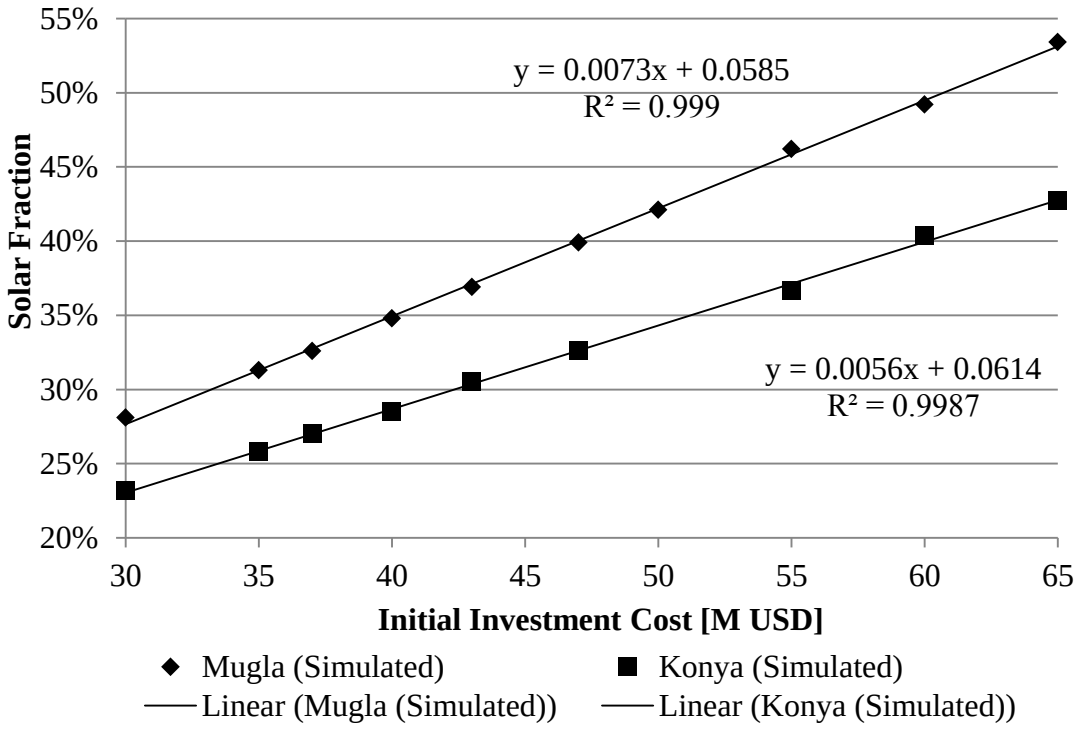

Figure 3.8 Change in Maximum Solar Fraction with Increasing Initial Investment Costs (35 – 65 M USD) for Muğla and Konya

In Figure 3.8, it can be inferred that over this range of initial investment the change in solar fraction with initial investment is linear for both Konya and Muğla. For some fixed initial investment, the difference in the solar fraction between Muğla and Konya for low initial investment cases is approximately 5% and it increases with initial investment to 10%. As stated in the weather model, average DNI for Konya 15.6% less than Muğla. From the trend lines in Figure 3.8, to provide the same solar fraction, 28% more initial investment should be done for Konya relative to Muğla.

3.5. Demand Analysis

Today, most solar power plants are designed for sustaining a peak load at noon time rather than meeting the base load. In this section, different demand profiles are

simulated for Muğla at a constant 50 M USD initial investment value. Four different demand profiles are used in these simulations, which are provided from IEA's CSP roadmap (International Energy Agency, 2010). For all demand profiles, the total daily generated energy is equal by requiring the total daily load mass flow be the same for all demand profile while the hourly mass flow rates can vary for the different demand profiles.

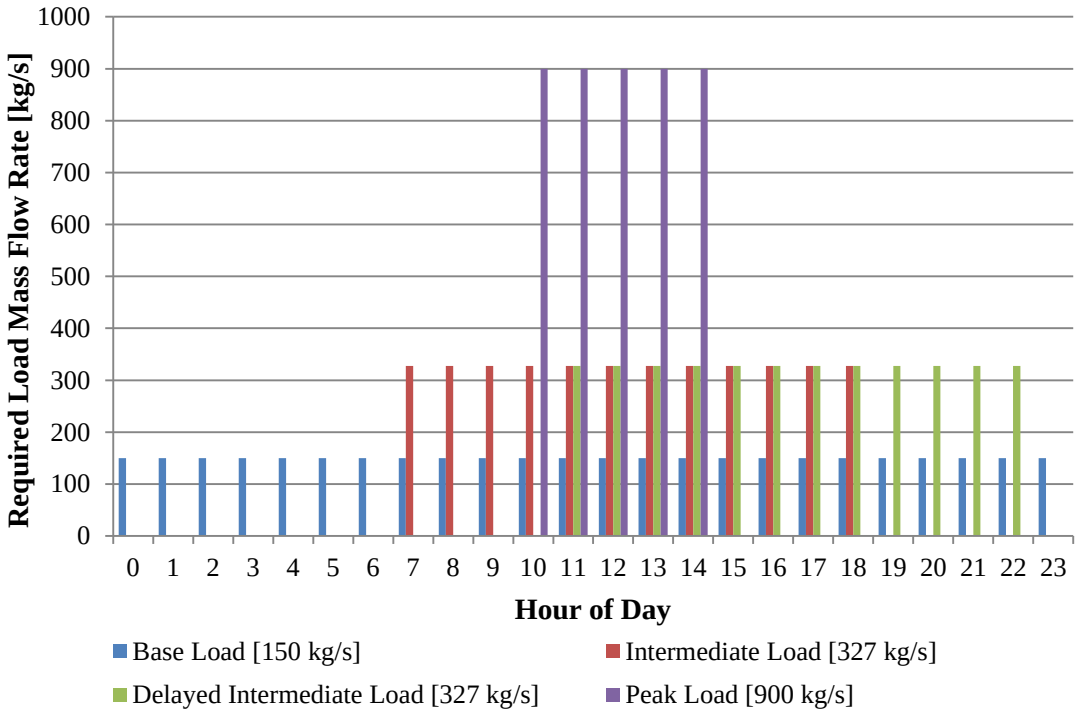

Figure 3.9 Load Profiles for Fixed Daily Output

In Figure 3.9, the four demand profiles used in the demand analysis are shown. All the previous simulations were performed by using the base load demand profile, which meets a constant demand for 24 hours. Meeting a base load profile is for solar power at night, as power is not generated and the TES must discharge for a long time. In the intermediate load demand profile, power is demanded from 08:00 to 19:00. This load configuration is designed for simulating energy generation when sunshine is available and it requires the minimum capacity of TES with respect to the other load profiles. In the delayed intermediate load profile, power generation is

shifted 4 hours and becomes from 12:00 to 23:00. Relative to the intermediate demand profile, shifting the demand 4 hours requires a larger-size TES, but also allows electricity to be generated at higher prices. The peak load profile is designed to meet an extreme load for a few hours. In Table 3.4, the solar fraction and TES size is shown for Muğla at fixed initial investment (50M USD) for the different load profiles.

Table 3.4 Results of Demand Analysis

Load Profile	**Maximum Solar Fraction (%)**	**Volume of TES Tanks [m^3]**	**Heat Capacity of TES [kWh_t]**
Intermediate	55.2	679	269.9
Base	41.5	3,142	1,249
Peak	37.0	3,142	1,249
Delayed Intermediate	36.9	4,181	1,662

Observing Table 3.4, it can be concluded that the demand profile is one of the most important parameters for designing a solar plant. The intermediate load has the highest solar fraction with the smallest size TES. This result is expected, since demand profile uses the power when it is generated. Thermal loses are also less than for the other profiles because of the small difference between charging and discharging times. Even for the same plant parameters, the peak load profile results in a 4.5% larger solar fraction than the base load profile. The main disadvantage of the peak load profile is after the demand stops: the plant charges the TES and the hot storage fluid cools until 10 am. For the delayed intermediate load profile, even when

the plant has a large size TES, it cannot sustain the demand properly when compared with other load profiles.

CHAPTER 4

4. CONCLUSIONS

4.1. Summary

Adding storage to solar energy systems can increase solar fractions, capacity factors, and dispatchability. Among the different energy storage technologies, Thermal Energy Storage (TES) is one of the most economically viable, and therefore Concentrating Solar Thermal (CST) systems with TES hold promise for providing thermal power that is reliable, affordable, and sustainable. In this thesis control strategies for CST systems with TES is investigated to predict and improve energetic and economic performance. In traditional fossil power plants, operation is controlled to maximize efficiency using a limited number of operational modes, and this approach is also preferred for CST systems. CST systems with storage typically operate in approximately 6 different modes based on the demand, solar resources, and state of storage. In the current work rather than limiting the system to these approximately 6 modes of operation, approximately 8 modes of operation is achieved through the independent control of valves.

The CST system primarily consisting of PTC's and TES is modeled in TRNSYS using existing libraries. A new control algorithm is developed and programmed using MatLab and then connected to the TRNSYS model. PTC collector string model is built as a combination of total enthalpy flow rate model, absorption model and heat loss model. As a result of interactions between these models, time rate of change of temperature and mass flow rate of heat transfer fluid is calculated. The results from this energetic model are used as inputs to an economic model developed in Excel

based on projected initial investments costs. For some fixed initial investment, the relative sizes of the PTC field and TES are varied to find the combination with the maximum solar fraction.

The initial design and sizing of the PTC field is based on an actual system installed in California and adapted to Muğla, Turkey. The maximum PTC outlet temperature is in part controlled by the string length, and an appropriate string length will vary with local solar resources.

In the parametric studies, weekly simulations for the summer season are performed using a time step in the range of 7-15 seconds. At each time step and based on a demand profile defined by a temperature and mass flow rate of HTF, the model optimizes the flow of fluids through the PTC's and TES by controlling the state of the valves and mass flow rates of the pumps. For each initial investment amount, the TES size is varied by a fixed step and optimization between steps is not performed. Similarly the PTC field size is varied by changing the number of strings in parallel while keeping the number of modules per string constant, and therefore only discrete changes in PTC field size equal to the area of 1-string are possible. The discrete nature of the steps used in the optimization process results in some irregular and unstable results at some conditions.

4.2. Conclusions

The major conclusions from this work are as follows:

- The main motivation of the thesis is demonstrating that solar energy can be a good future energy source. This can be achieved by using solar energy with other energy sources when solar power is unavailable or insufficient to supply peak demand. In the simulations, it is observed that up to 50% of load can be supplied with optimum size of collector and storage.

- From Daggett, California, to Muğla, Turkey, which has 40% less average DNI, string length should be increased around 10-15%. This result highlights the need for the PTC string length to be chosen based on the local DNI resources.
- For small size PTC sizes relative to the load, the predicted plant performance is sensitive to daily variations and results are unstable.
- For simulations for Muğla with a constant demand profile, and fixed 50M USD initial investment, a design with optimum sized TES has a 10% higher solar fraction than a design with no TES.
- For a fixed demand, the size and cost of TES increases with initial investment costs both in absolute terms and relative to the size and cost of the PTC field. For example, for an initial investment of 35M USD, 96% and 4% of the initial investment costs should go to the PTC field and TES, respectively, while for an initial investment of 65M USD the percentages are 80% and 20%, respectively.
- Simulations are run resulting in solar fractions ranging from approximately 20 to 80%, and over this range the solar fraction is found to scale approximately linearly with investment costs for solar fractions from 20% to 55%, and then asymptotically approach 1.
- It is observed that, for the conditions investigated in this thesis, once an initial investment of approximately 75 M USD is reached, to increase the solar fraction further investments should be made in hybridizing the plant with other energy sources rather than increasing the collector field or storage size further.
- For Konya, Turkey, which has lower DNI resources than Muğla, and for a constant demand profile and the same investment cost of 60M USD the solar fraction is approximately 10% less than Muğla and solar fraction is increasing less than for Muğla with increasing initial investment.
- Four different characteristic demand profiles (base load, intermediate load, delayed intermediate load, and peak load) were simulated for Muğla for a

fixed 50M USD initial investment. The intermediate demand profile is found to have the highest solar fraction and the smallest TES size. When comparing the relation between optimum TES size and solar fraction among the different demand profiles, an increase in TES size is related to a decrease in solar fraction. Extrapolating this result, among a set of demand profiles and for a fixed initial investment cost, the demand profile that requires no TES will have the highest solar fraction.

- Changing the demand profile changes the optimal design of the plant and for the same initial investment can change the solar fraction up to 18%.

4.3. Future Work

This study should be considered as an introduction for the design and optimization of a solar power plant consisting of a PTC field with TES but no power block. While general trends can be observed and conclusions drawn from the model and results for Konya and Muğla, there are several ways the work can be extended.

- The present model has a control algorithm but does not have a controller that sets the temperature of the outlet fluid by adjusting the mass flow rate. Implementing a controller will increase the solar fraction and the results can be more satisfactory.
- This model can be implemented to a power block for electricity generation and rather than analyzing initial investment cost, levelized cost of electricity can be investigated or a break-even analysis can be done. The new model can be compared with electricity consumption characteristics of Turkey.
- Fuel backup can be added to the model and the rate of fuel consumption can be calculated for characteristic load profiles.
- Annual simulations can be done and TES heaters can be implemented in the model for anti-freeze.

- The number of load profiles and geographical locations simulated can be increased.
- Simulations can be increased and step size can be decreased for finding the most efficient point.
- Components in the plant can be replaced with more accurate models.

REFERENCES

Abengoa. (2012, July 31). *Solar-thermal*. Retrieved August 1, 2014, from Abengoa: http://www.abengoa.com/web/en/negocio/energia/electricidad_solar/termosolar/index.html

Alstom. (2014). *Solar Power*. Retrieved August 1, 2014, from Alstom: http://www.alstom.com/power/renewables/solar-power/

Black, D. (2014). *Solar Fuels and Artificial Photosynthesis*. Retrieved August 8, 2014, from Royal Society of Chemistry: http://www.rsc.org/ScienceAndTechnology/Policy/Documents/solar-fuels.asp

Brittanica. (2013, March 6). *Oceanography*. Retrieved August 1, 2014, from Brittanica: http://global.britannica.com/EBchecked/topic/591544/thermocline

Brosseau, D. A., Hlava, P. F., & Kelly, M. J. (2004). *Testing Thermocline Filler Materials and Molten-Salt Heat Transfer Fluids for Thermal Energy Storage Systems Used in Parabolic Trough Solar Power Plants.* Albuquerque: Sandia National Laboratories.

Cohen, G. E., Kearney, D. W., & Kolb, G. J. (1999). *Final Report on the Operation and Maintenance Improvement Program for Concentrating Solar Power Plants.* Albuquerque: Sundia National Laboratories.

DLR. (2010, June 14). *Energy Question of the Week: Can Solar Power be Stored?* Retrieved August 1, 2014, from DLR Blogs: http://www.dlr.de/blogs/en/desktopdefault.aspx/tabid-6192/10184_read-147/

Dudley, V., Kolb, G. J., Mahoney, A. R., Mancini, T. R., Matthews, C. W., Sloan, M., et al. (1994). *Test Results: SEGS LS-2 Solar Collector.* Sandia National Laboratories.

Duffie, J. A., & Beckman, W. A. (2006). *Solar Engineering of Thermal Processes* (3rd ed.). New Jersey: John Wiley & Sons, Inc.

Fernandez-Garcia, A., Zarza, E., Valenzuela, L., & Perez, M. (2010). Parabolic-Trough Solar Collectors and Their Applications. *Renewable and Sustainable Energy Reviews, 14*, 1695-1721.

Forristall, R. (2003). *Heat Transfer Analysis and Modeling of a Parabolic Tough Solar Receiver Implemented in Engineering Equation Solver.* Golden, CA: National Revewable Energy Laboratory.

Garcia, I. L., Alvarez, J. L., & Blanco, D. (2011). Performance Model for Parabolic Trough Solar Thermal Power Plants with Thermal Storage: Comparison to Operating Plant Data. (A. Kribus, Ed.) *Solar Energy*(85), 2443-2460.

Greenhut, A. D. (2010). *Modeling and Analysis of Hybid Geothermal-Solar Thermal Energy Conversion Systems.* Mechanical Engineering. Massachusetts: Massachusetts Instittute of Technology.

Herrmann, U., Geyer, M., & Kearney, D. (2003). Overview on Thermal Storage Systems. *Parabolic Trough Thermal Energy Storage Workshop* (p. 23). Golden: NREL.

Incropera, F. P., DeWitt, D. P., Bergman, T. L., & Lavine, A. S. (2007). *Fundamentals of Heat and Mass Transfer* (6th b.). New Jersey: John Wiley & Sons.

International Energy Agency. (2010). *Technology Roadmap Concentrating Solar Power.* Retrieved August 1, 2014, from International Energy Agency:

http://www.iea.org/publications/freepublications/publication/csp_roadmap.pdf

International Energy Agency. (2011). *Solar Energy Perspectives: Executive Summary.* Retrieved August 1, 2014, from International Energy Agency: http://www.iea.org/publications/freepublications/publication/solar_energy_perspectives2011.pdf

Iqbal, M. (1983). *An Introduction to Solar Radiation.* Toronto: Academic.

Kalagirou, S. A. (2009). *Solar Energy Engineering Processes and Systems* (2nd ed.). Massachusetts: Elsevier.

Kryza, F. (2003). *The Power of Light; the Epic Story of Man's Quest to Harness the Sun* (1st ed.). New York: McGraw-Hill.

Lippke, F. (1995). *Simulation of the Part-Load Behavior of a 30 MWe SEGS Plant.* Solar Thermal Technology Department. Oak Ridge, TN: Sandia National Laboratories.

Lovegrove, K., & Stein, W. (2012). *Concentrating Solar Power Technology: Principles, Developments and Applications* (1st ed.). Cambridge: Woodhead Publising.

Marion, W., & Urban, K. (1995). *User's Manual for TMY2s.* Midwest Research Institute, Department of Energy. Golden: National Renewable Energy Laboratory.

Marion, W., & Urban, K. (1995). *User's Manual for TMY2s Derived from the 1961-1990 National Solar Radiation Data Base.* Denver, Colarado: National Renewable Energy Laboratory.

Mcmahan, A. C. (2006). *Design & Optimization of Organic Rankine Cycle Solar-Thermal Powerplants.* Madison, WI: University of Wisconsin-Madison.

Mills, D. (2004). Advances in Solar Thermal Electricity Technology. *Solar Energy*(12), 19-31.

Montes, M. J., Abanades, A., & Martinez-Val, J. M. (2010, May). Thermofluidynamic Model and Comparative Analysis of Parabolic Trough Collector Using Oil, Water/Steam, or Molten Salt as Heat Transfer Fluids. (M. Mehos, Ed.) *Journal of Solar Energy Engineering, 132*, 021001/1-7.

Montes, M. J., Abanades, A., Martinez-Val, J. M., & Valdes, M. (2009). Solar Multiple Optimization for a Solar-Only Thermal Power Plant, Using Oil as Heat Transfer Fluid in the Parabolic Trough Collectors. (R. Pitz-Paal, Ed.) *Solar Energy*(83), 2165-2176.

National Renewable Energy Laboratory. (2010, January 29). *Troughnet Parabolic Trough Solar Power Network*. Retrieved August 1, 2014, from National Renewable Energy Laboratory: http://www.nrel.gov/csp/troughnet/power_plant_data.html

Newport Corporations. (2014). *Introduction to Solar Radiation*. Retrieved August 29, 2014, from Newport Corporations: http://www.newport.com/Introduction-to-Solar-Radiation/411919/1033/content.aspx

Pacheco, J. E., Showalter, S. K., & Kolb, W. J. (2002, May). Development of a Molten-Salt Thermocline Thermal Storage System for Parabolic Trough Plants. *Journal of Solar Energy Engineering, 124*, 153-159.

Patnode, A. M. (2006). *Simulation and Performance Evaluation of Parabolic Trough Solar Power Plants.* Madison, WI: University of Wisconsin-Madison.

Perlin, J. (2013). *Let It Shine: The 6,000-Year Story of Solar Energy.* Novato: New World Library.

Plataforma Solar de Almería. (2014). *Dish Stirling Systems: Distal and Eurodish*. Retrieved August 1, 2014, from Plataforma Solar de Almería: http://www.psa.es/webeng/instalaciones/discos.php

Poullikkas, A. (2009). Economi Analysis of Power generation from Parabolic Trough Solar Thermal Plants for the Mediterranean Region - A Case Study for the Island of Cyprus. *Renewable and Sustainable Energy Reviews*(13), 2474-2484.

Price, H., Lüpfert, E., Kearney, D., Zarza, E., Cohen, G., Gee, R., et al. (2002). Advances in Parabolic Trough Solar Power Technology. *Journal Of Solar Energy Engineering, 124*, 109-125.

Rabl, A. (1976). Tower Reflector for Solar Power Plants. *Solar Energy*, 269-271.

RWE Innogy. (n.d.). *Andasol 3 - Facts & Figures.* Retrieved August 1, 2014, from RWE Innogy: https://www.rwe.com/web/cms/mediablob/en/1115150/data/1115144/1/rwe-innogy/sites/solar-power/andasol-3/facts-figures/Further-information-about-Andasol.pdf

Sargent & Lundy LLC Consulting Group. (2003). *Assessment of Parabolic Trough and Power Tower Solar Technology Cost and Performance Forecast.* Midwest Research Institute, U.S Department of Energy Laboratory. Golden: National Renewable Energy Laboratory.

Solar Millennium. (2014). *The Construction of the Andasol Power Plants*. Retrieved August 1, 2014, from Solar Millennium AG: http://www.solarmillennium.de/front_content.php?idart=155&lang=2

SOLAR MILLENNIUM AG. (2014). *SOLAR MILLENNIUM AG.* Retrieved August 5, 2014, from Downloads: http://www.solarmillennium.de/includes/force_download.php?client=1&path=upload/Download/Technologie/eng/Andasol1-3engl.pdf

Solarmundo Project. (2001). *Solarmundo Project*. Retrieved 2007, from Solarmundo Project: http://www.solarmundo-power.com

Steinfeld, A., & Palumbo, R. (2001). *Solar Thermochemical Process Technology*. Cambridge: R. A. Meyers Ed., Academic Press.

Stoddard, M., Faas, S., Chiang, C., & Dirks, J. (1987). *SOLERGY - A Computer Code for Calculating the Annual Energy from Central Receiver Plants.* Livermore, CA: Sandia National Laboratories.

Stuetzle, T. A. (2002). *Automatic Control of the 30 MWe SEGS VI Parabolic Trough Plant.* Madison, WI: University of Wisconsin Madison.

U.S. Energy Infomation Administration. (2014, March 8). Retrieved June 22, 2014, from http://www.eia.gov/forecasts/steo/realprices/

Uçkun, C. (2013). *Modeling and Simulations of Direct Steam Generation in Concentrating Solar Power Plants Using Parabolic Trough Collectors.* Ankara: Middle East Technical University.

Usta, Y. (2010). *Simulations of a Large Scale Solar Thermal Power Plant in Turkey Using Concentrating Parabolic Trough Collectors.* Ankara: Middle East Technical University.

Vogel, W., & Kalb, H. (2010). *Large-Scale Solar Thermal Power Technologies, Cost and Development.* Weinheim: Wiley-VCH.

Wikipeadia. (2014, July 18). *Fresnel Lens*. Retrieved August 1, 2014, from Wikipedia: http://en.wikipedia.org/wiki/Fresnel_lens

Wikipedia. (2014, April 14). *Compact Linear Fresnel Reflectors*. Retrieved August 1, 2014, from Wikipedia: http://en.wikipedia.org/wiki/Compact_Linear_Fresnel_Reflector

APPENDICES

A. PLANT SCREENSHOTS FROM TRNSYS 17

In this part, TRNSYS screenshots are provided for helping the future users for modeling the plant easily. TES model is shown in Figure A.1 separately and in Figure A.2, overall plant layout is given.

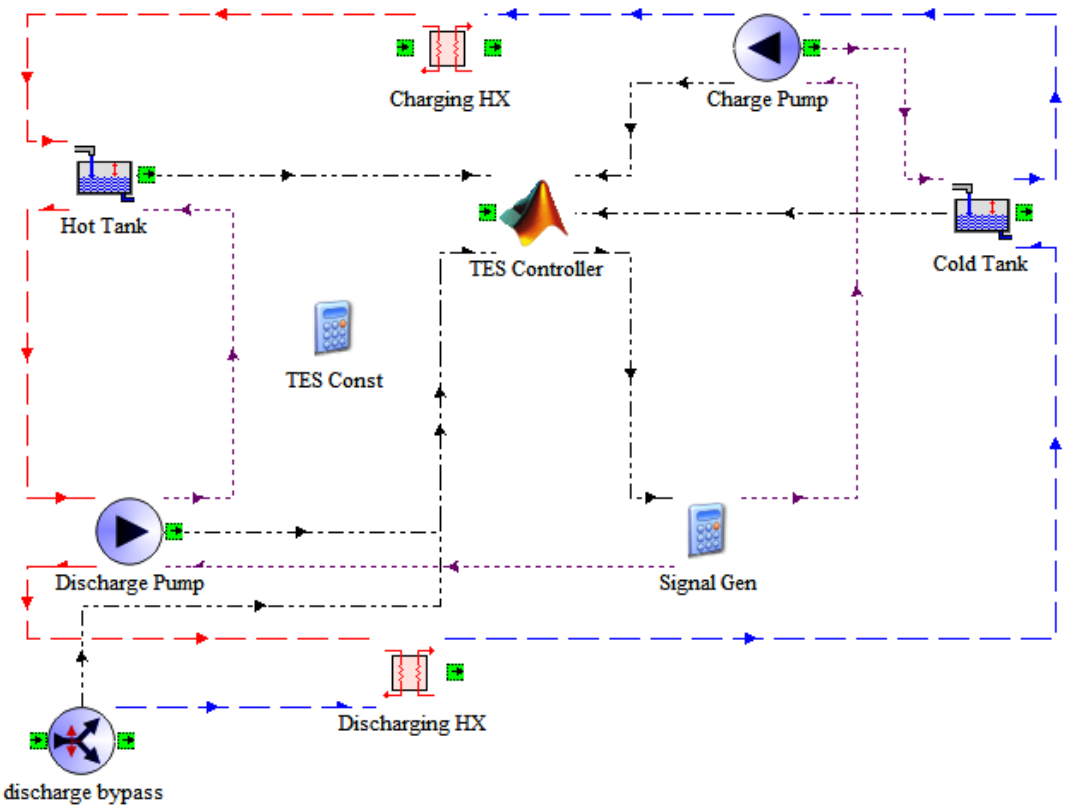

Figure A.1 Screenshot of TES Model in TRNSYS (Red Lines are Hot Storage Medium, Blue Lines are Cold Storage Medium, Black Lines are Input/Output Data to/from MatLab Calling Model, Purple Lines are Pump Signals)

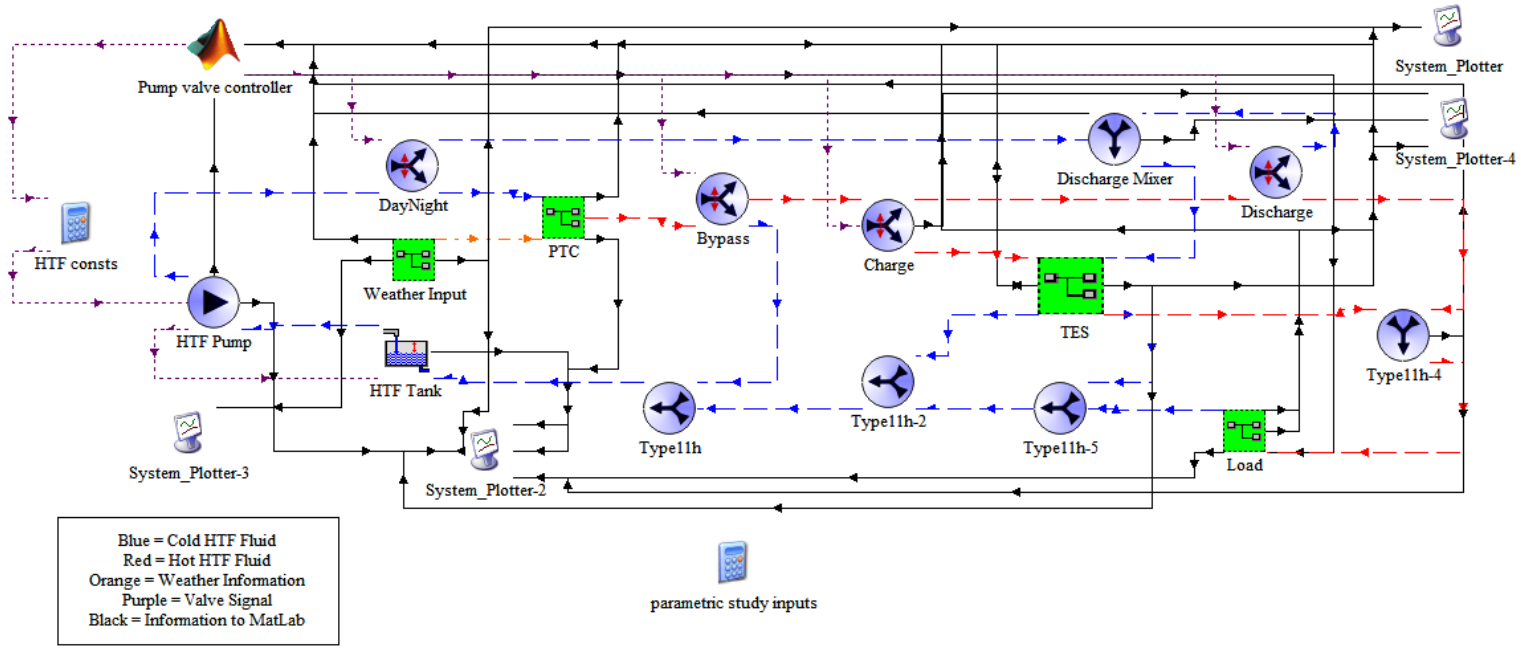

Figure A.2 Screenshot of Plant Model in TRNSYS (Red Lines are Hot HTF, Blue Lines are Cold HTF, Orange Line is Weather Data, Black Lines are Input/Output Data to/from MatLab Calling Model and Output Data, Purple Lines are Pump Signals)

B. DESIGN CONDITIONS OF TES

In Figure B.1, design conditions of the TES are shown, which are used for both MatLab codes. As a result of the change in TES size, the tanks' volumes changed and depending on the design value of HTF input mass flow rate, the heat transfer capacity of HEX and maximum flow rate of pumps are recalculated.

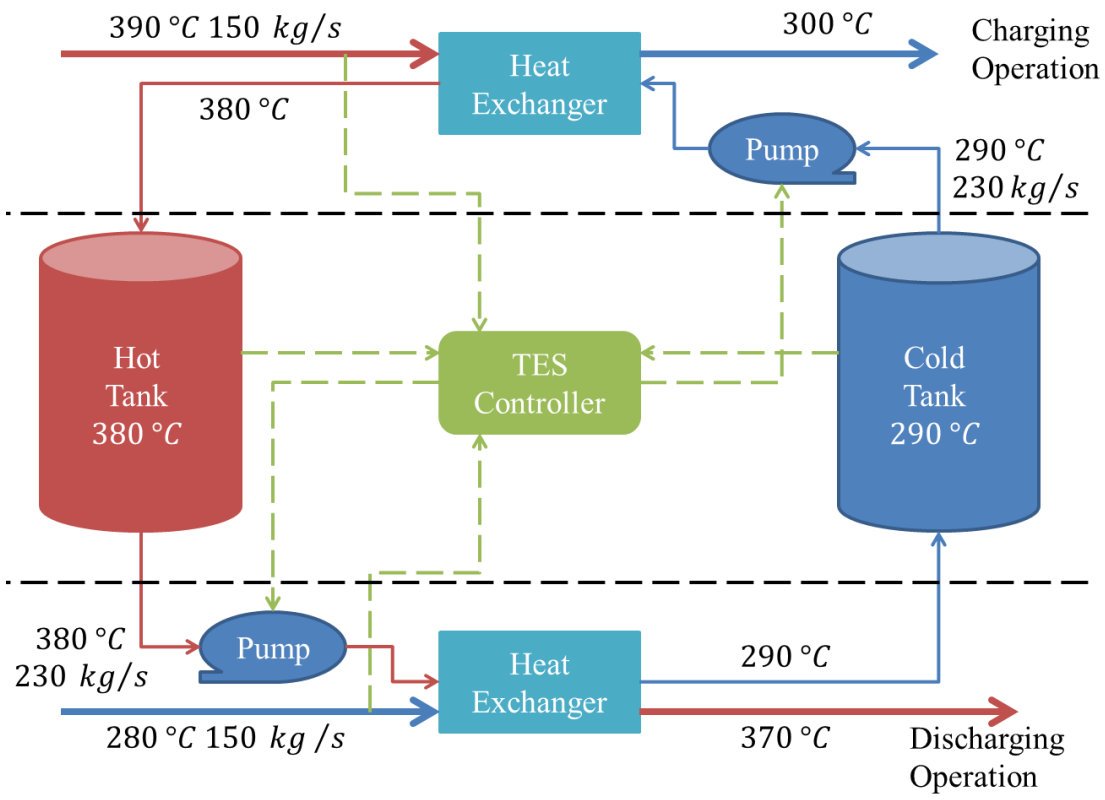

Figure B.1 Schematic Representation of TES Model in Design Conditions (Blue and red lines refer to cold and hot lines respectively, solid lines indicate mass flows, with a thick line for HTF flow and a thin line for storage medium flow, green dashed lines are information signals and all of them are connected to/from controller.)

C. MATLAB CODE FOR VALVE AND TES CONTROL

This part includes the MatLab code for the valve and TES control. Unlike the TRNSYS input file, the same code is used for all simulations. FORTRAN routine of TRNSYS communicates with MatLab module at beginning of every time step. In case of an error, MatLab sends a flag which is the last value of "mFileErrorCode" in the code.

For both codes, initial states of several components are sent from TRNSYS as input values and preset design conditions are provided as constants. The code compares states with design conditions and calculates states for every time step.

C.1. Code for Valve Control

This code part calculates the states of the components and sets the valves and HTF pump mass flow rate. The flow diagram of valve control code is presented in the related subsections of the plant model (Section 2.7).

```
% Type155_CallingMatlab.m
% ------------------------------------------------------------------------------------------------
------------------
%
% Example M-file called by TRNSYS Type 155
%
% Data passed from / to TRNSYS
% ----------------------------
%
% trnTime (1x1)        : simulation time
% trnInfo (15x1)       : TRNSYS info array
% trnInputs (nIx1)     : TRNSYS inputs
% trnStartTime (1x1)   : TRNSYS Simulation Start time
% trnStopTime (1x1)    : TRNSYS Simulation Stop time
```

```
% trnTimeStep (1x1)    : TRNSYS Simulation time step
% mFileErrorCode (1x1) : Error code for this m-file. It is set to 1 by TRNSYS and the m-file should set it to 0 at the
%                       end to indicate that the call was successful. Any non-zero value will stop the simulation
% trnOutputs (nOx1)    : TRNSYS outputs
%
%
% Notes:
% ------
%
% You can use the values of trnInfo(7), trnInfo(8) and trnInfo(13) to identify the call (e.g. first iteration, etc.)
% Real-time controllers (callingMode = 10) will only be called once per time step with trnInfo(13) = 1 (after convergence)
%
% The number of inputs is given by trnInfo(3)
% The number of expected outputs is given by trnInfo(6)
% WARNING: if multiple units of Type 155 are used, the variables passed from/to TRNSYS will be sized according to
%       the maximum required by all units. You should cope with that by only using the part of the arrays that is
%       really used by the current m-File. Example: use "nI = trnInfo(3); myInputs = trnInputs(1:nI);"
%                                               rather than "MyInputs = trnInputs;"
%       Please also note that all m-files share the same workspace in Matlab (they are "scripts", not "functions") so
%       variables like trnInfo, trnTime, etc. will be overwritten at each call.
%       "Local" variables like iCall, iStep in this example will also be shared by all units
%       (i.e. they should be given a different name in each m-File if required)
%
% ------------------------------------------------------------------------------------------------------------------


% TRNSYS sets mFileErrorCode = 1 at the beginning of the M-File for error detection
% This file increments mFileErrorCode at different places. If an error occurs in the m-file the last succesful step will
% be indicated by mFileErrorCode, which is displayed in the TRNSYS error message
% At the very end, the m-file sets mFileErrorCode to 0 to indicate that everything was OK
```

```
mFileErrorCode = 100;    % Beginning of the m-file

% --- Desired Temperatures ----------------------------------------------------------------
---------
% ------------------------------------------------------------------------------------------
------------------

T_ptc_des = 370;        %Limit for warm up
T_char_des = 390;       %Limit for TES charge
T_ptc_dchar_des=280;    %Limit for TES discharge
m_TES_max = 150*3600;   %Max limit of m for TES
day_limit = 250;        %Day DNI limit above is day time
T_hot_nom = 380;        %Nominal temp for hot tank
T_cold_nom = 290;       %Nominal temp for cold tank

mFileErrorCode = 110;    % After setting parameters

% --- Process Inputs and global parameters -----------------------------------------------
--------------------------
% ------------------------------------------------------------------------------------------
------------------

dni = trnInputs(1);
TES_level = trnInputs(2);
T_ptc = trnInputs(3);
m_ptc = trnInputs(4);
m_load = trnInputs(5);
T_load = trnInputs(6);
pump_max = trnInputs(7);
ptc_frac = trnInputs(8);
pump_ptc = pump_max*ptc_frac;
m_load_in = trnInputs(9);
T_pump_out = trnInputs(10);
m_dchar_in = trnInputs(11);
T_hot = trnInputs(12);
T_cold = trnInputs(13);

mFileErrorCode = 120;    % After processing inputs


% --- First call of the simulation: initial time step (no iterations) --------------------
------------------------
% ------------------------------------------------------------------------------------------
------------------
```

```
% (note that Matlab is initialized before this at the info(7) = -1 call, but the m-file is
not called)

if ( (trnInfo(7) == 0) && (trnTime-trnStartTime < 1e-2) )
   % This is the first call (Counter will be incremented later for this very first call)
   iCall = 0;
   % This is the first time step
   iStep = 1;
   % Do some initialization stuff, e.g. initialize history of the variables for plotting at
the end of the simulation
   % (uncomment lines if you wish to store variables)
   % No return, normal calculations are also performed during this call
   mFileErrorCode = 130;    % After initialization call
end

% --- Very last call of the simulation (after the user clicks "OK") ----------------------
---------------------------
% ----------------------------------------------------------------------------------------
------------------
if ( trnInfo(8) == -1 )
   mFileErrorCode = 1000;
   % Do stuff at the end of the simulation, e.g. calculate stats, draw plots, etc...
   mFileErrorCode = 0; % Tell TRNSYS that we reached the end of the m-file
without errors
   return
end
% --- Post convergence calls: store values -----------------------------------------------
-------------------------
% ----------------------------------------------------------------------------------------
------------------
if (trnInfo(13) == 1)
   mFileErrorCode = 140;   % Beginning of a post-convergence call
   % This is the extra call that indicates that all Units have converged. You should do
things like:
   % - calculate control signal that should be applied at next time step
   % - Store history of variables
   % Note: If Calling Mode is set to 10, Matlab will not be called during iterative
calls.
   % In that case only this loop will be executed and things like incrementing the
"iStep" counter should be done here
   mFileErrorCode = 0; % Tell TRNSYS that we reached the end of the m-file
without errors
   return  % Do not update outputs at this call
end
```

```
% --- All iterative calls ----------------------------------------------------------------------------
% ----------------------------------------------------------------------------------------------------
% --- If this is a first call in the time step, increment counter ---
if ( trnInfo(7) == 0 )
   iStep = iStep+1;
end
% --- Process Inputs ---
mFileErrorCode = 150;   % Beginning of iterative call
% Do calculations here

% bypass valve

if
(((TES_level<=0.01)&&(T_ptc<=T_ptc_des))||((T_ptc<T_ptc_dchar_des)||(m_ptc<
m_load)) )
   trnOutputs(3) = 1; % to expansion tank
else
   trnOutputs(3) = 0;
end
mFileErrorCode = 170;

% day night valve
if dni>day_limit%day check
   if (trnOutputs(3) == 1)&&((TES_level>0.01)&&(T_hot>=(T_hot_nom-3)))
%warmup but tes is not empty
      %warmup
      if (pump_ptc+m_load)>pump_max
        trnOutputs(2)=1-m_load/pump_max;
      else
        trnOutputs(2)= pump_ptc/(pump_ptc+m_load);
      end
   else
   trnOutputs(2) = 1;
   end
else%night
   trnOutputs(2) = 0;
end
mFileErrorCode = 160;

% TES charging valve
if (((T_ptc>T_char_des)&&(m_ptc>m_load))&&(TES_level<1))
   trnOutputs(4)=1-m_load/m_ptc;
else
```

```
   trnOutputs(4)=0;
end
mFileErrorCode = 180;

% TES discharging valve
if((TES_level>0.01)&&(((T_ptc>=T_ptc_dchar_des)&&((m_ptc<m_load)||(T_load>
T_ptc)))))

   if T_hot<(T_hot_nom-3)
      trnOutputs(5) = 0;
   else
      trnOutputs(5)=1;
   end
else
   trnOutputs(5)=0;
end
mFileErrorCode = 190;

% Load bypass valve

if m_load_in>m_load
   trnOutputs(6) = m_load/m_load_in;
else
   trnOutputs(6) = 1;
end

% TES discharge flow diverter

if m_dchar_in>m_TES_max
   trnOutputs(7) = m_TES_max/m_dchar_in;
else
   trnOutputs(7) = 1;
end

% HTF pump
if dni>day_limit
   if trnOutputs(3)==1 % bypass open
      if (TES_level>0.01)&&(T_hot>=(T_hot_nom-3)) % TES is not empty
         trnOutputs(1) = pump_ptc+m_load; % warm up + discharge
      else
         trnOutputs(1) = pump_ptc; % warm up
      end
   else
      if (TES_level>0.01)&&(T_hot>=(T_hot_nom-3)) %
         if ((T_ptc>T_ptc_dchar_des)&&(m_ptc>=m_load))
```

```
            trnOutputs(1) = pump_ptc;
            mFileErrorCode = 192;
         else
            trnOutputs(1) = m_load;
         end
      else
         trnOutputs(1) = pump_ptc;
      end
   end
else
   if (TES_level>0.01)&&(T_hot>=(T_hot_nom-3))
      trnOutputs(1) = m_load;
      mFileErrorCode = 193;
   else
      trnOutputs(1) = 0;
      mFileErrorCode = 194;
   end
end
mFileErrorCode = 195;   % Beginning of iterative call

mFileErrorCode = 0; % Tell TRNSYS that we reached the end of the m-file without
errors
return
```

C.2. Code for TES Control

TES control code gets the operation needed and depending on tank states, calculates mass flow rate for TES pumps. As a result of the calculations, the HEX give desired outlet temperatures for each operation. Charging and discharging are not allowed at the same time step. In case of unable to charge/discharge (full, empty or cold storage cases), HTF passes through HEX without any temperature change.

```
% Type155_CallingMatlab.m
% ------------------------------------------------------------------------------------------
------------------
%
% Example M-file called by TRNSYS Type 155
%
% Data passed from / to TRNSYS
% ----------------------------
%
% trnTime (1x1)        : simulation time
% trnInfo (15x1)       : TRNSYS info array
% trnInputs (nIx1)     : TRNSYS inputs
% trnStartTime (1x1)   : TRNSYS Simulation Start time
% trnStopTime (1x1)    : TRNSYS Simulation Stop time
% trnTimeStep (1x1)    : TRNSYS Simulation time step
% mFileErrorCode (1x1) : Error code for this m-file. It is set to 1 by TRNSYS and
the m-file should set it to 0 at the
%                        end to indicate that the call was successful. Any non-zero value will
stop the simulation
% trnOutputs (nOx1)    : TRNSYS outputs
%
%
% Notes:
% ------
%
% You can use the values of trnInfo(7), trnInfo(8) and trnInfo(13) to identify the call
(e.g. first iteration, etc.)
% Real-time controllers (callingMode = 10) will only be called once per time step
with trnInfo(13) = 1 (after convergence)
%
% The number of inputs is given by trnInfo(3)
```

```
% The number of expected outputs is given by trnInfo(6)
% WARNING: if multiple units of Type 155 are used, the variables passed from/to
TRNSYS will be sized according to
%       the maximum required by all units. You should cope with that by only using
the part of the arrays that is
%       really used by the current m-File. Example: use "nI = trnInfo(3); myInputs =
trnInputs(1:nI);"
%                                       rather than "MyInputs = trnInputs;"
%       Please also note that all m-files share the same workspace in Matlab (they
are "scripts", not "functions") so
%       variables like trnInfo, trnTime, etc. will be overwritten at each call.
%       "Local" variables like iCall, iStep in this example will also be shared by all
units
%       (i.e. they should be given a different name in each m-File if required)
%
% ----------------------------------------------------------------------------------------
------------------


% TRNSYS sets mFileErrorCode = 1 at the beginning of the M-File for error
detection
% This file increments mFileErrorCode at different places. If an error occurs in the
m-file the last succesful step will
% be indicated by mFileErrorCode, which is displayed in the TRNSYS error
message
% At the very end, the m-file sets mFileErrorCode to 0 to indicate that everything
was OK

mFileErrorCode = 100;    % Beginning of the m-file

% --- Storage Constants ------------------------------------------------------------
----
% ----------------------------------------------------------------------------------------
------------------

cp_htf=2.3;             %[kJ/kg/K]
cp_tes=1.5;             %[kJ/kg/K]
cp_s_c=cp_htf;
cp_l_c=cp_tes;
cp_s_d=cp_tes;
cp_l_d=cp_htf;
UA_c=11178000;      %[kJ/hr/K]
UA_d=UA_c;      %[kJ/hr/K]
T_l_out_c=380;      %[oC]
T_l_out_d=370;      %[oC]
```

```
T_hot_tank_des = 380;
T_cold_tank_des = 290;
max_flow = 150*3600;

mFileErrorCode = 110;    % After setting parameters

% --- Process Inputs and global parameters ---------------------------------------------
-------------------------
% --------------------------------------------------------------------------------------
-----------------

T_s_in_c = trnInputs(1);
T_l_in_c = trnInputs(2);
m_s_c = trnInputs(3);
level_hot = trnInputs(4);
T_s_in_d = trnInputs(5);
T_l_in_d = trnInputs(6);
m_l_d = trnInputs(7);
level_cold = trnInputs(8);
T_hot_tank = trnInputs(9);
T_cold_tank = trnInputs(10);

mFileErrorCode = 120;    % After processing inputs


% --- First call of the simulation: initial time step (no iterations) ------------------
-------------------------
% --------------------------------------------------------------------------------------
-----------------
% (note that Matlab is initialized before this at the info(7) = -1 call, but the m-file is
not called)

if ( (trnInfo(7) == 0) && (trnTime-trnStartTime < 1e-2) )

   % This is the first call (Counter will be incremented later for this very first call)
   iCall = 0;

   % This is the first time step
   iStep = 1;

   % Do some initialization stuff, e.g. initialize history of the variables for plotting at
the end of the simulation
   % (uncomment lines if you wish to store variables)

   T_s_in_d = 380;
```

```
    T_l_in_c = 290;

    % No return, normal calculations are also performed during this call
    mFileErrorCode = 130;    % After initialization call

end


% --- Very last call of the simulation (after the user clicks "OK") ----------------------
---------------------------
% ----------------------------------------------------------------------------------------
------------------

if ( trnInfo(8) == -1 )

    mFileErrorCode = 1000;

    % Do stuff at the end of the simulation, e.g. calculate stats, draw plots, etc...

    mFileErrorCode = 0; % Tell TRNSYS that we reached the end of the m-file
without errors
    return

end


% --- Post convergence calls: store values -----------------------------------------------
-------------------------
% ----------------------------------------------------------------------------------------
------------------

if (trnInfo(13) == 1)

    mFileErrorCode = 140;   % Beginning of a post-convergence call


    % This is the extra call that indicates that all Units have converged. You should do
things like:
    % - calculate control signal that should be applied at next time step
    % - Store history of variables
    % Note: If Calling Mode is set to 10, Matlab will not be called during iterative
calls.
    % In that case only this loop will be executed and things like incrementing the
"iStep" counter should be done here
```

```
   mFileErrorCode = 0; % Tell TRNSYS that we reached the end of the m-file
without errors
   return  % Do not update outputs at this call

end


% --- All iterative calls ----------------------------------------------------------------------
-------------------
% ---------------------------------------------------------------------------------------------
-------------------

% --- If this is a first call in the time step, increment counter ---

if ( trnInfo(7) == 0 )
   iStep = iStep+1;
end

% --- Process Inputs ---

mFileErrorCode = 150;   % Beginning of iterative call

% Do calculations here
% For charging HX
if ((m_s_c==0)||(level_hot==1))||(T_cold_tank<(0.95*T_cold_tank_des))% 1%
margin is given
   m_l_c=0;
elseif ((m_s_c==max_flow && T_s_in_c==390) && T_l_in_c==290) %special
cases
   m_l_c=m_s_c*cp_s_c/cp_l_c;
else
   mFileErrorCode = 165;
   T_s_out_c=fzero(@(T_s_out_c) UA_c*((T_s_in_c-T_l_out_c)-(T_s_out_c-
T_l_in_c))/log((T_s_in_c-T_l_out_c)/(T_s_out_c-T_l_in_c))-
m_s_c*cp_s_c*(T_s_in_c-T_s_out_c),[T_l_in_c T_s_in_c]);
   mFileErrorCode = 175;
   m_l_c=m_s_c*cp_s_c*(T_s_in_c-T_s_out_c)/cp_l_c/(T_l_out_c-T_l_in_c);
end
% For discharge HX
if ((m_l_d==0)||(level_cold==1))||(T_hot_tank<(0.99*T_hot_tank_des)) % 1%
margin is given
   m_s_d=0;
elseif ((m_l_d==max_flow && T_l_in_d==280)&& T_s_in_d==380) %special
cases
   m_s_d=m_l_d*cp_l_d/cp_s_d;
```

```
else
   mFileErrorCode = num2str(T_l_in_d);
   T_s_out_d=fzero(@(T_s_out_d) UA_d*((T_s_in_d-T_l_out_d)-(T_s_out_d-
T_l_in_d))/log((T_s_in_d-T_l_out_d)/(T_s_out_d-T_l_in_d))-
m_l_d*cp_l_d*(T_l_out_d-T_l_in_d),[T_l_in_d T_s_in_d]);
   mFileErrorCode = 195;
   m_s_d=m_l_d*cp_l_d*(T_l_out_d-T_l_in_d)/cp_s_d/(T_s_in_d-T_s_out_d);
end
mfileErrorCode = 205;
% --- Set outputs ---
trnOutputs(1) = m_l_c;
trnOutputs(2) = m_s_d;

mFileErrorCode = 0; % Tell TRNSYS that we reached the end of the m-file without
errors
return
```

D. TRNSYS MODEL INPUT FILE

In Appendix D, a sample FORTRAN code for simulation is shown which is generated by TRNSYS automatically before simulation starts. The code is for high demand analysis at 275M USD initial investment. It includes all the simulation parameters, initial values, constants and outputs of components and links between each component.

```
VERSION 17
**********************************************************************
**********
*** TRNSYS input file (deck) generated by TrnsysStudio
*** on Cumartesi, Temmuz 26, 2014 at 13:18
*** from TrnsysStudio project: D:\Dropbox\trnsys model\cases\high
cases\275Mdollar\case6\Project27 - Copy\Project27.tpf
***
*** If you edit this file, use the File/Import TRNSYS Input File function in
*** TrnsysStudio to update the project.
***
*** If you have problems, questions or suggestions please contact your local
*** TRNSYS distributor or mailto:software@cstb.fr
***
**********************************************************************
**********


**********************************************************************
**********
*** Units
**********************************************************************
**********

**********************************************************************
**********
*** Control cards
```

```
**********************************************************************
**********
* START, STOP and STEP
CONSTANTS 3
START=4680
STOP=4848
STEP=0.004
SIMULATION          START          STOP  STEP  ! Start time      End time
        Time step
TOLERANCES 0.05 0.05                    ! Integration     Convergence
LIMITS 5000 5000 5000                           ! Max iterations         Max
warnings        Trace limit
DFQ 1                                   ! TRNSYS numerical integration solver method
WIDTH 80                                ! TRNSYS output file width, number of
characters
LIST                                    ! NOLIST statement
                                        ! MAP statement
SOLVER 0 1 1                                    ! Solver statement      Minimum
relaxation factor       Maximum relaxation factor
NAN_CHECK 0                                     ! Nan DEBUG statement
OVERWRITE_CHECK 0                       ! Overwrite DEBUG statement
TIME_REPORT 0                           ! disable time report
EQSOLVER 1                              ! EQUATION SOLVER statement
* User defined CONSTANTS


* Model "Type15-2" (Type 15)
*

UNIT 23 TYPE 15      Type15-2
*$UNIT_NAME Type15-2
*$MODEL .\Weather Data Reading and Processing\Standard
Format\TMY2\Type15-2.tmf
*$POSITION 123 124
*$LAYER Weather - Data Files #
PARAMETERS 9
2               ! 1 File Type
31              ! 2 Logical unit
3               ! 3 Tilted Surface Radiation Mode
0.2             ! 4 Ground reflectance - no snow
0.7             ! 5 Ground reflectance - snow cover
1               ! 6 Number of surfaces
1               ! 7 Tracking mode
0.0             ! 8 Slope of surface
0               ! 9 Azimuth of surface
```

```
*** External files
ASSIGN "C:\Trnsys17\Weather\Meteonorm\Europe\TR-Mugla-172920.tm2" 31
*|? Which file contains the TMY-2 weather data? |1000
*-------------------------------------------------------------------------------

* EQUATIONS "PTC consts"
*
EQUATIONS 2
T_amb = [23,1]
PTC_Signal = Min(1,(max(0.00,0.00045*[22,3])))
*$UNIT_NAME PTC consts
*$LAYER Main
*$POSITION 300 167

*-------------------------------------------------------------------------------

* Model "Type1262" (Type 1262)
*

UNIT 22 TYPE 1262   Type1262
*$UNIT_NAME Type1262
*$MODEL .\High Temperature Solar (TESS)\Array Shading\Type1262.tmf
*$POSITION 263 78
*$LAYER Main #
*$# Parabolic Trough Shading: East-West Tracking
PARAMETERS 3
5.7             ! 1 Collector aperture width
15.             ! 2 Collector row spacing
Parallel_collectors             ! 3 Number of rows
INPUTS 4
23,25           ! Type15-2:Beam radiation for surface ->Incident beam radiation
23,16           ! Type15-2:Solar zenith angle ->Solar zenith angle
23,17           ! Type15-2:Solar azimuth angle ->Solar azimuth angle
23,29           ! Type15-2:Angle of incidence for surface ->Solar incidence angle
*** INITIAL INPUT VALUES
0.0 30.0 0. 30.0
*-------------------------------------------------------------------------------

* Model "Pump valve controller" (Type 155)
*

UNIT 35 TYPE 155    Pump valve controller
*$UNIT_NAME Pump valve controller
*$MODEL .\Utility\Calling External Programs\Matlab\Type155.tmf
*$POSITION 191 72
```

```
*$LAYER Main #
PARAMETERS 5
0               ! 1 Mode
13              ! 2 Number of inputs
7               ! 3 Number of outputs
0               ! 4 Calling Mode
0               ! 5 Keep Matlab open after simulation
INPUTS 13
23,25           ! Type15-2:Beam radiation for surface ->DNI-1
2,9             ! Hot Tank:Level indicator ->Level_Hot-2-2
T_PTC_out               ! Equa:T_PTC_out ->T_ptc-3
m_coll_out              ! Equa:m_coll_out ->m_ptc-4
m_req           ! Load Calc:m_req ->m_load-5
T_req           ! Load Calc:T_req ->T_load-6
htf_pump_max_flow               ! [equation] pump_max-7
PTC_Signal              ! PTC consts:PTC_Signal ->pump_frac-8
34,2            ! Type11h-4:Outlet flow rate ->m_load_in-9
25,1            ! HTF Pump:Outlet fluid temperature ->T_htf_pump-10
33,2            ! Discharge Mixer:Outlet flow rate ->m_discharge_in-11
2,1             ! Hot Tank:Fluid temperature ->T_hot_tank-12
3,1             ! Cold Tank:Fluid temperature ->T_cold_tank-13
*** INITIAL INPUT VALUES
0 0 0 0 0 0 htf_pump_max_flow 0 0 0 0 0 0
LABELS 1
"Matlab2.m"
*-------------------------------------------------------------------------------

* EQUATIONS "Equa"
*
EQUATIONS 5
Parallel_Coll = Parallel_collectors
m_coll_in = [26,4]/Parallel_Coll
m_coll_out = [26,4]
T_max = 400
T_PTC_out = min([40,1],T_max)
*$UNIT_NAME Equa
*$LAYER Main
*$POSITION 424 197

*-------------------------------------------------------------------------------


* Model "Type1257" (Type 1257)
*
```

```
UNIT 40 TYPE 1257   Type1257
*$UNIT_NAME Type1257
*$MODEL .\High Temperature Solar (TESS)\Trough Collector\Type1257.tmf
*$POSITION 623 197
*$LAYER Main #
*$# Parabolic Trough Model
PARAMETERS 31
5.7              ! 1 Width of Collector Aperture
HCE_length              ! 2 Length of single collector
0.07             ! 3 Inner diameter of absorber tube
1.8              ! 4 Focal length for collector
0.98             ! 5 Mirror accuracy
0.93             ! 6 Reflectivity of mirror
0.96             ! 7 Envelope transmittance
0.95             ! 8 Absorptance of receiver coating
150              ! 9 Initial temperature
HCE_series              ! 10 Number in collectors in series
12               ! 11 Number of collector nodes
800              ! 12 Number of Runge Kutta steps
0                ! 13 Mass calculation mode
1.               ! 14 IAM coefficient b0
0.000884                ! 15 IAM coefficient b1
-0.00005369             ! 16 IAM coefficient b2
-34.0669188             ! 17 Heat loss coefficient a0 (kJ/h.m)
1.09066176              ! 18 Heat loss coefficient a1 (kJ/h.m.K)
-0.0049925988                   ! 19 Heat loss coefficient a2 (kJ/h.m.K^2)
0.0000249452748                 ! 20 Heat loss coefficient a3 (kJ/h.m.K^3)
0.0764961               ! 21 Heat loss coefficient a4 (m)
0.0000001128818                 ! 22 Heat loss coefficient a5 (m/K^2)
1074.            ! 23 Fluid density coefficient r0 (kg/m3)
-0.6367                 ! 24 Fluid density coefficient r1 (kg/m3.K)
-0.0007762              ! 25 Fluid density coefficient r2 (kg/m3.K^2)
-18.34           ! 26 Fluid enthalpy coefficient h0 (kJ/kg)
1.498            ! 27 Fluid enthalpy coefficient h1 (kJ/kg.K)
0.001377                ! 28 Fluid enthalpy coefficient h2 (kJ/kg.K2)
-19.0000                ! 29 Fluid internal energy coefficient u0 (kJ/kg)
1.498            ! 30 Fluid internal energy coefficient u1 (kJ/kg.K)
0.001377                ! 31 Fluid internal energy coefficient u2 (kJ/kg)
INPUTS 10
26,3             ! DayNight:Temperature at outlet 2 ->Inlet fluid temperature
m_coll_in               ! Equa:m_coll_in ->Inlet mass flow rate
T_amb            ! [equation] Ambient temperature
22,3             ! Type1262:Shaded beam radiation: middle rows ->Beam radiation on
the tilted surface
23,29            ! Type15-2:Angle of incidence for surface ->Incidence angle
```

```
0,0             ! [unconnected] Tracking efficiency factor
0,0             ! [unconnected] Mirror cleanliness factor
0,0             ! [unconnected] Receiver glass dusting factor
0,0             ! [unconnected] Bellows shading factor
0,0             ! [unconnected] Miscellaneous efficiency factor
*** INITIAL INPUT VALUES
293.0 0. T_amb 0.0 0. 0.99 0.95 0.98 0.97 0.96
*--------------------------------------------------------------------------------

* Model "System_Plotter-3" (Type 65)
*

UNIT 42 TYPE 65      System_Plotter-3
*$UNIT_NAME System_Plotter-3
*$MODEL \Trnsys17\Studio\lib\System_Output\TYPE65d.tmf
*$POSITION 172 365
*$LAYER OutputSystem #
PARAMETERS 12
1               ! 1 Nb. of left-axis variables
0               ! 2 Nb. of right-axis variables
0.0             ! 3 Left axis minimum
3300            ! 4 Left axis maximum
0.0             ! 5 Right axis minimum
1000.0          ! 6 Right axis maximum
1               ! 7 Number of plots per simulation
7               ! 8 X-axis gridpoints
0               ! 9 Shut off Online w/o removing
-1              ! 10 Logical unit for output file
0               ! 11 Output file units
0               ! 12 Output file delimiter
INPUTS 1
22,3            ! Type1262:Shaded beam radiation: middle rows ->Left axis variable
*** INITIAL INPUT VALUES
Shading
LABELS  3
"Temperatures"
"Heat transfer rates"
"DNI"
*--------------------------------------------------------------------------------

* Model "System_Plotter-2" (Type 65)
*

UNIT 39 TYPE 65      System_Plotter-2
*$UNIT_NAME System_Plotter-2
```

```
*$MODEL \Trnsys17\Studio\lib\System_Output\TYPE65d.tmf
*$POSITION 396 378
*$LAYER OutputSystem #
PARAMETERS 12
7               ! 1 Nb. of left-axis variables
6               ! 2 Nb. of right-axis variables
0.0             ! 3 Left axis minimum
400             ! 4 Left axis maximum
0.0             ! 5 Right axis minimum
1350000             ! 6 Right axis maximum
1               ! 7 Number of plots per simulation
7               ! 8 X-axis gridpoints
0               ! 9 Shut off Online w/o removing
-1              ! 10 Logical unit for output file
0               ! 11 Output file units
0               ! 12 Output file delimiter
INPUTS 13
27,1            ! HTF Tank:Fluid temperature ->Left axis variable-1
25,1            ! HTF Pump:Outlet fluid temperature ->Left axis variable-2
T_PTC_out           ! Equa:T_PTC_out ->Left axis variable-3
34,1            ! Type11h-4:Outlet temperature ->Left axis variable-4
2,1             ! Hot Tank:Fluid temperature ->Left axis variable-5
3,1             ! Cold Tank:Fluid temperature ->Left axis variable-6
23,1            ! Type15-2:Dry bulb temperature ->Left axis variable-7
27,2            ! HTF Tank:Load flow rate ->Right axis variable-1
25,2            ! HTF Pump:Outlet flow rate ->Right axis variable-2
m_coll_out          ! Equa:m_coll_out ->Right axis variable-3
m_out           ! Load Calc:m_out ->Right axis variable-4
14,2            ! Charge Pump:Outlet flow rate ->Right axis variable-5
13,2            ! Discharge Pump:Outlet flow rate ->Right axis variable-6
*** INITIAL INPUT VALUES
Tank HTF_Pump ptc Load_in Hot_tank Cold_tank T_amb Tank HTF_pump ptc
Load_in
Charge_pump Discharge_pump
LABELS  3
"Temperatures"
"Mass Flow"
"Temp_M_dot"
*-------------------------------------------------------------------------------

* EQUATIONS "HTF consts"
*
EQUATIONS 3
htf_pump_max_flow = 300*3600/11*Parallel_collectors
Tank_load = [35,1]
```

```
htf_pump_sgn = [35,1]/htf_pump_max_flow
*$UNIT_NAME HTF consts
*$LAYER Main
*$POSITION 87 207

*-------------------------------------------------------------------------


* Model "System_Plotter" (Type 65)
*

UNIT 38 TYPE 65      System_Plotter
*$UNIT_NAME System_Plotter
*$MODEL \Trnsys17\Studio\lib\System_Output\TYPE65d.tmf
*$POSITION 1099 58
*$LAYER OutputSystem #
PARAMETERS 12
10              ! 1 Nb. of left-axis variables
2               ! 2 Nb. of right-axis variables
0               ! 3 Left axis minimum
1               ! 4 Left axis maximum
0               ! 5 Right axis minimum
1               ! 6 Right axis maximum
1               ! 7 Number of plots per simulation
7               ! 8 X-axis gridpoints
0               ! 9 Shut off Online w/o removing
-1              ! 10 Logical unit for output file
0               ! 11 Output file units
0               ! 12 Output file delimiter
INPUTS 12
35,2            ! Pump valve controller:DayNight-2 ->Left axis variable-1
35,3            ! Pump valve controller:Bypass-3 ->Left axis variable-2
35,4            ! Pump valve controller:Charge-4 ->Left axis variable-3
35,5            ! Pump valve controller:Discharge-5 ->Left axis variable-4
2,9             ! Hot Tank:Level indicator ->Left axis variable-5
3,9             ! Cold Tank:Level indicator ->Left axis variable-6
35,7            ! Pump valve controller:TES_discharge-7 ->Left axis variable-7
supplied                ! Load Calc:supplied ->Left axis variable-8
supplied_m              ! Load Calc:supplied_m ->Left axis variable-9
supplied_T              ! Load Calc:supplied_T ->Left axis variable-10
PTC_Signal              ! PTC consts:PTC_Signal ->Right axis variable-1
per             ! Dispatch percentage:per ->Right axis variable-2
*** INITIAL INPUT VALUES
DayNight-2 Bypass-3 Charge-4 Discharge-5 Hot_level Cold_Level
Discharge_bypass
```

```
supplied supplied_m suppiled_T DNI_signal sup_rat
LABELS  3
"Temperatures"
"Heat transfer rates"
"signals"
*------------------------------------------------------------------------

* Model "Bypass" (Type 11)
*

UNIT 28 TYPE 11      Bypass
*$UNIT_NAME Bypass
*$MODEL .\Hydronics\Flow Diverter\Other Fluids\Type11f.tmf
*$POSITION 572 188
*$LAYER Water Loop #
PARAMETERS 1
2               ! 1 Controlled flow diverter mode
INPUTS 3
T_PTC_out               ! Equa:T_PTC_out ->Inlet temperature
m_coll_out              ! Equa:m_coll_out ->Inlet flow rate
35,3            ! Pump valve controller:Bypass-3 ->Control signal
*** INITIAL INPUT VALUES
20.0 100.0 0.5
*------------------------------------------------------------------------

* Model "DayNight" (Type 11)
*

UNIT 26 TYPE 11      DayNight
*$UNIT_NAME DayNight
*$MODEL .\Hydronics\Flow Diverter\Other Fluids\Type11f.tmf
*$POSITION 339 163
*$LAYER Water Loop #
PARAMETERS 1
2               ! 1 Controlled flow diverter mode
INPUTS 3
25,1            ! HTF Pump:Outlet fluid temperature ->Inlet temperature
25,2            ! HTF Pump:Outlet flow rate ->Inlet flow rate
35,2            ! Pump valve controller:DayNight-2 ->Control signal
*** INITIAL INPUT VALUES
20.0 100.0 0.5
*------------------------------------------------------------------------

* Model "Charge" (Type 11)
*
```

```
UNIT 30 TYPE 11      Charge
*$UNIT_NAME Charge
*$MODEL .\Hydronics\Flow Diverter\Other Fluids\Type11f.tmf
*$POSITION 697 208
*$LAYER Water Loop #
PARAMETERS 1
2               ! 1 Controlled flow diverter mode
INPUTS 3
28,1            ! Bypass:Temperature at outlet 1 ->Inlet temperature
28,2            ! Bypass:Flow rate at outlet 1 ->Inlet flow rate
35,4            ! Pump valve controller:Charge-4 ->Control signal
*** INITIAL INPUT VALUES
20.0 100.0 0.5
*-------------------------------------------------------------------------------

* Model "Discharge" (Type 11)
*

UNIT 32 TYPE 11      Discharge
*$UNIT_NAME Discharge
*$MODEL .\Hydronics\Flow Diverter\Other Fluids\Type11f.tmf
*$POSITION 992 168
*$LAYER Water Loop #
PARAMETERS 1
2               ! 1 Controlled flow diverter mode
INPUTS 3
30,1            ! Charge:Temperature at outlet 1 ->Inlet temperature
30,2            ! Charge:Flow rate at outlet 1 ->Inlet flow rate
35,5            ! Pump valve controller:Discharge-5 ->Control signal
*** INITIAL INPUT VALUES
20.0 100.0 0.5
*-------------------------------------------------------------------------------

* Model "Load Bypass" (Type 11)
*

UNIT 44 TYPE 11      Load Bypass
*$UNIT_NAME Load Bypass
*$MODEL .\Hydronics\Flow Diverter\Other Fluids\Type11f.tmf
*$POSITION 729 338
*$LAYER Water Loop #
PARAMETERS 1
2               ! 1 Controlled flow diverter mode
INPUTS 3
```

```
34,1            ! Type11h-4:Outlet temperature ->Inlet temperature
34,2            ! Type11h-4:Outlet flow rate ->Inlet flow rate
35,6            ! Pump valve controller:Load_bypass-6 ->Control signal
*** INITIAL INPUT VALUES
20.0 100.0 0.5
*-------------------------------------------------------------------------------

* Model "Type11h-3" (Type 11)
*

UNIT 43 TYPE 11      Type11h-3
*$UNIT_NAME Type11h-3
*$MODEL .\Hydronics\Tee-Piece\Other Fluids\Type11h.tmf
*$POSITION 348 338
*$LAYER Water Loop #
PARAMETERS 1
1               ! 1 Tee piece mode
INPUTS 4
T_out           ! Load Calc:T_out ->Temperature at inlet 1
m_out           ! Load Calc:m_out ->Flow rate at inlet 1
44,1            ! Load Bypass:Temperature at outlet 1 ->Temperature at inlet 2
44,2            ! Load Bypass:Flow rate at outlet 1 ->Flow rate at inlet 2
*** INITIAL INPUT VALUES
20.0 100.0 20.0 100.0
*-------------------------------------------------------------------------------

* EQUATIONS "Load Calc"
*
EQUATIONS 7
m_out = [44,4]
T_out = [44,3]-100
m_req = 150*3600
T_req = 370
supplied_m = min(1,max(0,[44,4]/(m_req*0.99)))
supplied_T = ge([44,3],T_req*0.99)
supplied = supplied_m*supplied_T
*$UNIT_NAME Load Calc
*$LAYER Main
*$POSITION 559 298

*-------------------------------------------------------------------------------

* EQUATIONS "TES Const"
*
EQUATIONS 14
```

```
pump_max = 250*3600
UA = 11178000
cp_tes = 1.5
cp_htf = 2.3
den_tes = 1060
tank_h = tank_size
tank_cir = tank_h*2*3.14
tank_xsec = tank_h*tank_h*3.14
tank_vol = tank_h*tank_xsec
wet_loss = 0.05
dry_loss = 0.025
hot_ratio = 0.42
initial_vol_hot = tank_vol*hot_ratio
initial_vol_cold = tank_vol*(1-hot_ratio)
*$UNIT_NAME TES Const
*$LAYER Main
*$POSITION 394 330

*-------------------------------------------------------------------------------

* Model "discharge bypass" (Type 11)
*

UNIT 45 TYPE 11      discharge bypass
*$UNIT_NAME discharge bypass
*$MODEL .\Hydronics\Flow Diverter\Other Fluids\Type11f.tmf
*$POSITION 247 570
*$LAYER Water Loop #
PARAMETERS 1
2               ! 1 Controlled flow diverter mode
INPUTS 3
33,1            ! Discharge Mixer:Outlet temperature ->Inlet temperature
33,2            ! Discharge Mixer:Outlet flow rate ->Inlet flow rate
35,7            ! Pump valve controller:TES_discharge-7 ->Control signal
*** INITIAL INPUT VALUES
20.0 100.0 0.5
*-------------------------------------------------------------------------------

* Model "Discharging HX" (Type 5)
*

UNIT 8 TYPE 5        Discharging HX
*$UNIT_NAME Discharging HX
*$MODEL .\Heat Exchangers\Counter Flow\Type5b.tmf
*$POSITION 439 530
```

```
*$LAYER Main #
PARAMETERS 4
2               ! 1 Counter flow mode
cp_tes          ! 2 Specific heat of source side fluid
cp_htf          ! 3 Specific heat of load side fluid
0               ! 4 Not used
INPUTS 5
13,1            ! Discharge Pump:Outlet fluid temperature ->Source side inlet
temperature
13,2            ! Discharge Pump:Outlet flow rate ->Source side flow rate
45,3            ! discharge bypass:Temperature at outlet 2 ->Load side inlet
temperature
45,4            ! discharge bypass:Flow rate at outlet 2 ->Load side flow rate
UA              ! [equation] Overall heat transfer coefficient of exchanger
*** INITIAL INPUT VALUES
20.0 100.0 20.0 100.0 UA
*-------------------------------------------------------------------------------

* Model "TES Controller" (Type 155)
*

UNIT 20 TYPE 155    TES Controller
*$UNIT_NAME TES Controller
*$MODEL .\Utility\Calling External Programs\Matlab\Type155.tmf
*$POSITION 511 263
*$LAYER Main #
PARAMETERS 5
0               ! 1 Mode
10              ! 2 Number of inputs
2               ! 3 Number of outputs
0               ! 4 Calling Mode
0               ! 5 Keep Matlab open after simulation
INPUTS 10
30,3            ! Charge:Temperature at outlet 2 ->T_s_in_c-1
14,1            ! Charge Pump:Outlet fluid temperature ->T_l_in_c-2
30,4            ! Charge:Flow rate at outlet 2 ->m_s_c-3
2,9             ! Hot Tank:Level indicator ->level_hot-4
13,1            ! Discharge Pump:Outlet fluid temperature ->T_s_in_d-5
45,3            ! discharge bypass:Temperature at outlet 2 ->T_l_in_d-6
45,4            ! discharge bypass:Flow rate at outlet 2 ->m_l_d-7
3,9             ! Cold Tank:Level indicator ->level_cold-8
2,1             ! Hot Tank:Fluid temperature ->T_hot_tank-9
3,1             ! Cold Tank:Fluid temperature ->T_cold_tank-10
*** INITIAL INPUT VALUES
8 8 8 8 8 8 8 8 8 8
```

```
LABELS 1
"Matlab.m"
*-------------------------------------------------------------------------------

* Model "Cold Tank" (Type 39)
*

UNIT 3 TYPE 39       Cold Tank
*$UNIT_NAME Cold Tank
*$MODEL .\Thermal Storage\Variable Volume Tank\Type39.tmf
*$POSITION 771 262
*$LAYER Water Loop #
PARAMETERS 12
1               ! 1 Tank operation mode
tank_vol                ! 2 Overall tank volume
0               ! 3 Minimum fluid volume
tank_vol                ! 4 Maximum fluid volume
tank_cir                ! 5 Tank circumference
tank_xsec               ! 6 Cross-sectional area
wet_loss                ! 7 Wetted loss coefficient
dry_loss                ! 8 Dry loss coefficient
cp_tes          ! 9 Fluid specific heat
den_tes                 ! 10 Fluid density
290             ! 11 Initial fluid temperature
initial_vol_cold                ! 12 Initial fluid volume
INPUTS 4
8,1             ! Discharging HX:Source side outlet temperature ->Inlet temperature
8,2             ! Discharging HX:Source side flow rate ->Inlet flow rate
14,2            ! Charge Pump:Outlet flow rate ->Flow rate to load
T_amb           ! [equation] Environment temperature
*** INITIAL INPUT VALUES
25.0 100.0 75.0 T_amb
*-------------------------------------------------------------------------------

* EQUATIONS "Signal Gen"
*
EQUATIONS 5
pump_m_max = pump_max
sgn_char = min(pump_m_max,[20,1])/pump_m_max
sgn_dchar = min(pump_m_max,[20,2])/pump_m_max
hot_load = sgn_dchar*pump_m_max
cold_load = sgn_char*pump_m_max
*$UNIT_NAME Signal Gen
*$LAYER Main
*$POSITION 612 448
```

```
*-------------------------------------------------------------------------

* Model "Charge Pump" (Type 3)
*

UNIT 14 TYPE 3       Charge Pump
*$UNIT_NAME Charge Pump
*$MODEL .\Hydronics\Pumps\Variable Speed\Type3b.tmf
*$POSITION 647 166
*$LAYER Water Loop #
PARAMETERS 7
pump_max              ! 1 Maximum flow rate
cp_tes          ! 2 Fluid specific heat
539999.960046                 ! 3 Maximum power
0.05            ! 4 Conversion coefficient
0               ! 5 Power coefficient-1
2               ! 6 Power coefficient-2
-1              ! 7 Power coefficient-3
INPUTS 3
3,1             ! Cold Tank:Fluid temperature ->Inlet fluid temperature
3,2             ! Cold Tank:Load flow rate ->Inlet mass flow rate
sgn_char                ! Signal Gen:sgn_char ->Control signal
*** INITIAL INPUT VALUES
20.0 100.0 1.0
*-------------------------------------------------------------------------

* Model "Discharge Pump" (Type 3)
*

UNIT 13 TYPE 3       Discharge Pump
*$UNIT_NAME Discharge Pump
*$MODEL .\Hydronics\Pumps\Variable Speed\Type3b.tmf
*$POSITION 275 448
*$LAYER Water Loop #
PARAMETERS 7
pump_max              ! 1 Maximum flow rate
cp_tes          ! 2 Fluid specific heat
539999.960046                 ! 3 Maximum power
0.05            ! 4 Conversion coefficient
0               ! 5 Power coefficient-1
2               ! 6 Power coefficient-2
-1              ! 7 Power coefficient-3
INPUTS 3
2,1             ! Hot Tank:Fluid temperature ->Inlet fluid temperature
```

```
2,2             ! Hot Tank:Load flow rate ->Inlet mass flow rate
sgn_dchar               ! Signal Gen:sgn_dchar ->Control signal
*** INITIAL INPUT VALUES
380 100.0 1.0
*--------------------------------------------------------------------------

* Model "Charging HX" (Type 5)
*

UNIT 5 TYPE 5       Charging HX
*$UNIT_NAME Charging HX
*$MODEL .\Heat Exchangers\Counter Flow\Type5b.tmf
*$POSITION 461 166
*$LAYER Main #
PARAMETERS 4
2               ! 1 Counter flow mode
cp_htf          ! 2 Specific heat of source side fluid
cp_tes          ! 3 Specific heat of load side fluid
0               ! 4 Not used
INPUTS 5
30,3            ! Charge:Temperature at outlet 2 ->Source side inlet temperature
30,4            ! Charge:Flow rate at outlet 2 ->Source side flow rate
14,1            ! Charge Pump:Outlet fluid temperature ->Load side inlet temperature
14,2            ! Charge Pump:Outlet flow rate ->Load side flow rate
UA              ! [equation] Overall heat transfer coefficient of exchanger
*** INITIAL INPUT VALUES
20.0 100.0 20.0 100.0 UA
*--------------------------------------------------------------------------

* Model "Hot Tank" (Type 39)
*

UNIT 2 TYPE 39      Hot Tank
*$UNIT_NAME Hot Tank
*$MODEL .\Thermal Storage\Variable Volume Tank\Type39.tmf
*$POSITION 258 240
*$LAYER Water Loop #
PARAMETERS 12
1               ! 1 Tank operation mode
tank_vol                ! 2 Overall tank volume
0               ! 3 Minimum fluid volume
tank_vol                ! 4 Maximum fluid volume
tank_cir                ! 5 Tank circumference
tank_xsec               ! 6 Cross-sectional area
wet_loss                ! 7 Wetted loss coefficient
```

```
dry_loss                ! 8 Dry loss coefficient
cp_tes          ! 9 Fluid specific heat
den_tes                 ! 10 Fluid density
380             ! 11 Initial fluid temperature
initial_vol_hot         ! 12 Initial fluid volume
INPUTS 4
5,3             ! Charging HX:Load side outlet temperature ->Inlet temperature
5,4             ! Charging HX:Load side flow rate ->Inlet flow rate
13,2            ! Discharge Pump:Outlet flow rate ->Flow rate to load
T_amb           ! [equation] Environment temperature
*** INITIAL INPUT VALUES
25.0 100.0 75.0 T_amb
*------------------------------------------------------------------------------

* Model "HTF Pump" (Type 3)
*

UNIT 25 TYPE 3      HTF Pump
*$UNIT_NAME HTF Pump
*$MODEL .\Hydronics\Pumps\Variable Speed\Type3b.tmf
*$POSITION 191 266
*$LAYER Water Loop #
PARAMETERS 5
htf_pump_max_flow           ! 1 Maximum flow rate
cp_tes          ! 2 Fluid specific heat
539999.960046               ! 3 Maximum power
0.05            ! 4 Conversion coefficient
0.5             ! 5 Power coefficient
INPUTS 3
27,1            ! HTF Tank:Fluid temperature ->Inlet fluid temperature
27,2            ! HTF Tank:Load flow rate ->Inlet mass flow rate
htf_pump_sgn            ! HTF consts:htf_pump_sgn ->Control signal
*** INITIAL INPUT VALUES
20.0 100.0 1.0
*------------------------------------------------------------------------------

* Model "Type11h" (Type 11)
*

UNIT 29 TYPE 11     Type11h
*$UNIT_NAME Type11h
*$MODEL .\Hydronics\Tee-Piece\Other Fluids\Type11h.tmf
*$POSITION 532 346
*$LAYER Water Loop #
PARAMETERS 1
```

```
1               ! 1 Tee piece mode
INPUTS 4
31,1            ! Type11h-2:Outlet temperature ->Temperature at inlet 1
31,2            ! Type11h-2:Outlet flow rate ->Flow rate at inlet 1
28,3            ! Bypass:Temperature at outlet 2 ->Temperature at inlet 2
28,4            ! Bypass:Flow rate at outlet 2 ->Flow rate at inlet 2
*** INITIAL INPUT VALUES
20.0 100.0 20.0 100.0
*-------------------------------------------------------------------------------

* Model "Discharge Mixer" (Type 11)
*

UNIT 33 TYPE 11      Discharge Mixer
*$UNIT_NAME Discharge Mixer
*$MODEL .\Hydronics\Tee-Piece\Other Fluids\Type11h.tmf
*$POSITION 871 143
*$LAYER Water Loop #
PARAMETERS 1
1               ! 1 Tee piece mode
INPUTS 4
26,1            ! DayNight:Temperature at outlet 1 ->Temperature at inlet 1
26,2            ! DayNight:Flow rate at outlet 1 ->Flow rate at inlet 1
32,3            ! Discharge:Temperature at outlet 2 ->Temperature at inlet 2
32,4            ! Discharge:Flow rate at outlet 2 ->Flow rate at inlet 2
*** INITIAL INPUT VALUES
20.0 100.0 20.0 100.0
*-------------------------------------------------------------------------------

* Model "System_Plotter-4" (Type 65)
*

UNIT 46 TYPE 65      System_Plotter-4
*$UNIT_NAME System_Plotter-4
*$MODEL \Trnsys17\Studio\lib\System_Output\TYPE65d.tmf
*$POSITION 1249 100
*$LAYER OutputSystem #
PARAMETERS 12
8               ! 1 Nb. of left-axis variables
4               ! 2 Nb. of right-axis variables
250             ! 3 Left axis minimum
400             ! 4 Left axis maximum
0.0             ! 5 Right axis minimum
1080000.0               ! 6 Right axis maximum
1               ! 7 Number of plots per simulation
```

```
7               ! 8 X-axis gridpoints
0               ! 9 Shut off Online w/o removing
-1              ! 10 Logical unit for output file
0               ! 11 Output file units
0               ! 12 Output file delimiter
INPUTS 12
30,3            ! Charge:Temperature at outlet 2 ->Left axis variable-1
5,1             ! Charging HX:Source side outlet temperature ->Left axis variable-2
14,1            ! Charge Pump:Outlet fluid temperature ->Left axis variable-3
5,3             ! Charging HX:Load side outlet temperature ->Left axis variable-4
13,1            ! Discharge Pump:Outlet fluid temperature ->Left axis variable-5
8,1             ! Discharging HX:Source side outlet temperature ->Left axis variable-
6
33,1            ! Discharge Mixer:Outlet temperature ->Left axis variable-7
8,3             ! Discharging HX:Load side outlet temperature ->Left axis variable-8
5,2             ! Charging HX:Source side flow rate ->Right axis variable-1
5,4             ! Charging HX:Load side flow rate ->Right axis variable-2
8,2             ! Discharging HX:Source side flow rate ->Right axis variable-3
8,4             ! Discharging HX:Load side flow rate ->Right axis variable-4
*** INITIAL INPUT VALUES
Char_s_in Char_s_out Char_l_in Char_l_out DChar_s_in DChar_s_out DChar_l_in
DChar_l_out Char_source Char_load DChar_s DChar_l
LABELS  3
"Temperatures"
"Mass Flow"
"TES HX"
*-------------------------------------------------------------------------------

* Model "Type11h-4" (Type 11)
*

UNIT 34 TYPE 11      Type11h-4
*$UNIT_NAME Type11h-4
*$MODEL .\Hydronics\Tee-Piece\Other Fluids\Type11h.tmf
*$POSITION 1087 291
*$LAYER Water Loop #
PARAMETERS 1
1               ! 1 Tee piece mode
INPUTS 4
32,1            ! Discharge:Temperature at outlet 1 ->Temperature at inlet 1
32,2            ! Discharge:Flow rate at outlet 1 ->Flow rate at inlet 1
8,3             ! Discharging HX:Load side outlet temperature ->Temperature at inlet
2
8,4             ! Discharging HX:Load side flow rate ->Flow rate at inlet 2
*** INITIAL INPUT VALUES
```

```
20.0 100.0 20.0 100.0
*------------------------------------------------------------------------------

* Model "Type11h-5" (Type 11)
*

UNIT 47 TYPE 11      Type11h-5
*$UNIT_NAME Type11h-5
*$MODEL .\Hydronics\Tee-Piece\Other Fluids\Type11h.tmf
*$POSITION 827 346
*$LAYER Water Loop #
PARAMETERS 1
1               ! 1 Tee piece mode
INPUTS 4
45,1            ! discharge bypass:Temperature at outlet 1 ->Temperature at inlet 1
45,2            ! discharge bypass:Flow rate at outlet 1 ->Flow rate at inlet 1
43,1            ! Type11h-3:Outlet temperature ->Temperature at inlet 2
43,2            ! Type11h-3:Outlet flow rate ->Flow rate at inlet 2
*** INITIAL INPUT VALUES
20.0 100.0 20.0 100.0
*------------------------------------------------------------------------------

* Model "Type11h-2" (Type 11)
*

UNIT 31 TYPE 11      Type11h-2
*$UNIT_NAME Type11h-2
*$MODEL .\Hydronics\Tee-Piece\Other Fluids\Type11h.tmf
*$POSITION 698 326
*$LAYER Water Loop #
PARAMETERS 1
1               ! 1 Tee piece mode
INPUTS 4
5,1             ! Charging HX:Source side outlet temperature ->Temperature at inlet
1
5,2             ! Charging HX:Source side flow rate ->Flow rate at inlet 1
47,1            ! Type11h-5:Outlet temperature ->Temperature at inlet 2
47,2            ! Type11h-5:Outlet flow rate ->Flow rate at inlet 2
*** INITIAL INPUT VALUES
20.0 100.0 20.0 100.0
*------------------------------------------------------------------------------

* Model "HTF Tank" (Type 39)
*
```

```
UNIT 27 TYPE 39      HTF Tank
*$UNIT_NAME HTF Tank
*$MODEL .\Thermal Storage\Variable Volume Tank\Type39.tmf
*$POSITION 335 303
*$LAYER Water Loop #
PARAMETERS 12
1               ! 1 Tank operation mode
504             ! 2 Overall tank volume
2               ! 3 Minimum fluid volume
502             ! 4 Maximum fluid volume
34.6            ! 5 Tank circumference
95              ! 6 Cross-sectional area
2               ! 7 Wetted loss coefficient
1               ! 8 Dry loss coefficient
cp_tes          ! 9 Fluid specific heat
1060            ! 10 Fluid density
300             ! 11 Initial fluid temperature
450             ! 12 Initial fluid volume
INPUTS 4
29,1            ! Type11h:Outlet temperature ->Inlet temperature
29,2            ! Type11h:Outlet flow rate ->Inlet flow rate
25,2            ! HTF Pump:Outlet flow rate ->Flow rate to load
T_amb           ! [equation] Environment temperature
*** INITIAL INPUT VALUES
25.0 100.0 75.0 T_amb
*------------------------------------------------------------------------------

* Model "Type24" (Type 24)
*

UNIT 49 TYPE 24      Type24
*$UNIT_NAME Type24
*$MODEL .\Utility\Integrators\Quantity Integrator\Type24.tmf
*$POSITION 558 223
*$LAYER Main #
PARAMETERS 2
STOP            ! 1 Integration period
0               ! 2 Relative or absolute start time
INPUTS 1
supplied                ! Load Calc:supplied ->Input to be integrated
*** INITIAL INPUT VALUES
0.0
*------------------------------------------------------------------------------

* EQUATIONS "Dispatch percentage"
```

```
*
EQUATIONS 1
per = [49,1]/(time-start+step)
*$UNIT_NAME Dispatch percentage
*$LAYER Main
*$POSITION 651 212

*-------------------------------------------------------------------------------

* EQUATIONS "parametric study inputs"
*
EQUATIONS 4
tank_size = 13.75
Parallel_collectors = 73
HCE_length = 111.7
HCE_series = 16
*$UNIT_NAME parametric study inputs
*$LAYER Main
*$POSITION 658 506

*-------------------------------------------------------------------------------

END
```